

INSTITUTO NACIONAL DE PESQUISAS DA AMAZÔNIA
PROGRAMA DE PÓS-GRADUAÇÃO EM
CIÊNCIAS DE FLORESTAS TROPICAIS



Crescimento em biomassa de árvores de dossel em florestas com lençol freático superficial no centro-sul da Amazônia

Anderson Lozorio Canal Filho

Manaus – AM

Janeiro/2024

ANDERSON LOZORIO CANAL FILHO

**Crescimento em biomassa de árvores de dossel em florestas com lençol freático superficial
no centro-sul da Amazônia**

Orientadora: Dra. Juliana Schietti de Almeida

Dissertação apresentada ao Instituto Nacional de Pesquisas da Amazônia - INPA, como parte dos requisitos para obtenção do título de Mestre em Ciências de Florestas Tropicais.




Manaus – AM

PROGRAMA DE PÓS-GRADUAÇÃO EM CIÊNCIAS DE FLORESTAS TROPICAIS

ATA DE DEFESA PÚBLICA DE DISSERTAÇÃO - MESTRADO

Ata da Defesa remota de **ANDERSON LOZORIO CANAL FILHO**, ocorrida no dia 29/01/2024, via plataforma de videoconferência Google Meet.

Aos 29 dias de janeiro de 2024, às 14h00 (horário de Manaus/AM), realizou-se a Defesa Pública de Dissertação de **ANDERSON LOZORIO CANAL FILHO**, aluno do Programa de Pós-Graduação *Stricto sensu* em Ciências de Florestas Tropicais, intitulada "Crescimento em biomassa em árvore de dossel de florestas com lençol freático superficial no Centro - sul da Amazônia", sob a orientação da Dra. Juliana Schietti de Almeida (UFAM), em conformidade com o Art. 52 do Regimento Geral da Pós-Graduação do Instituto Nacional de Pesquisas da Amazônia (MCTI/INPA) e Art. 67 do Regimento Interno do Programa de Pós-Graduação em Ciências de Florestas Tropicais, como parte das atividades para conclusão e obtenção do Título de Mestre em Ciências de Florestas Tropicais. A Banca Examinadora foi constituída pelos seguintes membros: Flávia Machado Durgante (KIT), Jochen Shongart (INPA), Flávia Regina Capellotto Costa (INPA), e tendo como suplentes os seguintes membros: Izabela Fonseca Aleixo (INPA), Rafael Leandro de Assis (ITV), Thaiane Rodrigues de Sousa (INPA). O Presidente da Banca Examinadora deu início à sessão e informou os procedimentos do exame. O aluno fez uma exposição do seu estudo e ao término foi arguido oralmente pelos membros da Comissão. Após as arguições os membros da banca se reuniram para avaliação e chegaram ao seguinte parecer:

Nome	Parecer	Assinaturas
Flávia Machado Durgante	<input checked="" type="checkbox"/> Aprovou <input type="checkbox"/> Reprovou	 Documento assinado digitalmente FLAVIA MACHADO DURGANTE Data: 29/01/2024 18:12:29-0300 Verifique em https://validar.it.gov.br
Rafael Leandro de Assis	<input checked="" type="checkbox"/> Aprovou <input type="checkbox"/> Reprovou	
Flávia Regina Capellotto Costa	<input checked="" type="checkbox"/> Aprovou <input type="checkbox"/> Reprovou	 Documento assinado digitalmente FLAVIA REGINA CAPELLOTTO COSTA Data: 29/01/2024 19:03:07-0300 Verifique em https://validar.it.gov.br
Menção:	<input type="checkbox"/> "Com Distinção" <input type="checkbox"/> "Com Louvor"	<input type="checkbox"/> "Com Distinção e Louvor"

Nada mais havendo a tratar, foi lavrada a presente Ata que, após lida e aprovada, foi assinada pela Coordenação

L925c Lozorio, Anderson

Crescimento em biomassa de árvores de dossel em florestas com lençol freático superficial no centro-sul da Amazônia / Anderson Lozorio Canal Filho; orientadora Juliana Schietti de Almeida. - Manaus : [s.l.], 2024.

2,26 MB

90p. : il. color.

Dissertação (Mestrado - Programa de Pós-Graduação em Ciências de Florestas Tropicais) - Coordenação do Programa de Pós-Graduação, INPA, 2024.

1. Anéis de crescimento. 2. Interflúvio Purus-Madeira. 3. Mudanças climáticas. I. Almeida, Juliana Schietti de. II. Título

CDD 551.6 811 3

SINOPSE

O objetivo deste estudo foi determinar como o crescimento das árvores em biomassa acima do solo (inferido a partir de anéis de crescimento) responde às variações das condições climáticas e hidroedáficas na Amazônia central-sul, onde a paisagem é dominada por florestas com lençóis freáticos superficiais. Amostramos 1012 árvores do dossel ($DAP \geq 30$ cm) distribuídas em 54 parcelas para investigar como a interação entre o regime local de precipitação e a profundidade do lençol freático influencia o crescimento médio da árvore ao longo do interflúvio Purus-Madeira. Nossos resultados indicam que as florestas com lençóis freáticos superficiais apresentam suprimento suficiente de água do solo para sustentar um crescimento médio maior da biomassa arbórea em atmosferas mais secas e de maior demanda evaporativa. Esses achados suportam a hipótese de que o sequestro de carbono em florestas com lençóis freáticos superficiais pode compensar os menores ganhos de carbono das florestas com lençóis freáticos profundos em climas mais secos na Amazônia. No entanto, uma tendência discernível de aumento dos incrementos da biomassa em profundidades moderadas de lençóis freáticos e um declínio em solos encharcados sugerem que a hidrologia local, em conjunto com o clima, molda profundamente o impacto dos efeitos climáticos na floresta.

Palavras-chave: anéis de crescimento, floresta tropical, interflúvio Purus-Madeira, mudanças climáticas

DEDICATÓRIA

Este trabalho é dedicado
aos meus queridos avós maternos –
Maria Lúcia e Wilson (*in memoriam*),
que partiram de repente e
deixaram um vazio imensurável.
Agradeço imensamente por tudo.

AGRADECIMENTOS

Primeiramente, quero expressar minha mais profunda e sincera gratidão aos meus pais, Anderson e Ana. Eles não apenas me proporcionaram acesso à uma boa educação, mas também cultivaram em mim valores nobres que fundamentaram meu crescimento como ser humano. A confiança em minhas ideias foi acompanhada de um compromisso incansável, dedicando tempo, energia e recursos para me auxiliar em cada etapa deste meu novo caminho. Reconheço que não estaria onde estou hoje sem o apoio inabalável e a orientação amorosa. Sou profundamente grato por tudo que fizeram e fazem por mim.

Agradeço imensamente à minha orientadora, Juliana Schietti (“Ju”), pela atenção e presença constantes ao longo do desenvolvimento deste projeto, ações que foram verdadeiramente essenciais. Especialmente valorizo o tempo que generosamente dedicou às nossas reuniões mensais, especialmente quando entrei no projeto completamente perdido, com pouca compreensão da complexa ecologia florestal da Amazônia. Os conselhos, sugestões de leitura e orientações não foram apenas valiosos, mas também uma luz que iluminou (e muito) o caminho. Ju personifica uma mentora inspiradora e compassiva, demonstra empatia genuína e um compromisso sincero com o bem-estar e o progresso de todos no laboratório.

Quero, também, expressar meu sincero agradecimento àqueles que desempenharam um papel fundamental no desenvolvimento desta dissertação. Começando por Lucas (“Jão”) Tameirão, que não apenas se destacou como um parceiro de campo excepcional, mas também se tornou um amigo para todas as horas. Agradeço por toda assistência com a programação em R e pelas dicas de organização das minhas planilhas. Assim como sou grato ao Dr. Pedro Pequeno pela ajuda com os scripts dos modelos lineares e por sempre estar disposto a tirar minhas intermináveis dúvidas estatísticas. Agradeço ao Dr. Jochen Schöngart pela significativa contribuição no desenvolvimento dos resultados desta pesquisa. Seu vasto conhecimento no campo da dendroecologia foi um verdadeiro alicerce para conclusão deste trabalho. Agradeço também à Dra. Flavia Costa, que acompanhou de perto o desenvolvimento do trabalho e esteve sempre presente nos debates construtivos e nas reuniões de avaliação e perspectivas dos projetos do laboratório.

Expresso uma enorme gratidão à minha companheira de vida, Sthefane Gonzaga, por todo o amor, carinho, respeito, cumplicidade e paciência ao longo desta minha fase de vida. Sei que não foi uma jornada simples, pois os momentos difíceis frequentemente me acompanharam, mas você sempre esteve ao meu lado, me apoiando e ajudando a superar qualquer batalha. Além disso, quero expressar eterna gratidão pela nossa nova família formada aqui em terras amazônicas, composta por ‘apenas’ 8 gatos (Bruce, Floki, Jack, Jinx, Kali, Kiara, Kira e Mia) e 2 cachorros (Alaska e Alma). Essas criaturas não apenas trouxeram alegria aos nossos dias, mas também encheram nossa casa com amor, companhia e muitos pelos!

Quero estender meus agradecimentos ao Instituto Nacional de Pesquisas da Amazônia (INPA) pelo apoio e estrutura que proporciona aos alunos para o desenvolvimento de suas pesquisas. Com suas bases espalhadas por grande parte da Amazônia, o INPA desempenha um papel fundamental na promoção e divulgação da ciência brasileira. Sou grato pelos encontros com incríveis pesquisadores e professores, verdadeiras lendas da ciência, que tive o privilégio de conhecer e aprender. Por fim, expresso meu agradecimento pela bolsa de auxílio concedida pelo CNPq (Conselho Nacional de Desenvolvimento Científico e Tecnológico), cujo apoio foi essencial para minha permanência em Manaus e a realização deste trabalho. Essa bolsa possibilitou minha modesta contribuição para a pesquisa e desenvolvimento da Amazônia. Um ecossistema único e de vital importância, agora mais do que nunca, em meio às mudanças climáticas sem precedentes que ameaçam a vida neste pequeno e pálido ponto azul.

RESUMO

À medida que os extremos climáticos se intensificam, há evidências de que estão a levar a um declínio na absorção e armazenamento de carbono nas florestas tropicais. No entanto, os fatores que causam a variação do crescimento nas florestas com lençóis freáticos superficiais (<5 m de profundidade) permanecem em grande parte desconhecidos e pouco se sabe sobre o comportamento médio de crescimento nestas florestas. O objetivo deste estudo foi determinar como o crescimento das árvores em biomassa acima do solo (inferido a partir de anéis de crescimento) responde às variações das condições climáticas e hidroedáficas na Amazônia centro-sul, onde a paisagem é dominada por florestas com lençóis freáticos superficiais. Amostramos 1012 árvores do dossel (pelo menos 192 espécies, 36 famílias; DAP \geq 30 cm) distribuídas em 54 parcelas de 1 ha ao longo de um transecto de 600 km para investigar como a interação entre o regime local de precipitação e a profundidade do lençol freático influencia o crescimento médio da árvore ao longo do interflúvio Purus-Madeira, tanto no nível das parcelas quanto individual. Avaliamos também se a densidade da madeira modula o crescimento das árvores sob diferentes condições hidroedáficas e climáticas. Os dados foram analisados usando modelos lineares mistos. Nossos resultados revelam variações consideráveis no incremento médio individual da biomassa, variando de 5.89 a 103.15 kg/ano, e no crescimento diamétrico, de 0.02 a 20.56 mm/ano. O incremento médio da biomassa acima do solo no nível da parcela foi de 21.87 kg/ano (\pm 3.8), enquanto o crescimento diamétrico médio foi de 3.02 mm/ano (\pm 2.01). Notavelmente, apesar de sua menor fertilidade do solo, as florestas situadas na parte central do transecto exibiram os maiores incrementos de biomassa acima do solo. Os resultados no nível das parcelas indicam maiores incrementos de biomassa onde há mais fósforo disponível. Por outro lado, níveis totais mais elevados de fósforo no solo diminuíram o crescimento das árvores nos níveis da parcela e individual, e sugerimos que isso é controlado pela dinâmica de flutuação do lençol freático. Não encontramos uma interação explícita da profundidade do lençol freático com o clima influenciando o crescimento das árvores. Entretanto, encontramos uma correlação entre a profundidade do lençol freático e os incrementos de biomassa, indicando um fornecimento suficiente de água no solo para sustentar o crescimento em condições atmosféricas mais secas e exigentes, mas um crescimento limitado da biomassa quando os níveis máximos do lençol freático atingem a superfície. Essas descobertas corroboram a hipótese de que a hidrologia local impõe limitações significativas sobre a influência dos efeitos climáticos na floresta, com possíveis implicações para os feedbacks das mudanças climáticas.

Palavras-chave: anéis de crescimento, floresta tropical, interflúvio Purus-Madeira, mudanças climáticas.

ABSTRACT

As climate extremes intensify, there is evidence that they are leading to a decline in carbon absorption and storage in tropical forests. However, the factors driving growth variation in forests with shallow water tables (<5 m depth) remain largely unknown, and little is known about average growth behavior in these forests. The aim of this study was to determine how tree growth in aboveground biomass (inferred from growth rings) responds to variations in climatic and hydroedaphic conditions in the central-southern Amazon, where the landscape is dominated by forests with shallow water tables. We sampled 1012 canopy trees (at least 192 species, 36 families; DBH \geq 30 cm) distributed across 54 1-ha plots along a 600 km transect to investigate how the interaction between local precipitation regime and water table depth influences average tree growth along the Purus-Madeira interfluve, both at the plot and individual levels. We also assessed whether wood density modulates tree growth under different hydroedaphic and climatic conditions. Data were analyzed using mixed-effects linear models. Our results reveal considerable variations in individual mean biomass increment, ranging from 5.89 to 103.15 kg/year, and in diameter growth, from 0.02 to 20.56 mm/year. The mean aboveground biomass increment at the plot level was 21.87 kg/year (\pm 3.8), while mean diameter growth was 3.02 mm/year (\pm 2.01). Remarkably, despite their lower soil fertility, forests located in the central part of the transect exhibited the highest aboveground biomass increments. Results at the plot level indicate higher biomass increments where more phosphorus is available. Conversely, higher total phosphorus levels in the soil decreased tree growth at both plot and individual levels, suggesting that this is controlled by water table fluctuation dynamics. We did not find an explicit interaction of water table depth with climate influencing tree growth. However, we did find a direct correlation between water table depth and biomass increments, suggesting sufficient soil water supply to support growth in drier and more demanding atmospheric conditions, but a constrained biomass growth where the water table maximum levels reach the surface. These findings support the hypothesis that local hydrology imposes significant constraints on the influence of forest climate effects, with potential implications for climate change feedbacks.

Keywords: climate change, growth rings Purus-Madeira interfluve, tropical forest

SUMÁRIO

ATA DE DEFESA PÚBLICA DE DISSERTAÇÃO ASSINADA	3
FICHA CATALOGRÁFICA E SINOPSE	4
DEDICATÓRIA	5
AGRADECIMENTOS	6
RESUMO	7
ABSTRACT	8
LISTA DE TABELAS	10
LISTA DE FIGURAS	11
INTRODUÇÃO GERAL	12
OBJETIVOS	17
CAPÍTULO I	18
CONCLUSÃO GERAL	45
REFERÊNCIAS	46
TABELAS	70
FIGURAS	72
MATERIAL SUPLEMENTAR	76

LISTA DE TABELAS

Capítulo I

Tabela 1 - Resumo estatístico das variáveis estudadas para 1012 árvores de dossel em 11 módulos de estudo: mínimo (Min) e máximo (Max); média e desvio padrão (SD) dos incrementos médios de biomassa acima do solo (MABI) e incrementos médios de diâmetro (MDI) ao longo de 30 anos (1979-2009), diâmetro à altura do peito (DAP), altura estimada (m), densidade da madeira (g/cm^3) e idade (em anos). A tabela apresenta dados categorizados em dois níveis: individual (em cinza) e de parcela (em branco) (35)

Tabela 2 - Resumo estatístico dos melhores modelos lineares generalizados de efeitos mistos (GLMM) para explicar a relação entre os incrementos médios de biomassa acima do solo (MABI) e variáveis ambientais: fósforo disponível (P_{avail}), fósforo total (P_{tot}), temperatura máxima (T_{max}), déficit hídrico cumulativo máximo (MCWD), déficit de pressão de vapor (VPD) e temperatura mínima (T_{min}), considerando as 54 parcelas como unidades amostrais. Apresentamos os modelos com melhor suporte de acordo com o critério de Akaike. O local ("módulo") foi considerado um efeito aleatório em todos os modelos. Os valores de R^2 marginal (R^2_{marg}) referem-se a modelos ajustados considerando apenas os efeitos fixos, enquanto o R^2 condicional (R^2_{cond}) corresponde ao modelo completo, incluindo o efeito aleatório. A contribuição relativa dos preditores é dada pelos coeficientes beta padronizados dos LMMs, e a probabilidade para cada preditor é mostrada abaixo. Valores de $p < 0.05$ são destacados em negrito. O traço indica que a variável não contribuiu para explicar o MABI no modelo. Mostrando apenas os modelos com $\Delta\text{AIC} < 2$ (39)

Tabela 3 - Resumo estatístico dos melhores modelos lineares generalizados de efeitos mistos (GLMM) para explicar a relação entre os incrementos médios de biomassa acima do solo (MABI) e variáveis ambientais: fósforo total (P_{tot}), fósforo disponível (P_{avail}), profundidade média do lençol freático (WT_{med}), profundidade máxima do lençol freático (WT_{max}) e densidade da madeira (WD), considerando os 1012 indivíduos como unidades amostrais. Aqui, apresentamos os modelos com melhor suporte de acordo com o critério de Akaike. O local, referido como "módulo", foi considerado um efeito aleatório em todos os modelos. Os valores de R^2 marginal (R^2_{marg}) referem-se a modelos ajustados considerando apenas os efeitos fixos, enquanto o R^2 condicional (R^2_{cond}) corresponde ao modelo completo, incluindo o efeito aleatório. A contribuição relativa dos preditores é dada pelos coeficientes padronizados dos LMMs. A probabilidade para cada preditor é mostrada entre parênteses. Coeficientes padronizados em negrito indicam $p < 0.05$. O traço indica que a variável não foi incluída no modelo (40)

Tabela 4 - Resumo das métricas dendrométricas em cada local investigado ao longo do interflúvio Purus-Madeira, no centro-sul da Amazônia. Identificação da parcela (Plot Id.), incrementos médios de biomassa acima do solo (MABI), incrementos médios de diâmetro (MDI) e valores médios de diâmetro à altura do peito (DAP), altura estimada (m) e densidade da madeira (g/cm^3). Valores calculados para 16 a 23 árvores de dossel amostradas em cada parcela (69)

LISTA DE FIGURAS

Capítulo 1

Figura 1 - Mapa da região interfluvial Purus-Madeira mostrando o transecto de 600 km no centro-sul da Amazônia. Os onze locais de estudo são indicados por números pretos, e cada local possui cinco parcelas de 1 hectare onde as árvores foram medidas (exceto o “módulo” 3, que possui quatro parcelas). Reproduzido com permissão de Schiatti et al., 2016 (25)

Figura 2 - Os onze locais de pesquisa (M01 - M11) estão distribuídos ao longo do transecto de aproximadamente 600 km, conforme mostrado no eixo x. Os boxplots representam a variação em: a) incremento médio de biomassa acima do solo; b) incremento médio de diâmetro (MDI); e c) densidade da madeira (WD) (36)

Figura 3 - Histogramas de frequência mostrando a frequência de distribuição e os valores médios individuais para a nossa área de estudo com florestas de lençol freático superficial (linha tracejada vermelha). a) Incremento médio de biomassa acima do solo (kg/ano); b) Incremento médio de diâmetro (mm/ano); e c) Densidade da madeira (g/cm³) (37)

Figura 4 - Regressões parciais derivadas dos modelos de regressão múltipla com maior suporte (ver Tabela 3). Incremento médio da biomassa acima do solo a nível comunitário com base em indivíduos amostrados em 54 parcelas ao longo do interflúvio Purus-Madeira. As regressões parciais foram derivadas do modelo misto de regressão múltipla usando as variáveis preditoras consideradas nos modelos selecionados para explicar a variação nas taxas médias de incremento da biomassa acima do solo (kg/ano⁻¹). Efeito parcial de: a) fósforo disponível; b) fósforo total; c) temperatura máxima; d) temperatura mínima; e) déficit hídrico cumulativo máximo (valores mais altos indicam maior déficit hídrico); e f) déficit de pressão de vapor (VPD). A linha preta representa a linha de tendência média (72)

Figura 5 - Regressões parciais derivadas dos modelos de regressão múltipla com maior suporte (ver Tabela 4). Incremento médio da biomassa acima do solo a nível individual com base em 1012 indivíduos ao longo do interflúvio Purus-Madeira. As regressões parciais foram derivadas do modelo de regressão múltipla usando as variáveis preditoras consideradas nos modelos selecionados para explicar a variação nas taxas médias de incremento da biomassa acima do solo (kg/ano⁻¹). Efeito parcial de: a) fósforo total; b) fósforo disponível; e c) densidade da madeira. A linha preta representa a linha de tendência média (74)

Figura 6 - Regressões parciais obtidas a partir do modelo de regressão múltipla com Δ AIC = 2.15. Incremento médio da biomassa acima do solo versus medições do lençol freático, considerando 1012 indivíduos ao longo do interflúvio Purus-Madeira. As regressões parciais foram derivadas do modelo de regressão múltipla usando as variáveis preditoras incluídas no modelo selecionado para elucidar a variação nas taxas médias de incremento da biomassa acima do solo (kg/ano⁻¹). Efeitos parciais de: a) nível máximo do lençol freático (m); e b) nível médio do lençol freático. A linha preta representa a linha de tendência média. Valores negativos representam níveis subsuperficiais (75)

1. INTRODUÇÃO GERAL

As florestas tropicais representam os ecossistemas mais biodiversos do mundo e são um componente essencial do ciclo global de carbono e hidrológico, contribuindo mais para o sequestro e estoques de carbono do que qualquer outro bioma no planeta (Houghton et al., 2009; Pan et al., 2011; Esquivel-Muelbert et al., 2019). Dada a sua vasta extensão (aproximadamente 6 milhões de km²), reservatórios substanciais de carbono na biomassa viva (95 a 200 pentagramas de carbono) e notável diversidade de espécies (abrangendo até 15.000 espécies de árvores), as reações das florestas amazônicas a eventos extremos estão condicionadas para impactar não apenas a bacia, mas também exercer influência sobre os climas e a biodiversidade globais (Houghton et al., 2009; Pan et al., 2011; Feldspausch et al., 2012; Ter Steege et al., 2013; Nobre et al., 2016; Esquivel-Muelbert et al., 2019; Gatti et al., 2021). As incertezas associadas ao impacto dos déficits hídricos no crescimento das plantas e no funcionamento do ecossistema são ainda mais complicadas pelo fato de que os modelos em grande escala frequentemente falham em considerar a heterogeneidade da paisagem e a variação hidrológica local, assumindo, em vez disso, que a precipitação é a única fonte de déficit hídrico, levando a uma maior imprevisibilidade (Negrón-Juárez et al., 2015; Chitra-Tarak et al., 2018; Fan et al., 2019; Roebroek et al., 2020; Liu et al., 2023). Um melhor entendimento do incremento da biomassa acima do solo e do crescimento das árvores na Amazônia, especialmente ao longo das vastas áreas úmidas interfluviais da bacia, é de grande importância para compreender como o balanço de carbono dessa região responde à variabilidade climática. Além disso, há uma lacuna notável no nosso conhecimento sobre os fatores ambientais, incluindo clima, hidrologia e condições do solo, que controlam o aumento da biomassa lenhosa acima do solo nessas florestas caracterizadas por lençóis freáticos superficiais.

As condições climáticas e edáficas afetam indiretamente os incrementos da biomassa acima do solo ao atuarem como filtros ambientais para a estruturação da comunidade e impõem limitações fisiológicas na distribuição das espécies (Quesada et al., 2012; Esquivel-Muelbert et al., 2017; Marca-Zevallos et al., 2022; Garcia et al., 2023). Condições elevadas de Déficit de Pressão de Vapor (VPD) induzem uma diminuição na condutância estomática e na fotossíntese (Barkhordarian et al., 2019; Grossiord et al., 2020; López et al., 2021), e, por fim, levam ao fechamento estomático para mitigar a perda excessiva de água em meio à demanda atmosférica elevada (Oren et al., 1999; Grossiord et al., 2020). Essa resposta defensiva se manifesta como um impacto prejudicial no crescimento, esgotando as reservas de carboidratos e induzindo a fome de carboidratos no nível tecidual (McDowell et al., 2022). Nas florestas tropicais, o aumento da temperatura também tem um impacto direto no crescimento diamétrico das árvores, induzindo o fechamento estomático devido à demanda evaporativa elevada, levando a uma redução na fotossíntese e taxas de respiração aumentadas (Clark et al., 2003; Gliniars et al., 2013; Álvarez-

Dávila et al., 2017; Vilanova et al., 2018; Sullivan et al., 2020). A biomassa é significativamente influenciada não apenas pela temperatura, mas também pela disponibilidade de água, tornando-se mais proeminente em condições de chuva intermediária. Isso ocorre devido à ausência de secas extremas e à redução da limitação de luz causada pela cobertura de nuvens durante períodos de alta precipitação em florestas não inundadas (Poorter et al., 2016; Vilanova et al., 2018). No entanto, o impacto desses fatores ambientais no crescimento das árvores não apresenta um padrão consistente e as respostas das dinâmicas florestais ao clima exibem variações entre diferentes tipos de florestas (Schöngart et al., 2010). Por exemplo, a literatura sugere que um aumento na disponibilidade de água aprimora a produção (Pereira da Silva et al., 2002; Zuidema et al., 2022), mas o comportamento oposto é observado em florestas com lençóis freáticos superficiais (Sousa et al., 2022). Com o contínuo aumento das temperaturas globais, antecipa-se uma intensificação do estresse hídrico enfrentado pelas árvores, podendo resultar em efeitos adversos na resiliência dos ecossistemas florestais.

A quantidade de água disponível no solo para o crescimento das plantas é significativamente afetada por flutuações sazonais na chuva, e como resultado, as respostas fisiológicas das árvores em florestas tropicais exibem considerável variabilidade em resposta às mudanças na disponibilidade de água (Lin et al., 2012; Stahl et al., 2012). No entanto, o armazenamento de água no solo é impactado não apenas pelos padrões de precipitação, mas também por mudanças nos níveis do lençol freático e características físicas do solo, como textura e porosidade, que afetam diretamente a retenção de água (Hodnett & Tomasella 2002; Tomasella et al., 2007). Assim, a combinação de precipitação, topografia, propriedades do solo e lençol freático influencia a disponibilidade local de água no solo, conforme indicado pela profundidade do lençol freático (Marklund, 2009). Embora exista uma extensa literatura sobre os efeitos do solo, temperatura e clima no funcionamento das florestas tropicais (e.g. Quesada et al., 2012; Esquivel-Muelbert et al., 2017; Sullivan et al., 2020), pouco se sabe sobre essa relação no que diz respeito à hidrologia local regulada pela profundidade do lençol freático. Em florestas com lençóis freáticos profundos, as condições mais secas e quentes prevalentes durante secas extremas resultam em diminuição da umidade do solo, levando a uma redução na fotossíntese e na produção primária líquida (Santos et al., 2018; Zhao & Running, 2010). No entanto, esse cenário não se aplica necessariamente a florestas com lençóis freáticos superficiais (Sousa et al., 2020; Esteban et al., 2021; Costa et al., 2023). Nestes ambientes, a saturação do solo tende a diminuir durante as secas, expandindo a janela de crescimento e, assim potencialmente, promovendo o crescimento de maneira semelhante às observações em florestas de várzea (Schöngart et al., 2004; 2005). Com base em estimativas publicadas, as regiões amplamente inexploradas da bacia amazônica com lençóis freáticos superficiais (<5 m de profundidade) variam de 47% a 64%, dependendo do

modelo utilizado para simulação do lençol freático (Miguez-Macho & Fan, 2012; reanalisado por Costa et al., 2023). Pesquisas recentes destacam o potencial dessas áreas como pontos cruciais, instigando mudanças inesperadas nas dinâmicas globais de carbono, água e energia que podem contribuir para consequências imprevistas em cenários de mudança climática (Sousa et al., 2020; Costa et al., 2023). Isso sublinha a necessidade urgente de pesquisas adicionais para desvendar as complexidades desses ambientes. Além disso, nosso entendimento do incremento de biomassa nessas florestas permanece limitado, e são esperadas variações na resposta entre as árvores às condições de umidade do solo devido à presença de espécies diversas com estratégias de vida distintas e suas interações com as propriedades locais do solo e a hidrologia.

Os fatores edáficos, incluindo a textura e a fertilidade do solo, também desempenham um papel significativo na formação da estrutura e dinâmica das florestas (Quesada et al., 2012; Ali et al., 2017; Bordin & Muller, 2019). Notavelmente, o fósforo (P) emerge como um macronutriente crítico que limita a produtividade das florestas tropicais (Lambers et al., 2022) e a disponibilidade de P é principalmente derivada do material de origem do solo (Walker & Syers, 1976; Vitousek, 1984; Silver, 1994). No entanto, ao longo de milhões de anos, o material de origem sofre uma depleção gradual, e o fósforo disponível, juntamente com cátions básicos originários de rochas podem ser esgotados por lixiviação ou inacessíveis devido à oclusão por óxidos de ferro e alumínio (Walker & Syers, 1976; Crews et al., 1995). Consequentemente, solos altamente intemperizados, como os prevalentes na Amazônia Central, contêm quantidades limitadas de fósforo inorgânico prontamente disponíveis para absorção pelas plantas (Quesada et al., 2012; Cunha et al., 2022), e essas limitações contribuem para variações na composição de espécies e traços funcionais através de diferentes gradientes climáticos (Asner et al., 2014; Schietti et al., 2016; Villa et al., 2020; Marca-Zevallos, 2022; Alves et al., 2023). Compreender os elementos multifacetados que contribuem para as variações no crescimento das árvores é crucial para decifrar como estratégias de crescimento diversas moldam a dinâmica das florestas ao longo do tempo, impactando serviços ecossistêmicos essenciais, como produção de madeira e armazenamento de carbono. Esta intrincada interação entre as características das espécies e as condições ambientais é a chave para compreender os mecanismos que governam o crescimento das árvores em ecossistemas dinâmicos, sendo particularmente relevante para locais com lençóis freáticos superficiais, que são representativos da paisagem da bacia hidrográfica, mas ainda sub-representados nas redes de parcelas permanentes de balanço de carbono (Cintra et al., 2013; Schietti et al., 2016; Costa et al., 2023).

Apesar de um progresso significativo na dendroecologia tropical, informações cruciais sobre as taxas e padrões de crescimento das árvores permanecem limitadas (Worbes 1995, 2002; Schöngart et al., 2002; Rozendaal & Zuidema 2011; Sheil et al., 2017). Questões básicas, como

a extensão do crescimento das árvores e as taxas em que ocorre, permanecem sem resposta para árvores grandes (para mais detalhes, veja Sheil et al., 2017, e referências contidas). Além disso, as florestas tropicais enfrentam ameaças crescentes ao crescimento e persistência das árvores, principalmente impulsionadas pelo agravamento de restrições abióticas, como secas amplificadas pelo aquecimento global (Phillips et al., 2009). Notavelmente, estudos predominantes frequentemente negligenciam a correlação direta entre o crescimento da biomassa e os fatores subjacentes que o influenciam no nível individual da árvore. Em vez disso, eles se concentram predominantemente no desempenho agregado e nas características das espécies em média (por exemplo, Poorter & Bongers 2006; Wright et al., 2010). Uma vez que os indivíduos são as entidades que respondem aos gradientes ambientais, não as espécies (Clark et al., 2011), o desempenho das árvores do dossel, específico para cada espécie, pode ser influenciado por características de história de vida específicas da espécie que facilitam sua persistência no sub-bosque e eventual ascensão ao dossel. No entanto, é crucial reconhecer a considerável variação entre os indivíduos (Paine et al., 2011; Thomas et al., 2013), o que tem significado para seu desempenho ecológico e contribuições para o crescimento da população (Violle et al., 2007; Zuidema et al., 2009). Portanto, aprofundar-se em análises no nível individual da árvore pode fornecer informações valiosas sobre os determinantes subjacentes do crescimento das árvores (Binkley et al., 2010; Clark et al., 2011; Sterck et al., 2011; van der Sande et al., 2015).

Para compreender as diversas respostas dentro das florestas com regimes hidrológicos de lençóis freáticos superficiais, é crucial examinar árvores com diferentes taxas de crescimento e variados investimentos na construção de madeira. A densidade da madeira (DM) está diretamente ligada a vários aspectos da forma e função das plantas e desempenha um papel vital no refinamento das estimativas de biomassa em florestas amazônicas (Cornelissen et al., 2003; Nogueira et al., 2006, 2008; Fearnside, 2007; Chave et al., 2008, 2014). Variações na dinâmica espacial regional das florestas amazônicas têm sido associadas à variabilidade da densidade da madeira. Florestas com DM mais baixa na Amazônia ocidental exibem taxas elevadas de mortalidade e rápida rotatividade, enquanto a Amazônia central e oriental apresenta florestas com DM mais alta e menor mortalidade (Chao et al., 2008; Quesada et al., 2012). No entanto, a saturação do solo ou inundações, que tendem a limitar o crescimento, podem selecionar árvores de menor densidade de madeira (Cosme et al., 2017, Fontes et al., 2020). Condições ambientais menos favoráveis ao crescimento de espécies tropicais, caracterizadas por temperaturas baixas, déficit hídrico e solos menos férteis, geralmente estão correlacionadas com densidades de madeira mais altas. São nesses locais que as atividades cambiais e fisiológicas das plantas são reduzidas (Baker et al., 2004; Muller-Landau, 2004; Bergès et al., 2008). Em contraste, ambientes favoráveis ao crescimento, com temperaturas mais altas, grande disponibilidade de água e solos

férteis, estão associados a menores densidades de madeira (Baker et al., 2004; Muller-Landau, 2004; Quesada et al., 2012). Dado o conhecimento sobre variações nas propriedades da madeira nas taxas de crescimento individuais e entre grupos funcionais ao longo de gradientes de disponibilidade de água, parece razoável esperar que diferentes combinações de fatores hidroedáficos e climáticos levem a respostas diferentes no crescimento médio da árvore, indicando, assim, sensibilidades variadas da floresta às mudanças climáticas.

Neste estudo, examinamos a influência do clima, solo e profundidade do lençol freático no incremento médio da biomassa acima do solo de árvores do dossel com densidades de madeira diversas. Para entender os padrões de crescimento anual médio de árvores grandes (diâmetro acima de 30 cm) em florestas com lençóis freáticos superficiais, utilizamos uma rede de cinquenta e quatro parcelas distribuídas em locais de pesquisa ao longo de um transecto de 600 km em uma região de lençol freático superficial na Amazônia centro-sul. Abordamos duas questões centrais: (1) Como a interação entre a profundidade do lençol freático e a precipitação local influencia o incremento médio da biomassa acima do solo em árvores grandes?, e (2) A densidade da madeira modula o crescimento das árvores sob diferentes condições hidroedáficas e climáticas? Nossa previsão é que a disponibilidade de água no solo (ou seja, profundidade do lençol freático, LF) será o principal fator explicando as variadas respostas nas taxas médias de crescimento das árvores. O momento do período de crescimento mais favorável variará entre diferentes locais com base no conteúdo de água do solo. Solos saturados (LF mais superficial) podem limitar o crescimento das plantas, enquanto uma combinação de um lençol freático superficial em um clima mais seco e um lençol freático mais profundo em um clima úmido pode mitigar os déficits hídricos e levar a taxas de crescimento mais altas. Sob condições ótimas (chuva moderada, profundidade média do lençol freático, maiores concentrações de fósforo), espécies com madeiras mais leves devem exibir taxas de crescimento mais altas e incrementos de biomassa aumentados. Em condições de baixo oxigênio (altas taxas de precipitação, lençol freático superficial), hipotetizamos que não haverá diferença nas taxas de crescimento da biomassa de árvores com diferentes densidades de madeira. Também esperamos padrões de crescimento distintos entre várias classes de densidade da madeira, onde a disponibilidade nutricional elevada nos solos está pronta para impulsionar aumentos mais significativos nas categorias de madeira mais leves, resultando em taxas de crescimento mais altas.

2. OBJETIVOS

2.1 OBJETIVO GERAL

Compreender a influência das condições climáticas locais, das propriedades do solo e da profundidade do lençol freático no incremento médio em biomassa acima do solo em árvores de dossel (> 30 cm DAP) na região do interflúvio Purus-Madeira, centro-sul da Amazônia.

2.2 OBJETIVOS ESPECÍFICOS

1. Investigar como a interação entre a precipitação local e a profundidade do lençol freático afeta o crescimento médio das árvores ao longo do Interflúvio Purus-Madeira.
2. Avaliar se a densidade da madeira modula o crescimento das árvores nas diferentes condições hidroedáficas e climáticas locais.

CAPÍTULO 1

Biomass growth of canopy trees in shallow water table forests in central-southern Amazonia

Manuscrito em preparação para Journal of Ecology

Abstract

1. As climate extremes intensify, there is evidence that they are leading to a decline in carbon absorption and storage in tropical forests. However, the factors causing variation in the growth in forests with shallow water tables (<5m depth), remain largely unknown, and little is known about the average growth behaviour in these forests.
2. Our aim was to determine how tree growth in aboveground biomass (inferred from growth rings) responds to variations of hydroclimatic and edaphic conditions in the central-southern Amazon, where landscape is dominated by shallow water table (WT) forests. We sampled 1012 canopy trees (at least 192 species, 36 families; dbh \geq 30 cm) distributed across 54 1-ha plots along a 600 km transect to investigate how the interaction between local precipitation regime and water table depth influences the average tree growth along the Purus-Madeira interfluve at the community and individual levels. We also assessed whether wood density modulates tree growth under different hydro-edaphic and climatic conditions. We analysed the data using linear mixed models.
3. Results at the community level indicate higher biomass increments where there is more available phosphorus. Conversely, higher total soil phosphorus decreased tree biomass growth at the community and individual levels and we suggest this is controlled by WT fluctuation dynamics. We did not find an explicit interaction of the water table depth with climate influencing tree biomass growth. However, the mean and the maximum WT level directly influenced biomass increments. These results indicate sufficient soil water supply (higher mean WT level) supports more growth independent of drier or more demanding atmospheric conditions, but where the WT maximum levels reach the surface biomass growth is decreased. Wood density was important only at the individual level and unexpectedly, trees with higher wood densities exhibited the highest increment rates. We suggest this can be related to xylem allocation patterns in shallow WT forests but this needs further investigation.
4. *Synthesis: Higher tree biomass growth rates in shallow water table forests of central-southern Amazonia are sustained by higher P availability and higher mean WT levels, independent of climate. However, biomass growth is limited where the WT maximum*

levels reach the surface, leading to soil waterlogging and flooding. These findings support the hypothesis that local hydrology in shallow WT forests may impose significant constraints on the negative effects of drier climates.

Key words: *climate change, growth rings Purus-Madeira interfluve, tropical forest*

1. INTRODUCTION

Tropical forests represent the world's most biodiverse ecosystems and are an essential component of the global carbon and hydrological cycles, contributing more to carbon sequestration and stocks than any other biome on the planet (Houghton et al., 2009; Pan et al., 2011; Esquivel-Muelbert et al., 2019). Given their vast expanse (approximately 6 million km²), substantial carbon reservoirs in live biomass (95 to 200 petagrams of carbon), and remarkable species diversity (encompassing up to 15,000 tree species), the reactions of the Amazonian forests to extreme events are poised to impact not only the basin but also exert influence on global climates and biodiversity (Houghton et al., 2009; Pan et al., 2011; Feldspausch et al., 2012; Ter Steege et al., 2013; Nobre et al., 2016; Esquivel-Muelbert et al., 2019; Gatti et al., 2021). Uncertainties associated with the impact of water deficits on plant growth and ecosystem functioning are further complicated by the fact that large-scale models often fail to consider landscape heterogeneity and local hydrological variation, assuming instead that precipitation is the sole source of water deficit, leading to increased unpredictability (Negrón-Juárez et al., 2015; Chitra-Tarak et al., 2018; Fan et al., 2019; Roebroek et al., 2020; Liu et al., 2023). A better understanding of above-ground biomass increment and tree growth in the Amazon, especially across the vast interfluvial wetland areas of the basin, is crucial for comprehending how the carbon balance in this region responds to climatic variability. Additionally, there is a notable gap in our knowledge regarding environmental factors, including climate, hydrology, and soil conditions, that control the increase in above-ground woody biomass in these forests characterized by shallow water tables.

Climate and soil conditions indirectly impact above-ground biomass increments by acting as environmental filters for community structure and imposing physiological limitations on species distribution (Quesada et al., 2012; Esquivel-Muelbert et al., 2017; Marca-Zevallos et al., 2022; Garcia et al., 2023). Elevated Vapor Pressure Deficit (VPD) conditions lead to a reduction in stomatal conductance and photosynthesis (Barkhordarian et al., 2019; Grossiord et al., 2020; López et al., 2021), ultimately resulting in stomatal closure to mitigate excessive water loss amid high atmospheric demand (Oren et al., 1999; Grossiord et al., 2020). This defensive response manifests as a detrimental impact on growth, depleting carbohydrate reserves and inducing tissue-

level carbohydrate starvation (McDowell et al., 2022). In tropical forests, temperature increase also has a direct impact on tree diameter growth, inducing stomatal closure due to high evaporative demand, leading to reduced photosynthesis and increased respiration rates (Clark et al., 2003; Gliniars et al., 2013; Álvarez-Dávila et al., 2017; Vilanova et al., 2018; Sullivan et al., 2020). Biomass is significantly influenced not only by temperature but also by water availability, becoming more prominent under intermediate rainfall conditions. This is due to the absence of extreme droughts and reduced light limitation caused by cloud cover during periods of high precipitation in non-flooded forests (Poorter et al., 2016; Vilanova et al., 2018). However, the impact of these environmental factors on tree growth does not exhibit a consistent pattern, and forest dynamics responses to climate show variations among different forest types (Schöngart et al., 2010). For instance, the literature suggests that an increase in water availability enhances production (Pereira da Silva et al., 2002; Zuidema et al., 2022), but the opposite behavior is observed in forests with shallow water tables (Sousa et al., 2022). With the continuous increase in global temperatures, an intensification of water stress faced by trees is anticipated, potentially resulting in adverse effects on the resilience of forest ecosystems.

The amount of water available in the soil for plant growth is significantly affected by seasonal fluctuations in rainfall, leading to considerable variability in the physiological responses of trees in tropical forests to changes in water availability (Lin et al., 2012; Stahl et al., 2012). However, soil water storage is impacted not only by precipitation patterns but also by changes in groundwater levels and physical soil characteristics, such as texture and porosity, directly influencing water retention (Hodnett & Tomasella 2002; Tomasella et al., 2007). Therefore, the combination of precipitation, topography, soil properties, and groundwater level influences the local soil water availability, as indicated by the groundwater depth (Marklund, 2009). While there is extensive literature on the effects of soil, temperature, and climate on the functioning of tropical forests (e.g., Quesada et al., 2012; Esquivel-Muelbert et al., 2017; Sullivan et al., 2020), little is known about this relationship concerning local hydrology regulated by groundwater depth. In forests with deep water tables, drier and warmer conditions prevalent during extreme droughts result in soil moisture reduction, leading to a decrease in photosynthesis and net primary production (Santos et al., 2018; Zhao & Running, 2010). However, this scenario does not necessarily apply to forests with shallow water tables (Sousa et al., 2020; Esteban et al., 2021; Costa et al., 2023). In these environments, soil saturation tends to decrease during droughts, expanding the growth window and potentially promoting growth similarly to observations in floodplain forests (Schöngart et al., 2004; 2005). Based on published estimates, the widely unexplored regions of the Amazon basin with shallow water tables (<5 m deep) range from 47% to 64%, depending on the model used for groundwater simulation (Miguez-Macho & Fan, 2012; reanalyzed by Costa et al., 2023). Recent research highlights the potential of these areas as crucial

points, triggering unexpected changes in global carbon, water, and energy dynamics that may contribute to unforeseen consequences in climate change scenarios (Sousa et al., 2020; Costa et al., 2023). This underscores the urgent need for further research to unravel the complexities of these environments. Additionally, our understanding of biomass increment in these forests remains limited, and variations in tree responses to soil moisture conditions are expected due to the presence of diverse species with distinct life strategies and their interactions with local soil properties and hydrology.

Edaphic factors, including soil texture and fertility, also play a significant role in shaping the structure and dynamics of forests (Quesada et al., 2012; Ali et al., 2017; Bordin & Muller, 2019). Particularly, phosphorus (P) emerges as a critical macronutrient limiting the productivity of tropical forests (Lambers et al., 2022), and P availability is mainly derived from the soil parent material (Walker & Syers, 1976; Vitousek, 1984; Silver, 1994). However, over millions of years, the parent material undergoes gradual depletion, and available phosphorus, along with basic cations originating from rocks, can be leached or rendered inaccessible due to occlusion by iron and aluminum oxides (Walker & Syers, 1976; Crews et al., 1995). Consequently, highly weathered soils, such as those prevalent in Central Amazonia, contain limited amounts of readily available inorganic phosphorus for plant uptake (Quesada et al., 2012; Cunha et al., 2022), and these limitations contribute to variations in species composition and functional traits across different climatic gradients (Asner et al., 2014; Schiatti et al., 2016; Villa et al., 2020; Marca-Zevallos, 2022; Alves et al., 2023). Understanding the multifaceted elements contributing to variations in tree growth is crucial for deciphering how diverse growth strategies shape forest dynamics over time, impacting essential ecosystem services such as wood production and carbon storage. This intricate interaction between species characteristics and environmental conditions is key to comprehending the mechanisms governing tree growth in dynamic ecosystems, particularly relevant for sites with shallow water tables, representative of the watershed landscape but still underrepresented in permanent carbon balance plot networks (Cintra et al., 2013; Schiatti et al., 2016; Costa et al., 2023).

Despite significant progress in tropical dendroecology, crucial information about tree growth rates and patterns remains limited (Worbes 1995, 2002; Schöngart et al., 2002; Rozendaal & Zuidema 2011; Sheil et al., 2017). Fundamental questions, such as the extent and rates of tree growth, remain unanswered for large trees (for more details, see Sheil et al., 2017, and the references therein). Furthermore, tropical forests face increasing threats to tree growth and persistence, primarily driven by worsening abiotic constraints, such as droughts amplified by global warming (Phillips et al., 2009). Remarkably, predominant studies often overlook the direct correlation between biomass growth and the underlying factors influencing it at the individual

tree level. Instead, they predominantly focus on aggregate performance and species-level characteristics (e.g., Poorter & Bongers 2006; Wright et al., 2010). Since individuals, not species, respond to environmental gradients (Clark et al., 2011), canopy tree performance, specific to each species, may be influenced by species-specific life history traits facilitating their persistence in the understory and eventual ascent to the canopy. However, it is crucial to recognize the considerable variation among individuals (Paine et al., 2011; Thomas et al., 2013), which holds significance for their ecological performance and contributions to population growth (Violle et al., 2007; Zuidema et al., 2009). Therefore, delving into individual tree-level analyses can provide valuable insights into the underlying determinants of tree growth (Binkley et al., 2010; Clark et al., 2011; Sterck et al., 2011; van der Sande et al., 2015).

To comprehend the diverse responses within forests with shallow groundwater regimes, it is crucial to examine trees with varying growth rates and different investments in wood construction. Wood density (WD) is directly linked to various aspects of plant form and function, playing a vital role in refining biomass estimates in Amazonian forests (Cornelissen et al., 2003; Nogueira et al., 2006, 2008; Fearnside, 2007; Chave et al., 2008, 2014). Variations in the regional spatial dynamics of Amazonian forests have been associated with wood density variability. Western Amazon forests with lower WD exhibit high mortality rates and rapid turnover, while central and eastern Amazon forests have higher WD and lower mortality (Chao et al., 2008; Quesada et al., 2012). However, soil saturation or flooding, which tends to limit growth, may select for trees with lower wood density (Cosme et al., 2017, Fontes et al., 2020). Less favorable environmental conditions for tropical species growth, characterized by low temperatures, water deficit, and less fertile soils, are generally correlated with higher wood densities. In these locations, plant cambial and physiological activities are typically reduced (Baker et al., 2004; Muller-Landau, 2004; Bergès et al., 2008). In contrast, growth-friendly environments with higher temperatures, ample water availability, and fertile soils are associated with lower wood densities (Baker et al., 2004; Muller-Landau, 2004; Quesada et al., 2012). Given the understanding of wood property variations in individual growth rates and among functional groups along water availability gradients, it seems reasonable to expect that different combinations of hydro-edaphic and climatic factors will lead to diverse responses in average tree growth, indicating varied sensitivities of the forest to climate changes.

In this study, we examined the influence of climate, soil, and groundwater depth on the average aboveground biomass increment of canopy trees with various wood densities. To understand the patterns of average annual growth of large trees (diameter above 30 cm) in forests with shallow groundwater, we utilized a network of fifty-four plots distributed across research sites along a 600 km transect in a shallow groundwater region in central-southern Amazon. We

addressed two central questions: (1) How does the interaction between groundwater depth and local precipitation influence the average aboveground biomass increment in large trees?, and (2) Does wood density modulate tree growth under different hydro-edaphic and climatic conditions? Our prediction is that soil water availability (i.e., water table depth, WT) will be the primary factor explaining varied responses in average tree growth rates. The timing of the most favorable growth period will vary between different locations based on soil water content. Saturated soils (shallow WT) may limit plant growth, while a combination of shallow WT in drier climates and deeper WT in wetter climates may alleviate water deficits and lead to higher growth rates. Under optimal conditions (moderate rainfall, medium WT depth, higher phosphorus concentrations), species with lighter wood should exhibit higher growth rates and increased biomass increments. Under low oxygen conditions (high precipitation rates, shallow WT), we hypothesize no difference in biomass growth rates among trees with different wood densities. We also anticipate distinct growth patterns among various wood density classes, where elevated nutrient availability in soils is poised to drive more substantial increases in lighter wood categories, resulting in higher growth rates.

2. METHODS

2.1. Study area

The study was carried out along an approximately 600 km transect in the south of the Amazon River in Central Amazonia, between the Purus and Madeira Rivers (Fig. 1). The region lies along the BR-319 highway, which connects Manaus to Porto Velho, the capitals of the Amazonas and Rondônia states, respectively and has been largely abandoned for regular traffic since the 1970s (Fearnside, 2018). In this area, the mean annual precipitation varies from 2100–2700 mm (Hijmans et al. 2005) with the number of consecutive months with less than a 100 mm of precipitation (that is generally considered an indicator of the dry season) varying from one month in the north of the transect to four months per year in the south (Sombroek, 2000). The climate of the interfluvium is defined as Am (humid tropical) according to the Köppen classification, but it differs along the interfluvium, mainly by the intensification of dry months in the southern region of the interfluvium (RadamBrasil, 1978; Peel et al. 2007). The average monthly temperatures range from minimum of 24–26°C to maximum of 28°C (Salati & Vose, 1984; Junk & Piedade, 2020).

The Purus-Madeira interfluvial region is characterised by its relatively recent geological origin, consisting of unstable sediments from the Late Pleistocene or Early Holocene (Sombroek, 2000). Topography is generally flat (different from the dissected relief of Manaus region) with

elevation above sea level varying from 30–80 m over large distances (estimated by Shuttle Radar Topography Mission - SRTM data) (Rodríguez et al. 2006). This region is part of the Amazon basin's "loamy plains" (Sombroek, 2000), which cover approximately 11% of the entire basin. Dense Ombrophilous Lowland Forest is the predominant vegetation type in the north of the interfluvium, covering about 68% of the total region, while in the south there is a transition to more open lowland areas, with higher predominance of palm trees, probably due to increased rainfall seasonality (RadamBrasil, 1978; Sombroek, 2000; Junk & Piedade, 2020).

During the rainy season, large areas of the interfluvial region become waterlogged, and many small streams dry up during the dry season. The water table remains shallow, usually within 7 metres of the surface throughout the year, although certain areas may experience short-term flooding with water levels reaching approximately 50 centimetres (Moulatlet et al. 2014; J. Schietti et al. 2016). The predominant soil type for the whole interfluvial region is Plinthosols and Gleysols, the predominant texture is silt to fine sand, with poor drainage, low phosphorus availability and varying degrees of soil water saturation and anoxic conditions (Quesada et al. 2011; Martins et al. 2015). On a local scale, variations in the topography of a few metres create temporary pools on the lower and poorly drained areas during the rainy season and the soil physical structure is generally dense and restrictive to root growth (Rosetti et al. 2005; Quesada et al. 2011). Assuming that the water regime on the ground influences the distribution of trees, the species composition is variable and dependent on the frequency of hydro-geomorphological disturbances along the interfluvium (Marca-Zevallos, 2022; Costa et al., 2023).

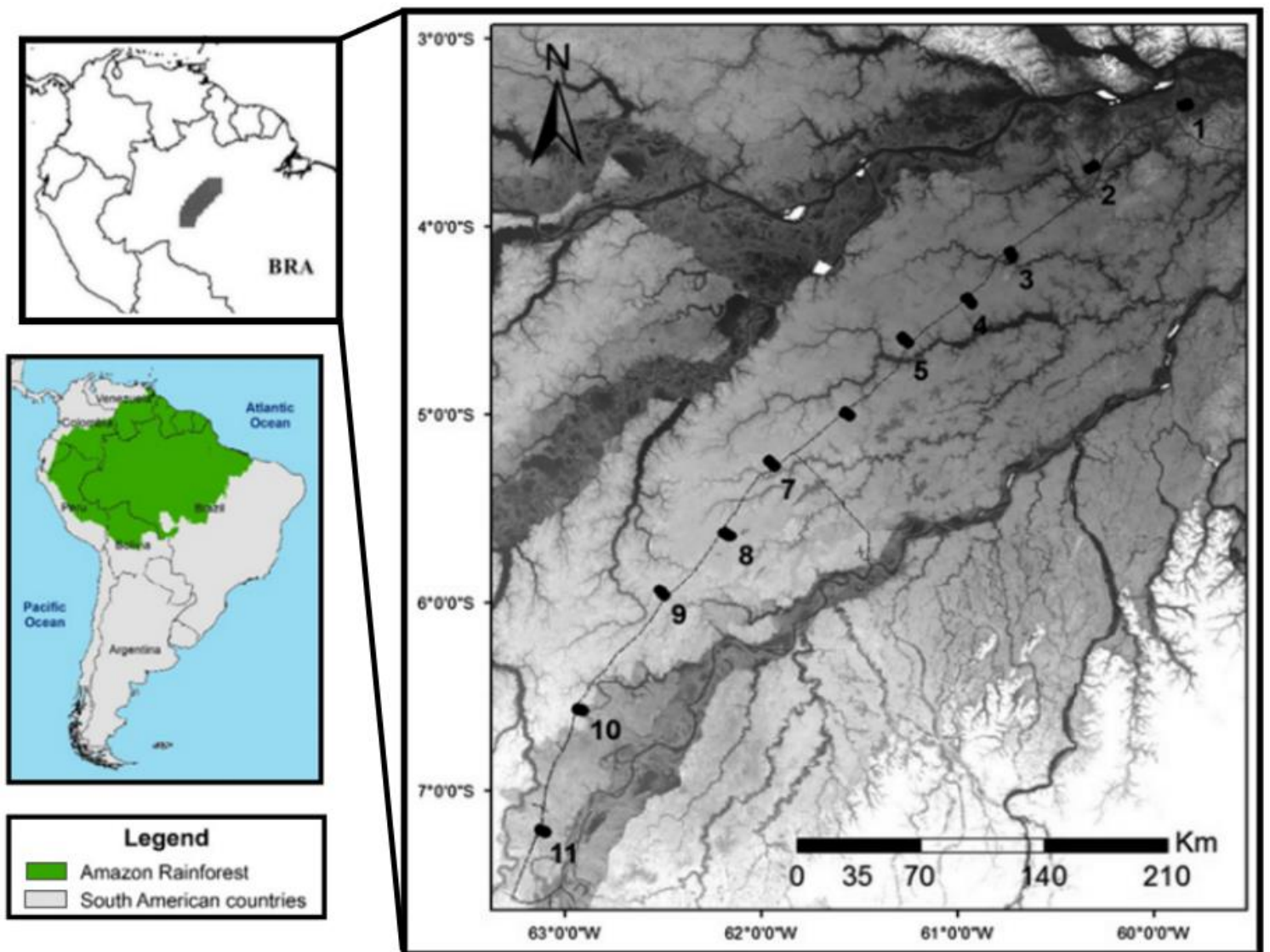


Figure 1. Map of the Purus-Madeira interfluvial area showing the 600 km transect in central southern Amazonia. The eleven study sites are indicated by black numbers and each site has five 1ha plots where trees were measured (except for Site 3 which has four plots). Reproduced with the permission from Schiatti et al., 2016.

2.2. Sampling design

The study was conducted using wood samples collected between 2009 and 2011 in 54 plots of 1ha each (250 m X 40 m) along the 600 km transect in the Purus-Madeira interfluve, in central southern Amazonia. Plots were distributed along the BR-319 highway approximately every 60 km from each other, at eleven research sites (modules) that are part of the Brazilian Program for Biodiversity Research (PPBio) network. At each site, a total of 5 plots were systematically distributed along a 5-km trail that originated from the highway, except for site “M3”, where only four plots were sampled (Figure 1). The plots were placed at a 1 km distance from each other, and with a minimum of 1 km distance from the highway to avoid secondary forests. Each plot follows a terrain contour line (topographical isocline), which keeps soil and hydrological properties less variable within a plot than between plots (RAPELD system, Magnusson et al., 2005). This method was designed to minimise altitudinal variation within plots, increasing the precision of estimates of predictor variables.

Approximately 1,100 trees distributed across the 54 study plots (18 - 23 trees/plot) had their trunk sampled for tree ring measurements, wood density and estimates of the average increment rates (Schietti et al. 2016). All sampled trees had diameter at breast height DBH \geq 30 cm and were randomly selected along each plot. After carefully curating the data, a comprehensive analysis was conducted on a total of 1012 individuals. Among them, 517 individuals (approximately 51.07% of the total) were identified up to the family level, representing 36 different botanical families. Additionally, 493 individuals were identified up to the species level, resulting in the identification of 192 distinct species. The most abundant species sampled included *Scleronema micranthum* (5% of identified individuals), *Eperua purpurea* (5%), *Brosimum utile* (4%), *Chrysophyllum sanguinolentum* (4%) and *Licania oblongifolia* (3%). Notably, *Scleronema micranthum*, *Brosimum utile* and *Chrysophyllum sanguinolentum* already have proven annual rings (Zuidema et al., 2012). The top five botanical families in descending order were: Fabaceae (20.08%), Sapotaceae (13.79%), Moraceae (about 11.76%), Chrysobalanaceae (8.72%), and Malvaceae (6.28%). Notably, these five families together represent approximately 60% of the total identified individuals.

2.3. Environmental data

2.3.1 Climate variables

The environmental variables considered in this study served as indicators for local-scale hydrological conditions and soil fertility. To capture the seasonality and local variability of climatic variables, such as temperature (°C), precipitation (mm/year¹), and vapour pressure deficit

(VPD), we utilised data from TerraClimate, an open-source global network database. This dataset provided high spatial resolution ($1/24^\circ$) with a pixel size of approximately 4km and covered a monthly time series from 1958 to 2020. TerraClimate climatological variables were derived by interpolating high-resolution data from the WorldClim dataset, combined with temporal data from the Climatic Research Unit (CRU) (Harris et al., 2014; Abatzoglou et al., 2018). This data integration approach improves the reliability and reduces the mean absolute error by validating the information against conventional weather stations.

To examine the impact of the average hydrological conditions on tree growth, we analysed a dataset comprising 360 monthly values (1979 - 2009) of cumulative water deficit (CWD) and cumulative water excess (CWE). These variables were computed using the methodology described in the study by Aragão et al. (2007) for CWD and Esteban et al. (2021) for CWE. For the calculation of CWD, we considered a constant moist tropical canopies' evapotranspiration rate of 100 mm and subtracted this value from the monthly rainfall values (Shuttleworth, 1988; Rocha et al., 2004). The CWD was calculated based on consecutive months that recorded a deficit in each hydrological year. If, at any point during a deficit computation, the following month experienced precipitation exceeding 100 mm, the cumulative CWD for that month is reset to zero. This process enabled us to determine the maximum cumulative water deficit (MCWD), which corresponded to the maximum value of the monthly accumulated climatic water deficit reached in each location (i.e., the difference between precipitation and evapotranspiration within each hydrological year; Muelbert et al., 2018). In essence, MCWD is an annual water deficit metric that considers both the duration and intensity of the dry season solely based on climatic variables, disregarding soil/groundwater properties. This deficit is determined by calculating the difference between precipitation (P) and evapotranspiration (E) for each month (n), and water deficit (WD) is quantified as:

$$\begin{aligned} &\text{if } WD_{n-1} - E_n + P_n < 0; \\ &\text{then } WD_n = WD_{n-1} - E_n + P_n; \\ &\text{else } WD_n = 0. \end{aligned}$$

The computation of MCWD doesn't strictly adhere to the calendar year. Consequently, the initial point, when $n = 1$, was determined climatologically as the wettest month in the first year of the time series (i.e., 1979), instead of the first month of that calendar year (following Muelbert et al., 2018). A more negative MCWD value indicated a higher degree of water deficit severity. Following the inverse logic of CWD, we calculated monthly CWE, to express the intensity of water excess. We calculated the MCWE values by accumulating the cumulative water excess (CWE) from the previous months, utilising the same approach. For each plot we calculated

an average MCWD and MCWE over the time series of precipitation between 1979 to 2009. Furthermore, when evaluating temperature anomalies represented by daily maximum and minimum temperatures for a given month, we averaged the highest and lowest temperatures for each year within the plots and then calculated the overall average across the entire historical series.

2.3.2 Water table depth (WTD)

In each of the 54 study plots along BR-319 highway piezometers with up to 7 m deep were installed in the soil in the period 2009/2010. Nine groundwater depth measurement campaigns were conducted between the months of August 2010 and March 2013, and the water table depth (WTD) was manually monitored three times per year (at highest and lowest levels). In order to assess the availability of belowground water resources and its impact on the overall hydrological conditions, we conducted an evaluation of maximum and minimum levels, fluctuation range, average and standard deviation of the water table depth (WTD) across all plots. The measurements of WTD provide valuable insights into the dynamics of water and its accessibility for plant roots, contributing to a comprehensive understanding of the local hydrological environment. Although the hydrological variables would be more correctly described by WTD values measured along the full census period, this temporal data is not available. However, the seasonal fluctuation of WTD in each plot is relatively similar across years (Sousa et al. 2020), meaning that we can use these average values of WTD, that is indicative of the potential hydrological conditions experienced by the trees.

2.3.3 Soil data

Phosphorus (P) has been identified as the most important nutrient for biomass production in Amazonian forests (Quesada et al. 2012; Cunha et al. 2022) and was also important in explaining the biomass stocks in the study area (Schietti et al. 2016). Thus, as an indicator of soil fertility, available phosphorus content was evaluated in compound topsoil samples, using the Mehlich-1 protocol (Embrapa, 2011). We also incorporated the soil concentration of exchangeable base cations ($\text{Ca}^{2+} + \text{Mg}^{2+} + \text{K}^{+}$) as a proxy of soil fertility.

In the laboratory, the collected samples were dried at ambient temperature and compound samples derived from six subsamples from the first 30 cm depth of the soil collected along the transect centerline in each of the 54 plots were prepared, resulting in a single sample per plot (Schietti et al., 2016). Despite being recognized as a crucial limiting nutrient for growth in tropical forests, the availability of total phosphorus was not measured for all plots. In this manner, for the plots lacking data, we compute the average of the corresponding site where the missing plots were

located, namely: *M1_TN_4500*, *M2_TN_0500*, *M2_TN_1500*, *M03_TS_0500*, *M03_TS_2500*, *M04_TN_(-)0500*, and *M07_TS_1500*.

We also incorporated a measure of physical soil constraints, as established by Quesada et al. (2010), to assess the extent of limitations imposed by the soil. This evaluation was conducted through the examination of two metre deep pits at each research site, as well as soil-profile samples collected from all plots (Martins et al. 2015). The index utilised in this assessment is based on factors such as soil effective depth, soil structure, anoxic conditions, and topography, providing a semi-quantitative measure. By summing the scores obtained for each category of soil constraints, we calculated the Index 1, which ranges from 0 to 16, indicating the degree of physical limitations imposed by the soil (Table 2 from Quesada et al. 2010).

2.4 Vegetation data

2.4.1 Collecting Wood Samples

In the 54 plots, cylindrical samples were extracted non-destructively from ~1100 individuals (DBH \geq 30 cm / 18 - 23 trees/plot) using the increment borer of 5.15 mm of diameter, as specified in the RAINFOR field manual to measure wood density in tropical forest trees (https://rainfor.org/wp-content/uploads/sites/129/2022/06/wood_density_english1.pdf). Most diameters were measured at 1.20 m above ground, avoiding the diameter measurement point of the trees (DBH = 1.30 m). The exceptions being when the tree individual had buttress roots or other challenges (e.g. bifurcated trees). Wood samples were glued on a support and then sanded and polished with sandpaper following a progressive sequence from G 100 up to G 600 grain and destined for the estimation of radial increment rates.

2.4.2 Biomass increment rates

Despite prior beliefs in consistently favourable growth conditions hindering annual ring formation in tropical environments (Lieberman et al., 1985; Whitmore, 1998), pioneering studies by Coster (1927) and others, using stable and radioactive carbon isotope dating, cambial activity measurements, and direct ring counting, revealed annual rings in tropical trees (Worbes, 2002; Rozendaal & Zuidema, 2011; Zuidema et al., 2012). Tropical dendrochronology revealed ring formation during adverse conditions when trees undergo cambial dormancy, such as in dry seasons or flooding periods (Worbes, 1999; Schöngart et al., 2002). The application of tree-ring data has recently proven successful in estimating wood biomass productivity across various forest types, including the central Amazon Basin where annual tree rings are present (Stadtler, 2007; Oliveira, 2010; Schöngart et al., 2010; Cintra et al., 2013).

The estimate of tree increment rates were based on the width of the growth rings obtained by the analysis of cylindrical samples extracted non-destructively from the trunk of the selected trees. The sampling was conducted to reach the trunk centre (pith). The samples glued on a wooden support were polished and sanded, until it was possible to identify and mark the growth rings in a stereo-microscope. The marked rings were then measured with a digital measuring device (LinTab) with 0.01 mm precision, which was attached to a computer with the software Time Series Analysis and Presentation (TSAP-WIN) to determine mean radial increments (Schöngart et al. 2004). Each ring was dated based on the last formed ring and the year of the sample collection. The wood samples were analysed at the Dendroecological Laboratory, housed within the National Institute for Amazon Research (INPA) in Manaus.

A sequential calculation of tree diameter was conducted to determine the diameter of each tree in the previous years before the wood sampling. For that, we used the annual increment in diameter (radial increment x 2) obtained from ring width measurements and the diameter of the tree at the time of fieldwork collection. This calculation assumes that the growth rings are annual. Based on the estimated diameter of the tree in different years, the biomass of the individual in each year and therefore the annual rate of increment in individual biomass was calculated. In this sense, tree-ring analyses were used to obtain estimates for the average diameter increment, that have been successfully applied to estimates of wood productivity in different forest types in Central Amazonia (Oliveira, 2010; Schöngart et al. 2010, Cintra et al. 2013; Worbes et al. 2019). Two levels of tree growth assessment were performed: (i) the mean increment of the plot (with the average of all trees sampled in a plot as the sampling unit), and (ii) the mean individual increment (where each tree will be a sample unit). In order to minimise the effects of ontogenetic changes on mean growth rates, only the last 30 years (1979-2009) of increment, identified through the growth rings, of the evaluated trees were considered in the analyses.

As there are no allometric models for biomass estimation available for the forest types in this study, we opted for a pantropical allometric model that uses diameter (D, in centimetres), wood density (ρ , in g cm³), and tree height (H, in metres) as independent parameters to improve the quality of above-ground biomass estimates (Chave et al. 2014). In this way, it is possible to reduce any biases caused by possible differences in tree height and wood density between the sites, which can be expected over large distances due to changes in the type of vegetation between the northern and southern regions of the interfluve (Chave et al. 2008, 2014; Nogueira et al. 2008; Feldpausch et al. 2011).

$$\textit{Tree biomass} = 0.0673 \times (\rho D^2 H)^{0.976}$$

Tree height was estimated using D-H allometric equations adjusted for each of the 11 research sites along the transect (Schietti et al. 2016). H-D models were adjusted using power functions ($H = b \cdot D^a$). Where (b) is the allometric constant and (a) scaling exponent (Table S1 from Schietti et al., 2016).

2.4.3 Wood density

Wood density (g/cm^3) was determined using a second wood sample obtained from approximately 20 trees selected per plot (Schietti et al., 2016). The sample length was adjusted to reach half the diameter whenever possible, allowing for the comprehensive sampling of the entire trunk radius, from sapwood to pith. In cases where trees exhibited wood decay, hollowness, or extremely dense wood, the sample length was shorter than the trunk radius. We calculated basic wood density (excluding bark), using the ratio between the dry mass and the volume of green wood (g/cm^3), following the approach recommended by Williamson & Wiemann (2010). The fresh volume was determined by calculating the cylinder volume, using the diameter (5.15 mm) times the length of the wood sample, which was measured immediately after extraction from the trunk with the increment borer. The dry mass of the wood was obtained with high precision (0.0001g) on an analytical balance after the sample, without bark, was subjected to drying at 105°C for 72 hours or until a consistent mass was achieved. Later, we categorised wood density into three groups: Soft ≤ 0.50 , Medium $0.50\text{--}0.72$, and Hard ≥ 0.72 , in accordance with Ibama's guidelines (for more details see: Brazil, 1997; Nogueira et al., 2006, 2007, 2008).

2.5. Data analyses

Our primary objective was to investigate the relationship between environmental gradients and tree biomass increment rates, focusing on large canopy trees ($\text{DBH} \geq 30$ cm). To explore the influence of local hydrological conditions on tree biomass increment and to account for potential spatial clustering and autocorrelation effects, we employed generalised linear mixed models (GLMM), assuming a Gamma distribution for aboveground biomass. Site was included in the models as a random effect, to control for potential spatial auto-correlation between plots nested in the same site (Zuur et al., 2009). These models, ranked by ΔAIC (difference in AIC), incorporated variables related to climate, water table depth, and soil characteristics. Hydro-climatological conditions were characterised by meteorological drought (MCWD) and water excess (MCWE), as well as water in the soil, which included mean, maximum, and minimum water table depth (WT), along with measures of water table fluctuation range and standard deviation. In particular, we hypothesised an interaction between water table depth and climatological conditions, which we believed played a significant role in influencing biomass

increment rates. Consequently, we included interaction terms for these factors in our model (water table depth metrics * MCWD and MCWE). Atmospheric conditions were represented by minimum and maximum temperature and Vapour Pressure Deficit (VPD). Soil constraints were delineated by an index of soil physical restriction (Table 2 from Quesada et al., 2010), along with concentrations of total and available phosphorus, and the sum of bases ($\text{Ca}^{2+} + \text{Mg}^{2+} + \text{K}^+$).

In addressing our second research question concerning the significance of wood density in moderating tree biomass increment rates across diverse hydroedaphic and climatic conditions, we categorised wood density into three distinct groups: Soft ($\leq 0.50 \text{ g/cm}^{-3}$), Medium ($0.50\text{--}0.72 \text{ g/cm}^{-3}$), and Hard ($\geq 0.72 \text{ g/cm}^{-3}$). This categorization allows us to examine whether there are discernible patterns or variations in biomass increment rates among these defined wood density groups (for more details see Brazil, 1997; Nogueira et al., 2006, 2007, 2008). All the analyses were performed at the plot (community average biomass growth rates) and individual level (tree average biomass growth rates). We did this to understand if wood density, an individual trait representing tree ecological strategy, would reveal tree response patterns that could be hidden by community averages, since divergent strategies within the plots could be expected.

All statistical analyses and graph visualisations were conducted using the R statistical environment (R Core Team, 2023). The Generalised Linear Mixed Models (GLMM) were constructed using the "*lme4*" package (Bates et al. 2015). To visually represent plots showing partial residuals, we employed the "*visreg*" package (Breheny & Burchett, 2017). To assess model fit, we calculated both the marginal and conditional R^2 (R^2m ; R^2c) using the "*MuMIn*" package (Bartón, 2022). Multicollinearity among independent variables was always checked, evaluating each model's Variance Inflation Factor (VIF), and values less than 5 indicates low multiple correlation of that predictor with others. Model performance was evaluated by examining model summaries and comparing their Akaike's information criterion (AIC) values. A lower AIC value signifies a better-fitting model. Furthermore, we used the ΔAIC (difference in AIC) to gauge the relative support for a specific model compared to others in the comparison. Following the recommendation of Burnham and Anderson (2004), a $\Delta\text{AIC} < 2$ indicates stronger support for a particular model. We employed the '*dredge*' function from the "*MuMIn*" package (Bartón, 2022) to conduct model ranking and selection. Our model selection criteria were based on lower AIC values, a parsimonious number of parameters, and the presence of significant relationships between response and predictor variables.

3. RESULTS

Climatic and hydroedaphic variation

Based on precipitation data recorded from 1979 to 2009, plots located in site M07 were the rainiest in the study region, with an annual average precipitation of 2535 mm, while the lower annual precipitation was site M09, with an annual average of 2116 mm, although the higher MCWD was observed at M11 (Figure S4f; Table S1). The study area showed, on average, annual anomalies of water deficit up to -2σ (MCWD = 204 mm, in plots further south - M11; Figure S4f) and annual anomalies of water excess (MCWE = 945 mm, in central plots of the transect - M05 and M06; Figure S4e). We observed that site M06 presented the highest 30 years average of maximum temperature throughout the study period, reaching 31.64 °C (Figure S4a). On the other hand, plots located further south on the transect (M11) presented the lowest average temperatures, recording a mean of 21.17 °C (Figure S4b), and the lowest VPD values, averaging 0.691 kPa (Figure S4d; Table S1).

The available superficial phosphorus concentrations exhibited a range between 0.6 and 6.3 mg/kg⁻¹, with higher values observed in the flooded forests of M01 (5.34 ± 1.21 mg/kg⁻¹), likely associated with seasonal inundation by river water. Total soil phosphorus varied from 97.4 to 197.3 mg/kg⁻¹, with elevated concentrations in sites M05 and M011, situated in the central and southernmost parts of the transect, respectively (Table S1). The sum of exchangeable bases ranged from 0.085 to 0.48 mg/kg⁻¹, with the highest concentrations also found in the flooded forests of M01 (0.31 ± 0.09 mg/kg⁻¹). The soil water saturation index displayed variations, ranging from 3 to 4 in seasonally flooded and waterlogged soils, and 1 to 2 in well-drained soils. As for the scored soil physical constraint index, it showed a range between 4 and 8 in well-drained soils but increased to an index of 8–10 in the seasonally flooded and waterlogged soils (Table S1). We observed no correlation between aboveground biomass increments and either the index or the sum of bases.

Tree growth and dendrometric variables

The average above-ground biomass increment exhibited significant variation among individuals, ranging from a minimum of 5.89 kg/year⁻¹ to a maximum of 103.15 kg/year⁻¹ during the study period (1979-2009). The overall mean for above-ground biomass increment was 21.87 ± 12 kg/year⁻¹ (Figure 2a, 3a, S1; Table 1 and 4). The plots with the higher averages were identified as M07 (27.88 ± 12.77 kg/year⁻¹), positioned near the centre of the transect. Notably, the most substantial individual average aboveground biomass increment was observed in a *Hymenaea parvifolia* (Fabaceae) tree, which recorded a remarkable increase of 223 kilograms in a single year.

Mean Diameter Increment (MDI) also showed substantial variation, ranging from a minimum of 0.02 mm/year⁻¹ to a maximum of 20.56 mm/year⁻¹, with an average of 3.02 mm/year⁻¹ (± 2.01) (Figure 3b, 3c; Table 1 and 4). The plots that displayed the highest mean diametric increment were situated at the extremes, with the northern module (M01) recording 3.34 mm/year⁻¹ (± 2.58) and the southern module (M11) measuring 3.22 mm/year⁻¹ (± 1.63), respectively. The lowest values were recorded at M09, with an annual diameter increment of 2.38 mm/year⁻¹ (± 1.25). Individually, among the identified species, the lowest mean annual diameter increments were observed for *Micrandra spruceana* (Euphorbiaceae) (1.36 ± 0.7 mm/year⁻¹) and *Chrysophyllum ucuquirana-branca* (Sapotaceae) (1.85 ± 0.5 mm year⁻¹). In contrast, *Hymenaea parvifolia* (Fabaceae) exhibited the highest diameter increment rates at 7.91 ± 4.1 mm year⁻¹.

Wood density (WD), a pivotal parameter for estimating aboveground woody biomass, exhibited a broad spectrum in our study, ranging from a minimum of 0.31 g/cm³, exemplified by *Parkia nitida* (Fabaceae), to a maximum of 1.27 g/cm³ for *Eschweilera laeviscarpa* (Lecythidaceae). The mean WD across all trees was 0.73 g/cm³ (± 0.16) (Figure 1c, 2c). Adopting classification intervals of ≤ 0.50 , 0.50–0.72, and ≥ 0.72 g/cm³ (Nogueira et al., 2006, 2007, 2008), trees were predominantly categorised as medium (43.2%) and hard (50.1%), with only 6.7% classified as soft (Figure S2).

The diameter at breast height (DBH) of individuals ranged from a minimum value of 29.3 cm, exemplified by a *Licania micranhta* (Chrysobalanaceae), to a maximum value of 112.5 cm for *Eperua purpurea* (Fabaceae). The average DBH was 43.09 cm (± 11.18) (\pm = S.E, standard error). Height estimates also varied considerably, with a minimum value of 18.6 m, and a maximum value of 33.14 m for the same individual with the largest DBH, an *Eperua purpurea* (M06_TN_1500). The average estimated height was 21.90 m (± 2.11). This height estimate variation resulted from the use of specific allometric equations for each of the 11 research sites along the transect, as detailed in the study by Schiatti et al. from 2016. Among all sampled trees, individuals with the highest age estimates had 286, 277, and 276 rings, respectively, without reaching the pith. This suggests an age estimate exceeding 400 years, extrapolating the number of rings counted in relation to the average trunk radius of the measured trees. The estimated age of individuals based on annual growth ring counting ranged from 37 to 286 years, with an average of 113 years (± 39). The oldest identified tree was a *Conceveiba guianensis* (Euphorbiaceae) with an estimated age of 276 years, based on ring counting.

Table 1: Statistical summary of the studied variables for 1012 canopy trees across the 11 studied modules: minimum (Min) and maximum (Max); mean, and standard deviation (SD) of 30 years (1979-2009) mean aboveground biomass increments (MABI) and mean diameter increments (MDI), diameter at breast height (DBH), estimated height (m), wood density (g/cm^3) and age (in years). The table presents data categorized into two levels: individual (in gray) and plot (white).

	Min - Max	Mean \pm SD
MABI (kg/year^{-1})	5.89 – 103.15	21.87 \pm 8.5
	12.46 – 39.28	21.74 \pm 3.8
MDI (mm/year^{-1})	0.02 – 20.56	3.02 \pm 1.4
	1.52 – 6.86	3.02 \pm 2.01
DBH (cm)	29.3 – 112.5	43.1 \pm 8.04
	32.8 – 51.05	39.2 \pm 3.38
Estimated Height (m)	18.6 – 34.54	22.8 \pm 2.02
	20.4 – 25.19	22.9 \pm 1.11
Wood Density (g/cm^3)	0.31 – 1.27	0.73 \pm 0.12
	0.60 – 0.92	0.73 \pm 0.06
Age (years)	37 - 286	113.26 \pm 31.3
	93 –128	113 \pm 15.6

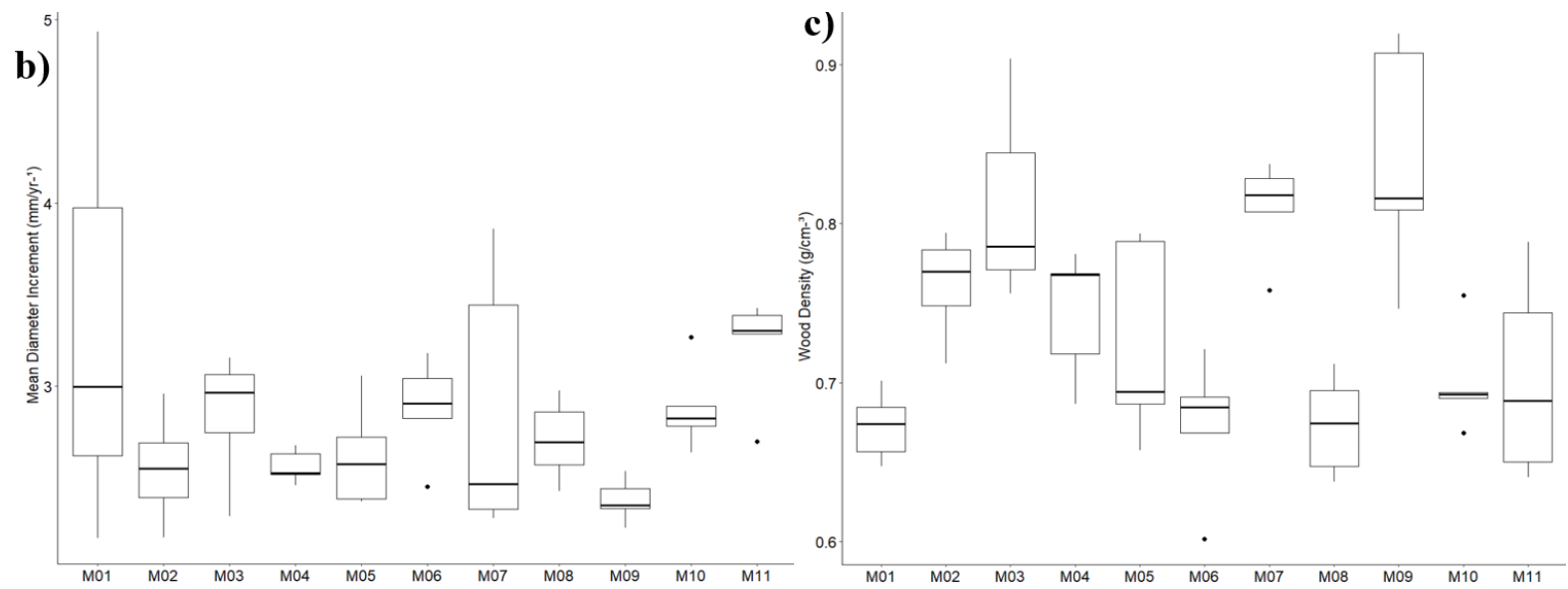
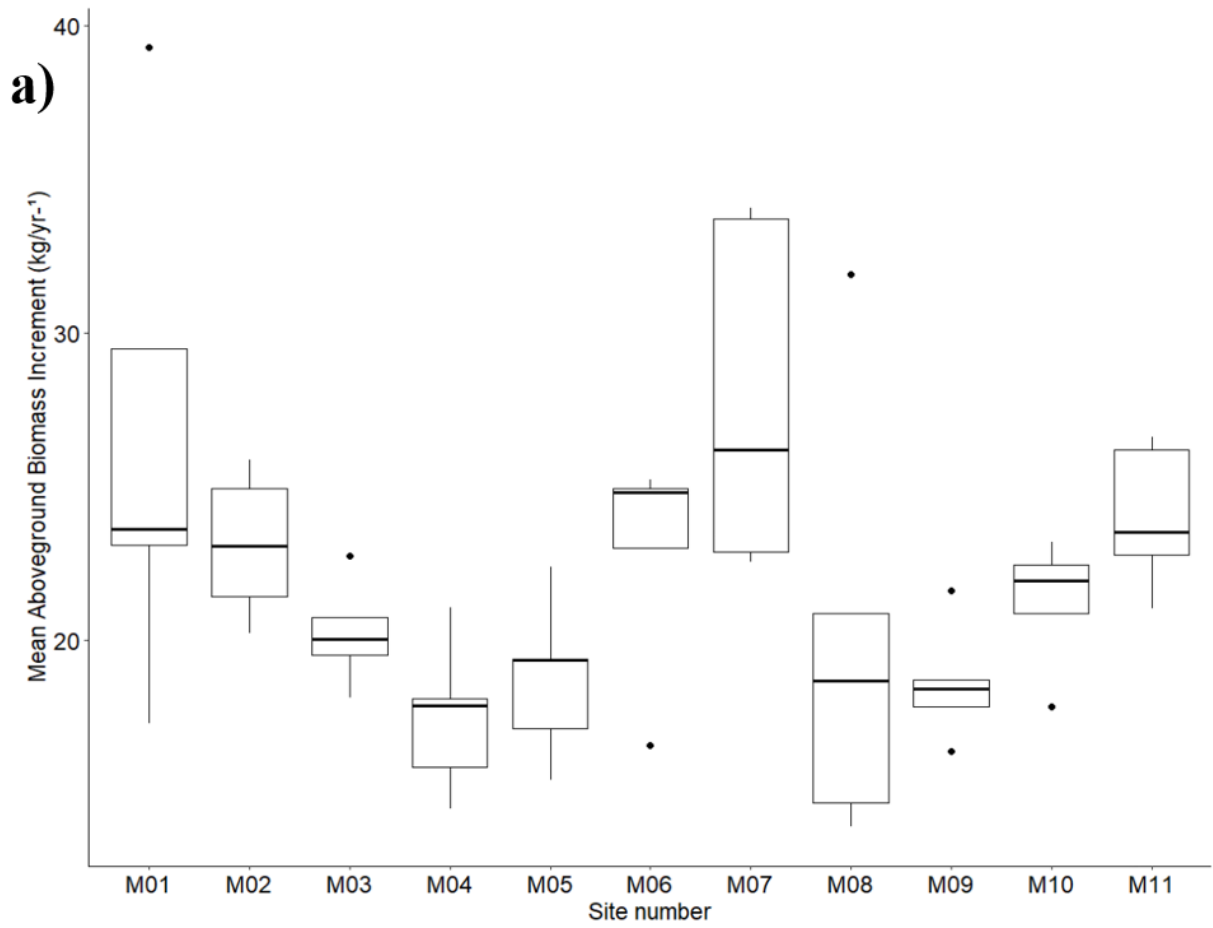


Figure 2: The eleven research sites (M01 - M11) located along the ~600 km transect shown on the x-axis. Boxplots depict the variation in: a) mean aboveground biomass increment; b) mean diameter increments (MDI); and c) wood density (WD).

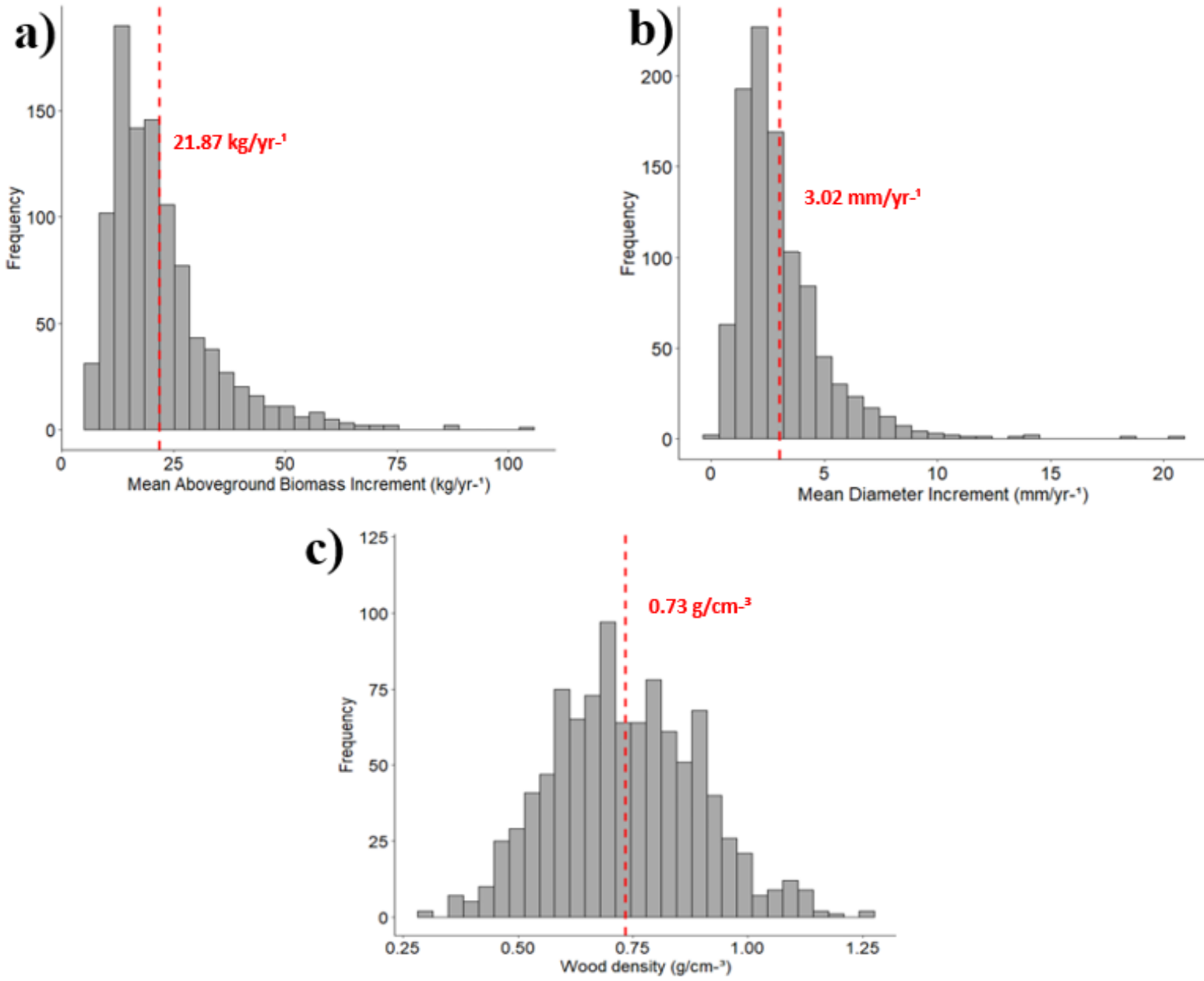


Figure 3: Density histograms showing distribution frequency and individual mean values for our study area with shallow water-table forests (dashed red line). a) mean aboveground biomass increment (kg/year⁻¹); b) mean diameter increment (mm/year⁻¹); and c) wood density (g/cm⁻³).

Relationships between tree growth, environmental conditions and wood density

We hypothesised that the average above-ground biomass increment varies with the average climate, local hydrology and soil structure, with interactions between climate and soil hydrology being important. The models with most support according to Akaike criterion ($\Delta\text{AIC} < 2$) did not support the hypothesis of climatic and hydrological interaction and did not show that water table depth or fluctuation range were important (Table 2), although water table depth variables were important at the individual level in a model with $\Delta\text{AIC} = 2.15$ (Table 3).

At the plot level, only available phosphorus exhibited a significant correlation with the average biomass increment, although the effects are quite subtle, with R^2 less than 0.1. Tree communities in plots with elevated available phosphorus demonstrated higher average biomass increment rates. Conversely, locations characterised by higher total phosphorus tended to exhibit lower average biomass increments ($p = 0.08$). The other variables selected in the models with $\Delta\text{AIC} < 2$ were maximum temperature (standardised beta coefficient, $\beta = -0.032$ to -0.054), MCWD ($\beta = 0.034$ to 0.046), VPD ($\beta = 0.027$), and minimum temperature ($\beta = 0.034$), but they did not show significant relationships with mean aboveground biomass increments at the plot level (Table 2). At the plot level wood density was also not significant for mean aboveground biomass increments.

At the individual level ($n = 1012$), the three models with higher support ($\Delta\text{AIC} < 2$) showed that trees with higher wood density ($\beta = 0.12$) and occurring in locals with higher available P ($\beta = 0.05$) have higher mean biomass increments. However, in locals with higher total P trees present lower mean biomass increments ($\beta = -0.06$) (Table 2). Wood density consistently correlated positively with biomass increment, contrary to our expectations (Figure 4c). Although, in simple correlations only wood densities categorised as "soft" ($p < 0.05$) and "medium" ($p = 0.01$) exhibited a statistically significant positive correlation with above-ground biomass increment (Figure S3a; Table S4). Together, these variables collectively contribute to explaining 11% of the increment variation in the models, accounting for the random effect of plots (Table 3). Nevertheless, the impact of phosphorus is relatively modest, as the positive correlation between wood density alone and the average above-ground biomass increment contributes to 6% of the variation explained.

A model with $\Delta\text{AIC} = 2.15$ showed the influence of both the maximum ($\beta = -0.15$) and mean ($\beta = 0.19$) water table levels on the biomass increment rates at the tree level. Tree biomass increments were higher where the mean water table level was more superficial but also where the maximum levels were deeper and more distance from soil surface (Figure 5). This model also included a positive effect of wood density ($\beta = 0.13$).

Table 2: Statistical summary of the best generalized linear mixed-effect models (GLMM) to explain the relationship between mean aboveground biomass increments (MABI) and environmental variables: available phosphorus (P_{avail}), total phosphorus (P_{tot}), maximum temperature (T_{max}), maximum cumulative water deficit (MCWD), vapour pressure deficit (VPD) and minimum temperature (T_{min}), considering the 54 plots as sample units. Here we show the models with better support according to Akaike criterion. Site ("module") was considered a random effect in all models. Marginal R^2 (R^2_{marg}) values pertain to models adjusted while considering only the fixed effects, and the conditional R^2 (R^2_{cond}) corresponds to the full model, including the random effect. The relative contribution of predictors is given by the standardized beta coefficients of the LMMs, and probability for each predictor is shown below. $p < 0.05$ are shown in bold. Dash indicates that the variable did not contribute to explain MABI in the model. Displaying only the models with $\Delta\text{AIC} < 2$.

MODEL	AIC	ΔAIC	R^2_{marg}	R^2_{cond}	P _{avail}	P _{tot}	T _{max}	MCWD	VPD	T _{min}
MABI ~ P _{avail}	156.1	0	0.07	0.29	0.06 $p = 0.08$	-	-	-	-	-
MABI ~ P _{tot}	157.3	1.17	0.06	0.32	-	-0.055 $p = 0.04$	-	-	-	-
MABI ~ T _{max}	157.7	1.58	0.05	0.28	-	-	-0.054 $p = 0.35$	-	-	-
MABI ~ T _{max} + MCWD + VPD	157.9	1.82	0.06	0.27	-	-	-0.032 $p = 0.78$	0.037 $p = 0.82$	0.027 $p = 0.85$	-
MABI ~ T _{max} + MCWD + T _{min}	158	1.86	0.06	0.27	-	-	-0.035 $p = 0.82$	0.046 $p = 0.72$	-	0.034 $p = 0.84$
MABI ~ MCWD	158	1.92	0.02	0.25	-	-	-	0.034 $p = 0.56$	-	-

Table 3: Statistical summary of the best generalized linear mixed-effect models (GLMM) to explain the relationship between mean aboveground biomass increments (MABI) and environmental variables: total phosphorus (P_tot), available phosphorus (P_avail), average water table depth (WT_med), maximum water table depth (WT_max), and wood density (WD), considering the 1012 individuals as sample units. Here we show the models with better support according to Akaike criterion. Site, referred to as "module," was considered a random effect in all models. Marginal R^2 (R^2_{marg}) values pertain to models adjusted while considering only the fixed effects, and the conditional R^2 (R^2_{cond}) corresponds to the full model, including the random effect. The relative contribution of predictors is given by the standardized coefficients of the LMMs. Probability for each predictor is shown in parentheses. Standardized coefficients in bold have $p < 0.05$. Dash indicates that the variable was not included in the model.

MODEL	AIC	AIC	R^2_{marg}	R^2_{cond}	WD	P_tot	P_avail	WT_med	WT_max
MABI ~ P_tot + WD	2744.1	0	0.06	0.11	0.12 <i>p</i> < 0.001	0.06 <i>p</i> < 0.001	-	-	-
MABI ~ WD	2744.2	0.05	0.06	0.1	0.13 <i>p</i> < 0.001	-	-	-	-
MABI ~ P_avail + WD	2744.9	0.82	0.05	0.09	0.12 <i>p</i> < 0.001	-	0.05 <i>p</i> = 0.01	-	-
MABI ~ wt_med + wt_max + WD	2746.3	2.15	0.01	0.06	0.13 <i>p</i> < 0.001	-	-	0.15 <i>p</i> = 0.01	-0.19 <i>p</i> = 0.01

4. DISCUSSION

This study constitutes one of the pioneering fieldwork-based efforts aimed to estimate above-ground woody biomass increments in large canopy trees of predominantly shallow water table forests (< 5m depth). This approach not only enabled us to investigate general trends at both the individual and community levels but also to explore the effects of tree associations with local climatic, edaphic, and hydrological characteristics. Our results showed mean above-ground biomass increments of 21.87 kg/year⁻¹ (± 12) for the trees in the Purus-Madeira region. These values are in the lowest range of observations in a semi-evergreen moist forest in Bolivia, where the average biomass increase was recorded at 105.4 kg/year⁻¹, with minimum values near 17.30 kg/year (van der Sande et al., 2015). Although few studies report tree growth in biomass, there are many studies in Amazonia reporting tree diameter growth. Annual growth averages derived from dendrometer measurements in upland forests across different Brazilian Amazon regions, eastern (near Santarém (PA), 3.1 mm/year⁻¹) and southwestern (near Rio Branco (AC), 3.9 mm/year⁻¹) (Vieira et al., 2004), are close to the average of 3.02 mm/year⁻¹ found in our study. However, growth rates reported for the central Amazon seem to be lower than the average for the Purus-Madeira region ranging from 1.2 to 2.2 mm per year (da Silva et al., 2002; Wagner et al., 2014; Dias & Marengo, 2016) (Table 5). The average wood density in the Purus-Madeira interfluvium (0.73 g/cm³) is similar to values of 0.75 g/cm³ reported to Manaus region (Dias & Marengo, 2016) but is higher than the average value of 0.64 g/cm³ reported for the whole Amazon (Nogueira et al., 2007). Our analyses unveiled a significant positive correlation between mean aboveground biomass increment and wood density (WD) across species. In contrast, there was no significant correlation between tree diameter growth and wood density (Figure S3b; Table S4).

Environmental variables effects on above-ground biomass increments

Our results showed the average above-ground biomass increment of canopy trees, both at the community and the individual level, revealed a negative relationship with the total soil phosphorus, while showing a positive correlation with available superficial phosphorus concentrations at the individual level. Previous study in the same area also found increased woody biomass productivity and lower stand aboveground biomass in available phosphorus-rich soils (Cintra et al., 2013, Schiatti et al., 2016). The observed correlations suggest that available phosphorus plays a role in fostering higher biomass production in forests characterised by lower stand biomass and more widely spaced stems (Schiatti et al., 2016). However, the central module "M07" displayed the highest average above-ground biomass increment (27.88 \pm 4.8 kg/year⁻¹), despite having lower available superficial phosphorus concentrations (0.92 \pm 0.2 mg/kg⁻¹). This inconsistency suggests the presence of additional factors influencing tree growth that were not considered in the models described here. Additional research is necessary to unravel the

mechanisms behind the higher biomass increment rates observed in soils with low phosphorus availability.

As described by Quesada et al. (2010, 2011), some of the most fertile soils in the Amazon basin can develop due to poor drainage and nutrient deposition. Plinthosols, predominant in our study area, develop under suboptimal soil conditions, enriching themselves with nutrients, notably iron molecules (Quesada et al., 2010, 2011). Phosphorus (P), an essential and limited element in these soils, maintains its primary association with iron molecules, being released when oxidised iron is reduced in the flooded plinthic layer (Chacon et al., 2006). In this context, it becomes plausible that hydrological conditions in our study region exert control over soil phosphorus availability, providing greater availability of this element to plants in more saturated areas. This hypothesis is supported by pronounced concentrations of phosphorus in plots located north of the transect, identified as seasonally flooded forests (Figure S5a). Cintra et al. (2013) also suggested that the M01 module, influenced by large river waters, exhibits soil chemical properties deviating from patterns observed in other modules due to flooding. In generally nutrient-poor soils like those in the Purus-Madeira Interfluve (Martins et al., 2015), the release or reduction of a growth-limiting nutrient could have significant impacts on the growth of these forests characterised by a shallow water table, and soil iron content could be the main chemical property affecting phosphorus availability to plants (Chacon et al., 2006). In more well-drained soils along the interfluve, iron deposition is likely mitigated, resulting in increased phosphorus unavailability for roots due to firm fixation by iron molecules present in the soil, which can lead to reduced tree growth (Cintra et al., 2013) and higher contents of total phosphorus in the soil. This phosphorus-iron dynamic may explain the negative relationship between total soil phosphorus and average above-ground biomass increment in the study region.

While temperature variables appeared in the best models to explain the rate of change in aboveground biomass increments at the plot level, they did not show statistical significance. This observed pattern contradicts conventional ecological expectations, where elevated temperatures are typically associated with constraints on tree growth, and extremely low minimum temperatures hinder the growth process (Clark et al., 2003, 2010; Lloyd & Farquar, 2008; Malhi, 2012; McDowell et al., 2018). Sullivan et al. (2020) observed a consistent negative linear relationship between maximum temperature and carbon stocks in tropical forests, underscoring the significant impact of higher daytime temperatures on forest thermal sensitivity. Their findings indicate that the detrimental effects become more pronounced beyond 32°C, suggesting an elevated risk of carbon stock loss with increased climate change magnitude. However, within our specific study area, the maximum daytime temperature range is narrowly constrained at 31.20 to 31.66 (± 0.11). This limited temperature range may elucidate the absence of a constraining effect

on the above-ground biomass increment in canopy trees within the Purus-Madeira interfluvial region. Temperature directly impacts biomass gain by influencing photosynthesis through crucial physiological processes like enzyme activity, the electron transport chain, and stomatal conductance (Lloyd & Farquhar, 2008; Marengo et al., 2014; Vinod et al., 2023). Rootzone temperature also regulates photosynthesis by affecting water absorption and stomatal conductance, driven by temperature-dependent effects on water viscosity and root permeability (Kaufmann, 1975; Delucia, 1986). In the Amazon, prolonged high temperatures during extreme droughts can reduce photosynthetic capacity due to high vapour pressure deficits (VPD), increasing mortality risk through stomatal closure, carbon starvation, or the formation of air bubbles in xylem vessels (cavitation/embolism), leading to hydraulic system collapse (McDowell & Allen, 2015; McDowell et al., 2018). Therefore, a continued monitoring of temperature and tree growth in this Amazon region is important since the increasing maximum temperatures expected (Gloor et al., 2015; Marengo & Espinoza 2016; Fontes et al., 2018; Gatti et al., 2021; López et al., 2021).

In well drained soils, the accumulation of climatological water deficit (CWD) results in increasing soil aridity, stressing plants due to limited water availability to roots, intensified by rising vapour pressure deficit (VPD). Elevated VPD not only affects soil water but also hampers tree growth before soil moisture becomes limiting (Novick et al., 2016; Cárcer et al., 2018). Higher VPD induces stomatal closure and increased respiration rates, a physiological acclimation to prevent excess water loss (Meinzer et al., 1993; Zhou et al., 2019), impacting vegetation growth and forest mortality significantly (Carnicer et al., 2012; Restaino et al., 2016). Moreover, elevated VPD and transpiration during the dry season may decrease stomatal conductance and, consequently, photosynthesis, contributing to negative carbon imbalance, depleting carbohydrate reserves, and causing tissue-level carbohydrate starvation (McDowell et al., 2008). Reduced soil water, coupled with high evaporative demand, can induce cavitation in xylem conduits and the rhizosphere, disrupting water flow, dehydrating plant tissues, and leading to plant death (McDowell et al., 2008). However, in the wetter Amazon regions (north and central), there is an observed increase in photosynthesis during the dry season in response to a slight VPD rise (Green et al., 2020). Similarly, Rowland et al. (2014) noted increased carbon accumulation during the dry season in an eastern Amazon forest with a pronounced seasonal rainfall pattern, correlated with increased solar radiation. We did not find a relationship between tree biomass increase and VPD or MCWD along the Purus-Madeira interfluve and this may support the hypothesis that in the central Amazon, areas with a shallow water table experience a relatively brief dry season, preventing soil water depletion beyond the root system's reach (Dias & Marengo, 2016). This may contribute to trees maintaining consistent growth rates throughout the year, even under relatively high VPD conditions, highlighting the potential resilience of regions with shallow water tables

(Costa et al., 2022). However, these areas may lack specific plant traits to endure severe water stress, potentially posing vulnerability to ecological collapse if drought severity exceeds critical thresholds. Identifying conditions triggering ecological tipping points, leading to forest die-off and breakdown of climate services in these areas, is crucial.

Both maximum ($\beta = -0.24$) and mean ($\beta = 0.27$) water table levels emerged as important factors in elucidating the variability of above-ground biomass increments in the Purus-Madeira interfluvium (model with $\Delta AIC = 2.15$). Regions with shallower average water table depths showed higher biomass increments. Conversely, in areas where the water table reaches the surface or there is soil inundation, biomass increments are likely to be constrained (Figure 5). This constraint may be attributed to anoxic conditions, resulting in reduced diameter growth (Worbes, 1999; Schongart et al., 2002; Piedade et al., 2010). However, observations of tree growth in floodplain forests suggest that trees initiate growth during the dry season, even when the forests are still flooded (Schöngart et al., 2002). This implies that saturation and flooding conditions may evoke distinct responses in tree growth, with water saturation favouring it, while flooding appears to be unfavourable. This emphasises the critical influence of water table depth on the ecological dynamics within the Purus-Madeira interfluvium, underscoring the significance of understanding these variations for comprehensive ecosystem understanding.

Despite extensive research efforts to evaluate the impact of climatic parameters on tree growth in tropical forests (Wagner et al., 2014; Dias & Marengo, 2016; Méndez, 2018), a consensus regarding the distinct importance of each climatic factor in this process remains elusive. In the Central Amazon region, the positive correlation between precipitation and tree growth exhibits limited evidence or fails to achieve statistical significance in years characterised by higher rainfall (Silva et al., 2003; Dias & Marengo, 2016). This phenomenon is attributed to increased cloudiness during the rainy season, leading to a substantial reduction in incident solar radiation. An investigation focusing on total above-ground productivity, carbon sequestration, and storage in selected plots within the same region observed an indirect increase in woody biomass productivity linked to elevated soil water saturation, mediated by phosphorus availability (Cintra et al., 2013). The influence of temperature and precipitation variability on tree growth in tropical forests is also a widely debated topic. In a tropical forest in La Selva, Costa Rica, Clark et al. (2003) noted a negative correlation between stem growth and mean and minimum temperatures over 16 years, without detecting a significant effect of maximum temperature and precipitation variability on tree diameter increment. Also in the central Amazon during the period from 2013 to 2017, the variation in mean and minimum temperatures had no impact on stem growth, while growth decreased in response to increased maximum temperature in various species (Marengo & Antezana-Vera, 2021). The complexity lies in the correlation between different

climatic variables, making it challenging to demonstrate the individual effects of these factors on tree growth or plant functioning. In our study, exploring the relationships between climatic variables and above-ground biomass increment in trees, we observed an absence of correlation with annual mean precipitation and temperature-derived variables (maximum and minimum). This discrepancy with previous study underscores the complexity of the forest dynamics, emphasising the need for further research for a comprehensive understanding of climatic effects on tree growth in tropical ecosystems.

Influence of wood density on tree biomass growth in shallow water table forests

Wood density tends to exhibit an inverse correlation with soil fertility (Baker et al., 2004; Muller-Landau, 2004; ter Steege et al., 2006; Nogueira et al., 2008; Quesada et al., 2012; Farias et al., 2023). Additionally, other factors, including natural disturbance frequency, understory light availability, humidity, and climatic life zones, can influence growth strategies and, consequently, wood density (Chudnoff, 1976; Wiemann & Williamson, 2002; Woodcock & Shier, 2003). The mean basic density of Amazonian forests is reported as 0.69 g/cm³ for heartwood, or 0.68 g/cm³ when adjusted for the volume and density of sapwood and bark (Fearnside, 1997). This average is 6.85% lower than our mean estimate of 0.73 g/cm³ (± 0.15) for canopy woody species in dense and open forests of the Purus-Madeira Interfluvium. Tree genera that could be contributing to this higher wood density community-averaged include *Licania* (average 0.90 ± 0.16 g/cm³; $n = 41$), *Eschweilera* (0.88 ± 0.14 g/cm³, $n = 17$), and *Pouteria* (0.85 ± 0.16 g/cm³, $n = 14$), particularly prevalent in central and eastern Amazonia but less so in northwest Amazonia (Baker et al., 2004; Schiatti et al., 2016). More recently, Dias and Marengo (2016) found that wood densities higher than 0.75 g/cm³ were present in 64.3% of the trees analyzed in a terra-firme rainforest in the central Amazon, while only 3.6% of species had wood densities lower than 0.50 g/cm³. In this study, we observed that 45.9% of the tree species analysed had wood densities equal to or higher than 0.75 g/cm³, and 6.72% of species had densities lower than 0.50 g/cm³ (Fig. S4). Utilizing data from the RAINFOR project and plots containing 40,077 stems with a diameter greater than 10 cm, encompassing various local and regional environmental gradients in Amazonia, Baker et al. (2004) identified the divergence between western and eastern Amazonia. This disparity is attributed to the high relative abundance of stems with a low specific gravity of 0.2–0.5 g/cm⁻³ in western Amazonia and stems with 0.7–0.9 g/cm⁻³ in central and eastern Amazon (Baker et al., 2004).

In general, our recorded values for all trees (ranging from 0.31 to 1.27 g/cm³) fall within the ranges reported in databases for tropical forest species (Chave et al., 2008; Zanne et al., 2009). Our average wood density values further corroborate the prevailing notion that in the Amazon basin, high wood density values are frequently encountered in central Amazonia (Baker et al.,

2004; Malhi et al., 2004; Nogueira et al., 2008; Dias & Marengo, 2016). Our study provides a noteworthy extension of high average wood density values to the southern region of Manaus, contributing valuable insights to the comprehension of wood density in this area. The average wood density in the Southwestern Amazon (SSWA) was estimated at 0.58 g/cm^3 using commercial wood inventories from the RadamBrasil Project (Nogueira et al., 2007), which is 17% lower compared to our southernmost plots ($0.7 \text{ g/cm}^3 \pm 0.03$). As water table depths and regimes closely correlate with topography, they can exhibit considerable variation within small areas at the landscape level. In the shallow water table forests of the Purus-Madeira interfluve, Costa et al. (2023) identified a compositional turnover along the gradient of water table depth fluctuation for all taxonomic levels analysed. However, wood density did not show the anticipated variation along the gradient of water table depth (WTD) fluctuation. Contrary to the initial hypothesis suggesting divergent modes of trait selection or coordination among leaf and wood traits based on water table fluctuation, higher wood density was associated with increased WTD fluctuation, especially in drier climates with longer seasonal dry periods (Costa et al., 2023). These results are consistent with earlier findings, highlighting that climate seasonality, coupled with WTD characteristics, influences tree wood density and potentially affects the filtering patterns of other traits across the Amazon basin (Marca-Zevallos et al., 2022).

In our study, we identified a positive correlation (Figure 4c) between the mean aboveground biomass increment of species and wood density. This indicates that species with higher wood densities exhibit greater average above-ground biomass increments, contrary to expectations that lighter woods would have higher growth rates. Besides that, no correlation was found between tree diameter growth and wood density. As indicated in the individual-level models, wood density is an important variable for explaining the variation in biomass increment, as it appeared in the three most robust models and alone explained approximately 10% of the observed variation. Additionally, we observed a significant correlation between softwood densities and aboveground biomass increments, as well as a positive correlation between medium-density woods and mean aboveground biomass increments, although with low explanation power (Table S4 / Figure S5). Differently, a study conducted in a terra-firme forest in the north of Manaus, reported no correlation between species stem growth (SG) and wood density ($p = 0.44$) (Camargo & Marengo, 2023). We did not find in the literature other studies reporting positive correlations between tree biomass growth and wood density. Maybe this unexpected pattern can be elucidated by further investigations on the allocation patterns in different elements of xylem of the trees. The xylem volume allocation results in different wood properties and ecological strategies. A higher allocation towards fibre wall volume increases wood density and can favour resistance against embolism. However, this defensive strategy incurs a trade-off, with lower investments in parenchyma and in fibre lumen volumes, which results in lower wood

density, specific conductivity and sapwood capacitance (Janssen et al., 2019). In the context of wet forests, tree species exhibit a tendency to allocate more xylem to axial parenchyma at the expense of fibre walls, favouring higher hydraulic conductivity and growth. This allocation pattern results in decreased embolism resistance and heightened vulnerability to drought-induced mortality, irrespective of the given wood density (Janssen et al., 2019). While it is commonly observed that trees with low wood density tend to grow faster than those with high-density wood (Suzuki, 1999; Osunkoya et al., 2007), this pattern was not observed in forests situated over shallow water tables in the Purus-Madeira interfluvium and may be related to different xylem allocation investment, in soft and medium wood density trees.

Limitations of this study

Although the monitoring of the water table level in 54 plots, 11 sites, along 600 km in an interfluvial area of the Amazon basin is an unprecedented effort, we recognize that 2010- 2013 data may not represent the groundwater regime of 30 years. The water table level is influenced by the precipitation regime, among other factors such as topography and soil properties (Marklund, 2007; Fan et al., 2013, 2019; Costa et al., 2022) and studies showed that precipitation over the Amazon basin is changing in the last 40 years (Marengo 2004, 2006; Gloor et al., 2015; Marengo & Spinoza, 2016; Barichivich et al., 2018; Motta Paca et al., 2020). Despite the general trend of precipitation increase, there was a decrease in the total annual precipitation in part of the studied transect (Motta Paca et al., 2020). These changes in the patterns of precipitation along the years could have changed the water table levels across the sites differently. Additionally, while we have successfully delineated major trends, it is noteworthy that the variables integrated into our most robust models contribute to approximately 30% of the explanatory power for above-ground biomass increment variation at the community level and a modest 10% at the individual level. Within our analysis, about 20% of the variability is attributed to differences among sites (modules). These conditions underscore the necessity of considering a broad spectrum of environmental and biological factors when attempting to comprehend and predict changes in tropical ecosystem dynamics. Such insights are crucial for developing more accurate models and effective conservation strategies, particularly in the face of global environmental changes. This pattern implies that pivotal variables and underlying processes remain unaddressed, with additional variation likely linked to species composition and emerging functional traits as prominent factors.

Notably, these regions characterised by shallow water tables may indeed represent a critical Achilles' heel within the broader context of the Amazon, as highlighted by Costa et al. (2022). Such variations in the landscape might present a more substantial vulnerability than previously anticipated, surpassing the vulnerabilities initially envisaged for seasonally inundated

forests highly sensitive to drought and fire (Flores et al., 2017). This realisation underscores the urgency for thorough investigations that delve into the intricate interplay of factors shaping tree growth in this ecologically significant region.

Conclusions

The Amazon's hydrological cycle is undergoing changes due to climate change, with projections suggesting further intensification in the future (Gloor et al., 2015). Global climate models highlight substantial impacts on the Amazon basin, affecting carbon stocks and uptake, particularly due to changes in hydrological regimes and temperature increase (Dufresne et al., 2002; Betts et al., 2004; Cook et al., 2012). The Purus-Madeira interfluve region is currently under significant pressure from deforestation expansion and the reconstruction of the BR-319 highway, rendering it highly susceptible to human impacts. While the effects of climatic extremes on Amazonian forests are well-studied in regions with deep water tables, 30% to 50% of the Amazon basin hosts forests with a shallow water table (<5m deep), and little is known about tree responses in these conditions (Costa et al., 2022, 2023). Our research reveals significant variability in average biomass increments among canopy trees in the Purus-Madeira interfluve, ranging from 5.8 to 103.1 kg/year⁻¹, with an average of 21.9 kg/year⁻¹. Forests near Manaus and in central plots (M07) exhibited the most substantial biomass increments. Diametric growth varied significantly, ranging from 0.02 to 20.56 mm/year⁻¹, with an average of 3.02 mm/year⁻¹, higher than showed in prior studies in proximity to the Central Amazon (Vieira et al., 2004; Dias and Marengo, 2016). Wood density played a crucial role only at the individual level, and contrary to expectations, trees with higher wood densities showed the highest increment rates. We did not find an explicit interaction of the water table depth with climate. However, we did find a direct correlation between water table depth and biomass increments, suggesting sufficient soil water supply to support growth in drier and more demanding atmospheric conditions, but a constrained biomass growth where the water table maximum levels reach the surface. These findings support the hypothesis that local hydrology imposes significant constraints on the influence of forest climate effects, with potential implications for climate change feedbacks.

Finally, our findings highlight the need for additional studies on hydraulic strategies and functional traits across plant species. Understanding the functional variability of Amazonian forests over a shallow water table is crucial, particularly as these areas have the potential to mitigate extreme heat and drought effects, becoming refuges for biodiversity (Sousa et al., 2020; Esteban et al., 2021; Costa et al., 2022). Bridging this knowledge gap contributes to biodiversity-driven variability in terrestrial system functioning models, aiding in predicting resilience and adaptations to evolving climate scenarios. Moreover, it informs sustainable management practices and conservation strategies in this critical region.

CONCLUSÃO GERAL

O ciclo hidrológico da Amazônia está sendo impactado por mudanças climáticas, prevendo-se uma intensificação futura. Modelos climáticos globais indicam impactos substanciais na bacia amazônica, afetando carbono e estoques devido a mudanças nos regimes hidrológicos e aumento da temperatura. A região Purus-Madeira, especialmente sob pressão de desmatamento e reconstrução da rodovia BR-319, enfrenta significativa suscetibilidade a impactos humanos. Apesar dos estudos focados em extremos climáticos em florestas amazônicas com lençóis freáticos profundos, 30-50% da bacia possui lençol freático superficial, com poucos estudos sobre as respostas das árvores nessas condições. Este presente estudo revela grande variabilidade nos incrementos médios de biomassa entre árvores de dossel no interflúvio Purus-Madeira, indicando uma média de 21.9 kg/ano, variando de 5.8 até 103 kg/ano. Florestas próximas a Manaus e parcelas centrais mostraram os maiores incrementos. O crescimento diamétrico variou de 0.02 a 20.56 mm/ano⁻¹, com uma média de 3.02 mm/ano⁻¹. Surpreendentemente, árvores com maior densidade da madeira apresentaram as maiores taxas de incremento, sem interação explícita entre a profundidade do lençol freático e o clima. No entanto, foi identificada uma correlação entre a profundidade do lençol freático e os incrementos de biomassa, indicando fornecimento adequado de água no solo para sustentar o crescimento em condições atmosféricas mais secas. Esses resultados suportam a hipótese de que a hidrologia local limita a influência dos efeitos climáticos na floresta, com implicações para feedbacks das mudanças climáticas. As descobertas ressaltam a necessidade de estudos adicionais sobre estratégias hidráulicas e características funcionais entre espécies vegetais ao longo da região interfluvial. Compreender a variabilidade funcional das florestas amazônicas sobre lençol freático superficial é crucial, pois essas áreas têm potencial para mitigar os efeitos extremos de calor e seca, servindo como refúgios para a biodiversidade. Preencher essa lacuna de conhecimento contribui para modelos de funcionamento de sistemas terrestres, prevendo resiliência e adaptações a cenários climáticos em evolução, informando práticas de gestão sustentável e estratégias de conservação nesta região.

REFERENCES

- Ali, A., Yan, E. R., Chang, S. X., Cheng, J. Y., & Liu, X. Y. (2017). Community-weighted mean of leaf traits and divergence of wood traits predict aboveground biomass in secondary subtropical forests. *Science of the Total Environment*, 574, 654-662.
- Alves, Y. L. A., Durgante, F. M., Piedade, M. T. F., Wittmann, F., & Schöngart, J. (2023). Tree growth performance and xylem functional arrangements of *Macrolobium* Schreb.(Fabaceae) in different wetland forests in the Central Amazon basin. *Trees*, 1-12.
- Antezana-Vera, S. A., & Marengo, R. A. (2021). Intra-annual tree growth responds to micrometeorological variability in the central Amazon. *iForest-Biogeosciences and Forestry*, 14(3), 242.
- Asner, G. P., & Mascaro, J. (2014). Mapping tropical forest carbon: Calibrating plot estimates to a simple LiDAR metric. *Remote Sensing of Environment*, 140, 614-624.
- Baker, T. R., Phillips, O. L., Malhi, Y., Almeida, S., Arroyo, L., Di Fiore, A., ... & Vasquez Martinez, R. (2004). Variation in wood density determines spatial patterns in Amazonian forest biomass. *Global Change Biology*, 10(5), 545-562.
- Baraloto, C., Rabaud, S., Molto, Q., Blanc, L., Fortunel, C., Hérault, B., ... & Fine, P. V. (2011). Disentangling stand and environmental correlates of aboveground biomass in Amazonian forests. *Global Change Biology*, 17(8), 2677-2688.
- Barichivich, J., Gloor, E., Peylin, P., Brienen, R. J., Schöngart, J., Espinoza, J. C., & Pattnayak, K. C. (2018). Recent intensification of Amazon flooding extremes driven by strengthened Walker circulation. *Science advances*, 4(9), eaat8785.
- Barkhordarian, A., Saatchi, S. S., Behrangi, A., Loikith, P. C., & Mechoso, C. R. (2019). A recent systematic increase in vapor pressure deficit over tropical South America. *Scientific reports*, 9(1), 15331.
- Bartón, K. (2022). *MuMIn: Multi-model inference*. R package version 1.47.1.
- Bastin, J. F., Rutishauser, E., Kellner, J. R., Saatchi, S., Pélissier, R., Hérault, B., ... & Zebaze, D. (2018). Pan-tropical prediction of forest structure from the largest trees. *Global Ecology and Biogeography*, 27(11), 1366-1383.

Becknell, J. M., Kucek, L. K., & Powers, J. S. (2012). Aboveground biomass in mature and secondary seasonally dry tropical forests: A literature review and global synthesis. *Forest Ecology and Management*, 276, 88-95.

Bennett, A. C., Rodrigues de Sousa, T., Monteagudo-Mendoza, A., Esquivel-Muelbert, A., Morandi, P. S., Coelho de Souza, F., ... & Phillips, O. L. (2023). Sensitivity of South American tropical forests to an extreme climate anomaly. *Nature Climate Change*, 13(9), 967-974.

Bergès, L., Nepveu, G., & Franc, A. (2008). Effects of ecological factors on radial growth and wood density components of sessile oak (*Quercus petraea* Liebl.) in Northern France. *Forest Ecology and Management*, 255(3-4), 567-579.

Betts, R. A., Cox, P. M., Collins, M., Harris, P. P., Huntingford, C., & Jones, C. D. (2004). The role of ecosystem-atmosphere interactions in simulated Amazonian precipitation decrease and forest dieback under global climate warming. *Theoretical and applied climatology*, 78, 157-175.

Binkley, D., Stape, J. L., Bauerle, W. L., & Ryan, M. G. (2010). Explaining growth of individual trees: light interception and efficiency of light use by Eucalyptus at four sites in Brazil. *Forest ecology and management*, 259(9), 1704-1713.

Bordin, K. M., & Müller, S. C. (2019). Drivers of subtropical forest dynamics: The role of functional traits, forest structure and soil variables. *Journal of Vegetation Science*, 30(6), 1164-1174.

Brazil, I. B. A. M. A. (1997). *Madeiras da Amazônia: Características e Utilização, Amazônia Oriental*.

Brienen, R. J., Phillips, O. L., Feldpausch, T. R., Gloor, E., Baker, T. R., Lloyd, J., ... & Zagt, R. J. (2015). Long-term decline of the Amazon carbon sink. *Nature*, 519(7543), 344-348.

Brienen, R. J., Schöngart, J., & Zuidema, P. A. (2016). Tree rings in the tropics: insights into the ecology and climate sensitivity of tropical trees. *Tropical tree physiology: adaptations and responses in a changing environment*, 439-461.

Brienen, R. J., Caldwell, L., Duchesne, L., Voelker, S., Barichivich, J., Baliva, M., ... & Gloor, E. (2020). Forest carbon sink neutralized by pervasive growth-lifespan trade-offs. *Nature communications*, 11(1), 4241.

Cárcer, S. P., Vitasse, Y., Peñuelas, J., Jasey, V. E., Buttler, A., & Signarbieux, C. (2018). Vapor–pressure deficit and extreme climatic variables limit tree growth. *Global Change Biology*, 24(3), 1108-1122.

Carnicer, J., Brotons, L., Stefanescu, C., & Penuelas, J. (2012). Biogeography of species richness gradients: linking adaptive traits, demography and diversification. *Biological Reviews*, 87(2), 457-479.

Chacon, N., Silver, W. L., Dubinsky, E. A., & Cusack, D. F. (2006). Iron reduction and soil phosphorus solubilization in humid tropical forests soils: the roles of labile carbon pools and an electron shuttle compound. *Biogeochemistry*, 78, 67-84.

Chapotin, S. M., Razanameharizaka, J. H., & Holbrook, N. M. (2006). Water relations of baobab trees (*Adansonia* spp. L.) during the rainy season: does stem water buffer daily water deficits?. *Plant, Cell & Environment*, 29(6), 1021-1032.

Chave, J., Andalo, C., Brown, S., Cairns, M. A., Chambers, J. Q., Eamus, D., ... & Yamakura, T. (2006). Tree allometry and improved estimation of carbon stocks and balance in tropical forests. *Oecologia*, 145, 87-99.

Chave, J., Olivier, J., Bongers, F., Châtelet, P., Forget, P. M., van Der Meer, P., ... & Charles-Dominique, P. (2008). Above-ground biomass and productivity in a rain forest of eastern South America. *Journal of tropical Ecology*, 24(4), 355-366.

Chave, J., Réjou-Méchain, M., Búrquez, A., Chidumayo, E., Colgan, M. S., Delitti, W. B., ... & Vieilledent, G. (2014). Improved allometric models to estimate the aboveground biomass of tropical trees. *Global change biology*, 20(10), 3177-3190.

Chitra-Tarak, R., Ruiz, L., Dattaraja, H. S., Mohan Kumar, M. S., Riotte, J., Suresh, H. S., ... & Sukumar, R. (2018). The roots of the drought: Hydrology and water uptake strategies mediate forest-wide demographic response to precipitation. *Journal of Ecology*, 106(4), 1495-1507.

Cintra, B. B. L., Schiatti, J., Emillio, T., Martins, D., Moulatlet, G., Souza, P., ... & Schöngart, J. (2013). Soil physical restrictions and hydrology regulate stand age and wood biomass turnover rates of Purus–Madeira interfluvial wetlands in Amazonia. *Biogeosciences*, 10(11), 7759-7774.

Clark, D. A., Piper, S. C., Keeling, C. D., & Clark, D. B. (2003). Tropical rain forest tree growth and atmospheric carbon dynamics linked to interannual temperature variation during 1984–2000. *Proceedings of the national academy of sciences*, *100*(10), 5852-5857.

Clark, D. B., Clark, D. A., & Oberbauer, S. F. (2010). Annual wood production in a tropical rain forest in NE Costa Rica linked to climatic variation but not to increasing CO₂. *Global Change Biology*, *16*(2), 747-759.

Cook, B. I., Wolkovich, E. M., Davies, T. J., Ault, T. R., Betancourt, J. L., Allen, J. M., ... & Travers, S. E. (2012). Sensitivity of spring phenology to warming across temporal and spatial climate gradients in two independent databases. *Ecosystems*, *15*, 1283-1294.

Cornelissen, J. H. C., Cerabolini, B., Castro-Díez, P., Villar-Salvador, P., Montserrat-Martí, G., Puyearavaud, J. P., ... & Aerts, R. (2003). Functional traits of woody plants: correspondence of species rankings between field adults and laboratory-grown seedlings?. *Journal of Vegetation Science*, *14*(3), 311-322.

Cosme, L. H., Schiatti, J., Costa, F. R., & Oliveira, R. S. (2017). The importance of hydraulic architecture to the distribution patterns of trees in a central Amazonian forest. *New Phytologist*, *215*(1), 113-125.

Costa, F. R., Schiatti, J., Stark, S. C., & Smith, M. N. (2022). The other side of tropical forest drought: do shallow water table regions of Amazonia act as large-scale hydrological refugia from drought?. *New Phytologist*, *237*(3), 714-733.

Costa, F. R., Lang, C., Sousa, T. R., Emilio, T., Esquivel-Muelbert, A., & Schiatti, J. (2023). Fine-grained water availability drives divergent trait selection in Amazonian trees. *Frontiers in Forests and Global Change*, *6*, 1112560.

Coster, C. (1927). Zur anatomie und physiologie der zuwachszone- und jahresringbildung in den tropen. [internal PhD, WU, Wageningen University]. Brill.

Cox, P. M., Harris, P. P., Huntingford, C., Betts, R. A., Collins, M., Jones, C. D., ... & Nobre, C. A. (2008). Increasing risk of Amazonian drought due to decreasing aerosol pollution. *Nature*, *453*(7192), 212-215.

Crews, T. E., Kitayama, K., Fownes, J. H., Riley, R. H., Herbert, D. A., Mueller-Dombois, D., & Vitousek, P. M. (1995). Changes in soil phosphorus fractions and ecosystem dynamics across a long chronosequence in Hawaii. *Ecology*, *76*(5), 1407-1424.

Cunha, H. F. V., Andersen, K. M., Lugli, L. F., Santana, F. D., Aleixo, I. F., Moraes, A. M., ... & Quesada, C. A. (2022). Direct evidence for phosphorus limitation on Amazon forest productivity. *Nature*, 608(7923), 558-562.

Davidson, E. A., Ishida, F. Y., & Nepstad, D. C. (2004). Effects of an experimental drought on soil emissions of carbon dioxide, methane, nitrous oxide, and nitric oxide in a moist tropical forest. *Global Change Biology*, 10(5), 718-730.

Dias, D. P., & Marengo, R. A. (2016). Tree growth, wood and bark water content of 28 Amazonian tree species in response to variations in rainfall and wood density. *Volume 9, Número JUNE2016, Pags. 445-451*.

Doughty, C. E., Asner, G. P., & Martin, R. E. (2011). Predicting tropical plant physiology from leaf and canopy spectroscopy. *Oecologia*, 165, 289-299.

Dufresne, J. L., Friedlingstein, P., Berthelot, M., Bopp, L., Ciais, P., Fairhead, L., ... & Monfray, P. (2002). Effects of climate change due to CO₂ increase on land and ocean carbon uptake. *Geophys. Res. Lett*, 29(10), 1405.

Esquivel-Muelbert, A., Baker, T. R., Dexter, K. G., Lewis, S. L., Ter Steege, H., Lopez-Gonzalez, G., ... & Phillips, O. L. (2017). Seasonal drought limits tree species across the Neotropics. *Ecography*, 40(5), 618-629.

Esquivel-Muelbert, A., Baker, T. R., Dexter, K. G., Lewis, S. L., Brienen, R. J., Feldpausch, T. R., ... & Phillips, O. L. (2019). Compositional response of Amazon forests to climate change. *Global change biology*, 25(1), 39-56.

Esteban, E. J., Castilho, C. V., Melgaço, K. L., & Costa, F. R. (2021). The other side of droughts: wet extremes and topography as buffers of negative drought effects in an Amazonian forest. *New Phytologist*, 229(4), 1995-2006.

Fan, Y., Li, H., & Miguez-Macho, G. (2013). Global patterns of groundwater table depth. *Science*, 339(6122), 940-943.

Fan, Y., Miguez-Macho, G., Jobbágy, E. G., Jackson, R. B., & Otero-Casal, C. (2017). Hydrologic regulation of plant rooting depth. *Proceedings of the National Academy of Sciences*, 114(40), 10572-10577.

Fan, Y., Clark, M., Lawrence, D. M., Swenson, S., Band, L. E., Brantley, S. L., ... & Yamazaki, D. (2019). Hillslope hydrology in global change research and earth system modeling. *Water Resources Research*, 55(2), 1737-1772.

Farias, H. L. S., Pequeno, P. A. C. L., Silva, W. R., Melo, V. F., Carvalho, L. C. D. S., Perdiz, R. D. O., ... & Barbosa, R. I. (2023). Amazon forest biomass: intra-and interspecific variability in wood density drive divergences in Brazil's far north. *iForest-Biogeosciences and Forestry*, 16(2), 95.

Fauset, S., Johnson, M. O., Gloor, M., Baker, T. R., Monteagudo M, A., Brienen, R. J., ... & Phillips, O. L. (2015). Hyperdominance in Amazonian forest carbon cycling. *Nature communications*, 6(1), 1-9.

Fearnside, P. M. (1997). Wood density for estimating forest biomass in Brazilian Amazonia. *Forest ecology and management*, 90(1), 59-87.

Fearnside, P. M. (2007). Brazil's Cuiabá-Santarém (BR-163) Highway: The environmental cost of paving a soybean corridor through the Amazon. *Environmental management*, 39, 601-614.

Fearnside, P. M. (2018). Brazil's Amazonian forest carbon: the key to Southern Amazonia's significance for global climate. *Regional Environmental Change*, 18, 47-61.

Feldpausch, T. R., Lloyd, J., Lewis, S. L., Brienen, R. J., Gloor, M., Monteagudo Mendoza, A., ... & Phillips, O. L. (2012). Tree height integrated into pantropical forest biomass estimates. *Biogeosciences*, 9(8), 3381-3403.

Ferri, M. G., & Jones, W. H. (1979). Determinants of financial structure: A new methodological approach. *The Journal of finance*, 34(3), 631-644.

Fontes, C. G., Dawson, T. E., Jardine, K., McDowell, N., Gimenez, B. O., Anderegg, L., ... & Chambers, J. Q. (2018). Dry and hot: the hydraulic consequences of a climate change-type drought for Amazonian trees. *Philosophical Transactions of the Royal Society B: Biological Sciences*, 373(1760), 20180209.

Fletcher, Jr, R. J., Ries, L., Battin, J., & Chalfoun, A. D. (2007). The role of habitat area and edge in fragmented landscapes: definitively distinct or inevitably intertwined?. *Canadian journal of zoology*, 85(10), 1017-1030.

Friedlingstein, P., Andrew, R. M., Rogelj, J., Peters, G. P., Canadell, J. G., Knutti, R., ... & Le Quéré, C. (2014). Persistent growth of CO₂ emissions and implications for reaching climate targets. *Nature geoscience*, 7(10), 709-715.

Garcia, M. N., Domingues, T. F., Oliveira, R. S., & Costa, F. R. (2023). The biogeography of embolism resistance across resource gradients in the Amazon. *Global Ecology and Biogeography*, 32(12), 2199-2211.

Gatti, L. V., Basso, L. S., Miller, J. B., Gloor, M., Gatti Domingues, L., Cassol, H. L., ... & Neves, R. A. (2021). Amazonia as a carbon source linked to deforestation and climate change. *Nature*, 595(7867), 388-393.

Gliniars, R., Becker, G. S., Braun, D., & Dalitz, H. (2013). Monthly stem increment in relation to climatic variables during 7 years in an East African rainforest. *Trees*, 27, 1129-1138.

Gloor, M., Barichivich, J., Ziv, G., Brienen, R., Schöngart, J., Peylin, P., ... & Baker, J. (2015). Recent Amazon climate as background for possible ongoing and future changes of Amazon humid forests. *Global Biogeochemical Cycles*, 29(9), 1384-1399.

Gourlet-Fleury, S., Rossi, V., Rejou-Mechain, M., Freycon, V., Fayolle, A., Saint-André, L., ... & Picard, N. (2011). Environmental filtering of dense-wooded species controls above-ground biomass stored in African moist forests. *Journal of Ecology*, 99(4), 981-990.

Green, J. K., Berry, J., Ciais, P., Zhang, Y., & Gentine, P. (2020). Amazon rainforest photosynthesis increases in response to atmospheric dryness. *Science Advances*, 6(47), eabb7232.

Grossiord, C., Buckley, T. N., Cernusak, L. A., Novick, K. A., Poulter, B., Siegwolf, R. T., ... & McDowell, N. G. (2020). Plant responses to rising vapor pressure deficit. *New Phytologist*, 226(6), 1550-1566.

Héroult, B., Bachelot, B., Poorter, L., Rossi, V., Bongers, F., Chave, J., ... & Baraloto, C. (2011). Functional traits shape ontogenetic growth trajectories of rain forest tree species. *Journal of ecology*, 99(6), 1431-1440.

Hijmans, R. J., Cameron, S. E., Parra, J. L., Jones, P. G., & Jarvis, A. (2005). Very high resolution interpolated climate surfaces for global land areas. *International Journal of Climatology: A Journal of the Royal Meteorological Society*, 25(15), 1965-1978.

Hodnett, M. G., & Tomasella, J. (2002). Marked differences between van Genuchten soil water-retention parameters for temperate and tropical soils: a new water-retention pedo-transfer functions developed for tropical soils. *Geoderma*, *108*(3-4), 155-180.

Houghton, R. A., Lawrence, K. T., Hackler, J. L., & Brown, S. (2001). The spatial distribution of forest biomass in the Brazilian Amazon: a comparison of estimates. *Global Change Biology*, *7*(7), 731-746.

Houghton, R. A. (2003). Why are estimates of the terrestrial carbon balance so different?. *Global change biology*, *9*(4), 500-509.

Houghton, R. A. (2005). Aboveground forest biomass and the global carbon balance. *Global change biology*, *11*(6), 945-958.

Houghton, R. A., Hall, F., & Goetz, S. J. (2009). Importance of biomass in the global carbon cycle. *Journal of Geophysical Research: Biogeosciences*, *114*(G2).

Hughes, R. F., Asner, G. P., Mascaro, J., Uowolo, A., & Baldwin, J. (2014). Carbon storage landscapes of lowland Hawaii: the role of native and invasive species through space and time. *Ecological Applications*, *24*(4), 716-731.

Junk, W. J., Piedade, M. T. F., Schöngart, J., Cohn-Haft, M., Adeney, J. M., & Wittmann, F. (2011). A classification of major naturally-occurring Amazonian lowland wetlands. *Wetlands*, *31*, 623-640.

Konings, A. G., Williams, A. P., & Gentine, P. (2017). Sensitivity of grassland productivity to aridity controlled by stomatal and xylem regulation. *Nature Geoscience*, *10*(4), 284-288.

Lambers, H. (2022). Phosphorus acquisition and utilization in plants. *Annual Review of Plant Biology*, *73*, 17-42.

Lambers, H., & Shane, M. W. (2007). Role of root clusters in phosphorus acquisition and increasing biological diversity in agriculture. *Frontis*, 235-248.

Laurance, S. G., Laurance, W. F., Nascimento, H. E., Andrade, A., Fearnside, P. M., Rebello, E. R., & Condit, R. (2009). Long-term variation in Amazon forest dynamics. *Journal of Vegetation Science*, *20*(2), 323-333.

Laurance, W. F., Fearnside, P. M., Laurance, S. G., Delamonica, P., Lovejoy, T. E., Rankin-de Merona, J. M., ... & Gascon, C. (1999). Relationship between soils and Amazon forest biomass: a landscape-scale study. *Forest ecology and management*, 118(1-3), 127-138.

Lieberman, D., Lieberman, M., Peralta, R., & Hartshorn, G. S. (1985). Mortality patterns and stand turnover rates in a wet tropical forest in Costa Rica. *The Journal of Ecology*, 915-924.

Lin, L., Comita, L. S., Zheng, Z., & Cao, M. (2012). Seasonal differentiation in density-dependent seedling survival in a tropical rain forest. *Journal of Ecology*, 100(4), 905-914.

Liu, X., Zhang, Y., Xiao, T., Li, P., Zhang, L., Liu, Y., & Deng, W. (2023). Runoff velocity controls soil nitrogen leaching in subtropical restored forest in southern China. *Forest Ecology and Management*, 548, 121412.

Lloyd, J., & Farquhar, G. D. (2008). Effects of rising temperatures and [CO₂] on the physiology of tropical forest trees. *Philosophical Transactions of the Royal Society B: Biological Sciences*, 363(1498), 1811-1817.

López, J., Way, D. A., & Sadok, W. (2021). Systemic effects of rising atmospheric vapor pressure deficit on plant physiology and productivity. *Global Change Biology*, 27(9), 1704-1720.

Malhi, Y. (2012). The productivity, metabolism and carbon cycle of tropical forest vegetation. *Journal of Ecology*, 100(1), 65-75.

Malhi, Y., Baker, T. R., Phillips, O. L., Almeida, S., Alvarez, E., Arroyo, L., ... & Lloyd, J. (2004). The above-ground coarse wood productivity of 104 Neotropical forest plots. *Global change biology*, 10(5), 563-591.

Malhi, Y., Doughty, C. E., Goldsmith, G. R., Metcalfe, D. B., Girardin, C. A., Marthews, T. R., ... & Phillips, O. L. (2015). The linkages between photosynthesis, productivity, growth and biomass in lowland Amazonian forests. *Global Change Biology*, 21(6), 2283-2295.

Marca-Zevallos, M. J., Moulatlet, G. M., Sousa, T. R., Schietti, J., Coelho, L. D. S., Ramos, J. F., ... & Costa, F. R. (2022). Local hydrological conditions influence tree diversity and composition across the Amazon basin. *Ecography*, 2022(11), e06125.

Marengo, J. A. (2004). Interdecadal variability and trends of rainfall across the Amazon basin. *Theoretical and applied climatology*, 78, 79-96.

Marengo, J. A. (2006). On the hydrological cycle of the Amazon Basin: A historical review and current state-of-the-art. *Revista brasileira de meteorologia*, 21(3), 1-19.

Marengo, J. A., & Espinoza, J. C. (2016). Extreme seasonal droughts and floods in Amazonia: causes, trends and impacts. *International Journal of Climatology*, 36(3), 1033-1050.

Markesteyn, L., Poorter, L., Bongers, F., Paz, H., & Sack, L. (2011). Hydraulics and life history of tropical dry forest tree species: coordination of species' drought and shade tolerance. *New phytologist*, 191(2), 480-495.

Marklund L. 2009. Topographical control of groundwater flow. PhD Thesis, Department of Land and Water Resources Engineering. Royal Institute of Technology, Stockholm, Sweden.

Martins, D. L., Schiatti, J., Feldpausch, T. R., Luizão, F. J., Phillips, O. L., Andrade, A., ... & Quesada, C. A. (2015). Soil-induced impacts on forest structure drive coarse woody debris stocks across central Amazonia. *Plant Ecology & Diversity*, 8(2), 229-241.

McDowell, N. G., & Allen, C. D. (2015). Darcy's law predicts widespread forest mortality under climate warming. *Nature Climate Change*, 5(7), 669-672.

McDowell, N., Allen, C. D., Anderson-Teixeira, K., Brando, P., Brienens, R., Chambers, J., ... & Xu, X. (2018). Drivers and mechanisms of tree mortality in moist tropical forests. *New Phytologist*, 219(3), 851-869.

McDowell, N. G., Sapes, G., Pivovarov, A., Adams, H. D., Allen, C. D., Anderegg, W. R., ... & Xu, C. (2022). Mechanisms of woody-plant mortality under rising drought, CO₂ and vapour pressure deficit. *Nature Reviews Earth & Environment*, 3(5), 294-308.

McGregor, I. R., Helcoski, R., Kunert, N., Tepley, A. J., Gonzalez-Akre, E. B., Herrmann, V., ... & Anderson-Teixeira, K. J. (2021). Tree height and leaf drought tolerance traits shape growth responses across droughts in a temperate broadleaf forest. *New Phytologist*, 231(2), 601-616.

McLaughlin, B. C., Ackerly, D. D., Klos, P. Z., Natali, J., Dawson, T. E., & Thompson, S. E. (2017). Hydrologic refugia, plants, and climate change. *Global change biology*, 23(8), 2941-2961.

Meinzer, F. C., Andrade, J. L., Goldstein, G., Holbrook, N. M., Cavelier, J., & Jackson, P. (1997). Control of transpiration from the upper canopy of a tropical forest: the role of stomatal,

boundary layer and hydraulic architecture components. *Plant, Cell & Environment*, 20(10), 1242-1252.

Mencuccini, M., Martínez-Vilalta, J., Vanderklein, D., Hamid, H. A., Korakaki, E., Lee, S., & Michiels, B. (2005). Size-mediated ageing reduces vigour in trees. *Ecology letters*, 8(11), 1183-1190.

Mitchard, E. T., Feldpausch, T. R., Brienen, R. J., Lopez-Gonzalez, G., Monteagudo, A., Baker, T. R., ... & Phillips, O. L. (2014). Markedly divergent estimates of Amazon forest carbon density from ground plots and satellites. *Global ecology and biogeography*, 23(8), 935-946.

Motta Paca, V. H., Espinoza-Dávalos, G. E., Moreira, D. M., & Comair, G. (2020). Variability of trends in precipitation across the Amazon River Basin determined from the CHIRPS precipitation product and from station records. *Water*, 12(5), 1244.

Moulatlet, G. M., Costa, F. R., Rennó, C. D., Emilio, T., & Schiatti, J. (2014). Local hydrological conditions explain floristic composition in lowland Amazonian forests. *Biotropica*, 46(4), 395-403.

Muller-Landau, H. C. (2004). Interspecific and inter-site variation in wood specific gravity of tropical trees. *Biotropica*, 36(1), 20-32.

Negrón-Juárez, R. I., Koven, C. D., Riley, W. J., Knox, R. G., & Chambers, J. Q. (2015). Observed allocations of productivity and biomass, and turnover times in tropical forests are not accurately represented in CMIP5 Earth system models. *Environmental Research Letters*, 10(6), 064017.

Nimer, E. (1989). Climatologia do brasil. *IBGE*.

Nobre, C. A., Sampaio, G., Borma, L. S., Castilla-Rubio, J. C., Silva, J. S., & Cardoso, M. (2016). Land-use and climate change risks in the Amazon and the need of a novel sustainable development paradigm. *Proceedings of the National Academy of Sciences*, 113(39), 10759-10768.

Nogueira, E. M., Nelson, B. W., & Fearnside, P. M. (2006). Volume and biomass of trees in central Amazonia: influence of irregularly shaped and hollow trunks. *Forest Ecology and Management*, 227(1-2), 14-21.

Nogueira, E. M., Fearnside, P. M., Nelson, B. W., & França, M. B. (2007). Wood density in forests of Brazil's 'arc of deforestation': Implications for biomass and flux of carbon from land-use change in Amazonia. *Forest ecology and management*, 248(3), 119-135.

Nogueira, E. M., Fearnside, P. M., & Nelson, B. W. (2008). Normalization of wood density in biomass estimates of Amazon forests. *Forest Ecology and Management*, 256(5), 990-996.

Novick, K. A., Ficklin, D. L., Stoy, P. C., Williams, C. A., Bohrer, G., Oishi, A. C., ... & Phillips, R. P. (2016). The increasing importance of atmospheric demand for ecosystem water and carbon fluxes. *Nature climate change*, 6(11), 1023-1027.

Olson, M. E., Soriano, D., Rosell, J. A., Anfodillo, T., Donoghue, M. J., Edwards, E. J., ... & Méndez-Alonzo, R. (2018). Plant height and hydraulic vulnerability to drought and cold. *Proceedings of the National Academy of Sciences*, 115(29), 7551-7556.

Ometto, J. P., Aguiar, A. P., Assis, T., Soler, L., Valle, P., Tejada, G., ... & Meir, P. (2015). Amazon forest biomass density maps: tackling the uncertainty in carbon emission estimates. *Uncertainties in Greenhouse Gas Inventories: Expanding Our Perspective*, 95-110.

Oren, R., Sperry, J. S., Katul, G. G., Pataki, D. E., Ewers, B. E., Phillips, N., & Schäfer, K. V. R. (1999). Survey and synthesis of intra-and interspecific variation in stomatal sensitivity to vapour pressure deficit. *Plant, cell & environment*, 22(12), 1515-1526.

Osunkoya, O. O., Sheng, T. K., MAHMUD, N. A., & Damit, N. (2007). Variation in wood density, wood water content, stem growth and mortality among twenty-seven tree species in a tropical rainforest on Borneo Island. *Austral Ecology*, 32(2), 191-201.

Paine, C. T., Baraloto, C., Chave, J., & Hérault, B. (2011). Functional traits of individual trees reveal ecological constraints on community assembly in tropical rain forests. *Oikos*, 120(5), 720-727.

Pan, Y., Birdsey, R. A., Fang, J., Houghton, R., Kauppi, P. E., Kurz, W. A., ... & Hayes, D. (2011). A large and persistent carbon sink in the world's forests. *Science*, 333(6045), 988-993.

Pansini, S., Sampaio, A. F., Reis, N. F. C., Quesada, C. A. N., de Andrade, R. T. G., & Manzatto, A. G. (2016). Riqueza e seletividade de palmeiras ao longo de gradientes ambientais na região do interflúvio Purus-Madeira em Porto Velho, RO. *Biota Amazônia (Biote Amazonie, Biota Amazonia, Amazonian Biota)*, 6(2), 93-100.

- Paoli, G. D., Curran, L. M., & Slik, J. W. F. (2008). Soil nutrients affect spatial patterns of aboveground biomass and emergent tree density in southwestern Borneo. *Oecologia*, *155*, 287-299.
- Parolin, P., Lucas, C., Piedade, M. T. F., & Wittmann, F. (2010). Drought responses of flood-tolerant trees in Amazonian floodplains. *Annals of botany*, *105*(1), 129-139.
- Peel, M. C., Finlayson, B. L., & McMahon, T. A. (2007). Updated world map of the Köppen-Geiger climate classification. *Hydrology and earth system sciences*, *11*(5), 1633-1644.
- Phillips, O. L., & Gentry, A. H. (1994). Increasing turnover through time in tropical forests. *Science*, *263*(5149), 954-958.
- Phillips, O. L., Baker, T. R., Arroyo, L., Higuchi, N., Killeen, T. J., Laurance, W. A. E., ... & Vinceti, B. (2004). Pattern and process in Amazon tree turnover, 1976–2001. *Philosophical Transactions of the Royal Society of London. Series B: Biological Sciences*, *359*(1443), 381-407.
- Phillips, O. L., Lewis, S. L., Baker, T. R., Chao, K. J., & Higuchi, N. (2008). The changing Amazon forest. *Philosophical Transactions of the Royal Society B: Biological Sciences*, *363*(1498), 1819-1827.
- Phillips, O. L., Aragão, L. E., Lewis, S. L., Fisher, J. B., Lloyd, J., López-González, G., ... & Torres-Lezama, A. (2009). Drought sensitivity of the Amazon rainforest. *Science*, *323*(5919), 1344-1347.
- Piedade, M. T. F., Schöngart, J., & Junk, W. J. (2005). O manejo sustentável das áreas alagáveis da Amazônia Central e as comunidades de herbáceas aquáticas. *Uakari*, *1*(1), 29-38.
- Piedade, M. T., Ferreira, C. S., Wittmann, A. D. O., Buckeridge, M., & Parolin, P. (2011). Biochemistry of Amazonian floodplain trees. *Amazonian floodplain forests: ecophysiology, biodiversity and sustainable management*, 127-139.
- Poorter, L., van der Sande, M. T., Thompson, J., Arets, E. J., Alarcón, A., Álvarez-Sánchez, J., ... & Peña-Claros, M. (2015). Diversity enhances carbon storage in tropical forests. *Global Ecology and Biogeography*, *24*(11), 1314-1328.
- Poorter, L., Bongers, F., Aide, T. M., Almeyda Zambrano, A. M., Balvanera, P., Becknell, J. M., ... & Rozendaal, D. M. (2016). Biomass resilience of Neotropical secondary forests. *Nature*, *530*(7589), 211-214.

Quesada, C. A., Lloyd, J., Schwarz, M., Baker, T. R., Phillips, O. L., Patiño, S., ... & Ramírez, H. (2009). Regional and large-scale patterns in Amazon forest structure and function are mediated by variations in soil physical and chemical properties. *Biogeosciences Discussion*, 6, 3993-4057.

Quesada, C. A., Lloyd, J., Schwarz, M., Patiño, S., Baker, T. R., Czimczik, C., ... & Paiva, R. (2010). Variations in chemical and physical properties of Amazon forest soils in relation to their genesis. *Biogeosciences*, 7(5), 1515-1541.

Quesada, C. A., Lloyd, J., Anderson, L. O., Fyllas, N. M., Schwarz, M., & Czimczik, C. I. (2011). Soils of Amazonia with particular reference to the RAINFOR sites. *Biogeosciences*, 8(6), 1415-1440.

Quesada, C. A., Phillips, O. L., Schwarz, M., Czimczik, C. I., Baker, T. R., Patiño, S., ... & Lloyd, J. (2012). Basin-wide variations in Amazon forest structure and function are mediated by both soils and climate. *Biogeosciences*, 9(6), 2203-2246.

RADAMBRASIL. (1978). Folha SC.20—Porto Velho: Levantamento de Recursos Naturais. Rio de Janeiro: Ministério das Minas e Energia, Departamento Nacional da Produção Mineral.

Ramírez Méndez, C. (2018). Influência do El Niño 2015-2016 no incremento diamétrico das árvores da Amazônia Central. Master dissertation, Instituto Nacional de Pesquisas da Amazônia, Manaus, Amazonas, Brasil.

Restaino, C. M., Peterson, D. L., & Littell, J. (2016). Increased water deficit decreases Douglas fir growth throughout western US forests. *Proceedings of the National Academy of Sciences*, 113(34), 9557-9562.

Rodriguez, E., Morris, C. S., & Belz, J. E. (2006). A global assessment of the SRTM performance. *Photogrammetric Engineering & Remote Sensing*, 72(3), 249-260.

Roebroek, C. T., Melsen, L. A., Hoek van Dijke, A. J., Fan, Y., & Teuling, A. J. (2020). Global distribution of hydrologic controls on forest growth. *Hydrology and Earth System Sciences*, 24(9), 4625-4639.

Rossetti, D., de Toledo, P. M., & Góes, A. M. (2005). New geological framework for Western Amazonia (Brazil) and implications for biogeography and evolution. *Quaternary research*, 63(1), 78-89.

Rowe, N., & Speck, T. (2005). Plant growth forms: an ecological and evolutionary perspective. *New phytologist*, *166*(1), 61-72.

Rowland, L., Hill, T. C., Stahl, C., Siebicke, L., Burban, B., Zaragoza-Castells, J., ... & Williams, M. (2014). Evidence for strong seasonality in the carbon storage and carbon use efficiency of an Amazonian forest. *Global Change Biology*, *20*(3), 979-991.

Rozendaal, D. M., & Zuidema, P. A. (2011). Dendroecology in the tropics: a review. *Trees*, *25*(1), 3-16.

Salati, E., & Vose, P. B. (1984). Amazon basin: a system in equilibrium. *Science*, *225*(4658), 129-138.

Santiago, L. S., Goldstein, G., Meinzer, F. C., Fisher, J. B., Machado, K., Woodruff, D., & Jones, T. (2004). Leaf photosynthetic traits scale with hydraulic conductivity and wood density in Panamanian forest canopy trees. *Oecologia*, *140*, 543-550.

Schiatti, J., Martins, D., Emilio, T., Souza, P. F., Levis, C., Baccaro, F. B., ... & Magnusson, W. E. (2016). Forest structure along a 600 km transect of natural disturbances and seasonality gradients in central-southern Amazonia. *Journal of Ecology*, *104*(5), 1335-1346.

Schöngart, J., Piedade, M. T. F., Ludwigshausen, S., Horna, V., & Worbes, M. (2002). Phenology and stem-growth periodicity of tree species in Amazonian floodplain forests. *Journal of Tropical Ecology*, *18*(4), 581-597.

Schöngart, J., Junk, W. J., Piedade, M. T. F., Ayeares, J. M., Hüttermann, A., & Worbes, M. (2004). Teleconnection between tree growth in the Amazonian floodplains and the El Niño–Southern Oscillation effect. *Global Change Biology*, *10*(5), 683-692.

Schöngart, J., Piedade, M. T. F., Wittmann, F., Junk, W. J., & Worbes, M. (2005). Wood growth patterns of *Macaranga acaciifolia* (Benth.) Benth.(Fabaceae) in Amazonian black-water and white-water floodplain forests. *Oecologia*, *145*, 454-461.

Schöngart, J., & Wittmann, F. (2011). Biomass and net primary production of central Amazonian floodplain forests. *Amazonian floodplain forests: Ecophysiology, biodiversity and sustainable management*, 347-388.

Sheil, D., Eastaugh, C. S., Vlam, M., Zuidema, P. A., Groenendijk, P., van der Sleen, P., ... & Vanclay, J. (2017). Does biomass growth increase in the largest trees? Flaws, fallacies and alternative analyses. *Functional Ecology*, *31*(3), 568-581.

Silver, W. L. (1994). Is nutrient availability related to plant nutrient use in humid tropical forests?. *Oecologia*, 98, 336-343.

Sombroek, W. (2000). Amazon landforms and soils in relation to biological diversity. *Acta Amazonica*, 30, 81-81.

Sousa, T. R., Schiatti, J., Coelho de Souza, F., Esquivel-Muelbert, A., Ribeiro, I. O., Emílio, T., ... & Costa, F. R. (2020). Palms and trees resist extreme drought in Amazon forests with shallow water tables. *Journal of Ecology*, 108(5), 2070-2082.

Sousa, T. R., Schiatti, J., Ribeiro, I. O., Emílio, T., Fernández, R. H., Ter Steege, H., ... & Costa, F. R. (2022). Water table depth modulates productivity and biomass across Amazonian forests. *Global ecology and biogeography*, 31(8), 1571-1588.

Sperry, J. S., Meinzer, F. C., & McCulloh, K. A. (2008). Safety and efficiency conflicts in hydraulic architecture: scaling from tissues to trees. *Plant, Cell & Environment*, 31(5), 632-645.

Stadtler, E. W. C. (2007). Estimativas de biomassa lenhosa, estoque e seqüestro de carbono acima do solo ao longo do gradiente de inundação em uma floresta de igapó alagada por água preta na Amazônia Central, Master Dissertation, Instituto Nacional de Pesquisas da Amazônia, Manaus, Brasil.

Stahl, C., Hérault, B., Rossi, V., Burban, B., Bréchet, C., & Bonal, D. (2013). Depth of soil water uptake by tropical rainforest trees during dry periods: does tree dimension matter?. *Oecologia*, 173(4), 1191-1201

Sterck, F., Markesteijn, L., Schieving, F., & Poorter, L. (2011). Functional traits determine trade-offs and niches in a tropical forest community. *Proceedings of the National Academy of Sciences*, 108(51), 20627-20632.

Suzuki, E. (1999). Diversity in specific gravity and water content of wood among Bornean tropical rainforest trees. *Ecological research*, 14(3), 211-224.

Ter Steege, H., Pitman, N. C., Phillips, O. L., Chave, J., Sabatier, D., Duque, A., ... & Vásquez, R. (2006). Continental-scale patterns of canopy tree composition and function across Amazonia. *Nature*, 443(7110), 444-447.

Ter Steege, H., Pitman, N. C., Sabatier, D., Baraloto, C., Salomão, R. P., Guevara, J. E., ... & Silman, M. R. (2013). Hyperdominance in the Amazonian tree flora. *Science*, *342*(6156), 1243092.

Thomas, S. C., Frye, S., Gale, N., Garmon, M., Launchbury, R., Machado, N., ... & Winsborough, C. (2013). Biochar mitigates negative effects of salt additions on two herbaceous plant species. *Journal of Environmental Management*, *129*, 62-68.

Tomasella, J., Hodnett, M. G., Cuartas, L. A., Nobre, A. D., Waterloo, M. J., & Oliveira, S. M. (2008). The water balance of an Amazonian micro-catchment: the effect of interannual variability of rainfall on hydrological behaviour. *Hydrological Processes: An International Journal*, *22*(13), 2133-2147.

Tyearee, M. T., & Zimmermann, M. H. (2013). Xylem structure and the ascent of sap. *Springer Science & Business Media*.

Van der Sande, M. T., Zuidema, P. A., & Sterck, F. (2015). Explaining biomass growth of tropical canopy trees: the importance of sapwood. *Oecologia*, *177*, 1145-1155.

Van Schaik, C. P., & Mirmanto, E. (1985). Spatial variation in the structure and litterfall of a Sumatran rain forest. *Biotropica*, 196-205.

Vieira, S., de Camargo, P. B., Selhorst, D., Da Silva, R., Hutyeara, L., Chambers, J. Q., ... & Martinelli, L. A. (2004). Forest structure and carbon dynamics in Amazonian tropical rain forests. *Oecologia*, *140*, 468-479.

Vilanova, E., Ramirez-Angulo, H., Torres-Lezama, A., Aymard, G., Gamez, L., Duran, C., ... & Ettl, G. J. (2018). Environmental drivers of forest structure and stem turnover across Venezuelan tropical forests. *PLoS One*, *13*(6), e0198489.

Villa, P. M., Martins, S. V., de Oliveira Neto, S. N., Rodrigues, A. C., Hernández, E. P., & Kim, D. G. (2020). Policy forum: Shifting cultivation and agroforestry in the Amazon: Premises for REDD+. *Forest policy and economics*, *118*, 102217.

Violle, C., Navas, M. L., Vile, D., Kazakou, E., Fortunel, C., Hummel, I., & Garnier, E. (2007). Let the concept of trait be functional!. *Oikos*, *116*(5), 882-892.

Vital, B. R. (1984). Métodos de determinação da densidade da madeira. *Viçosa, MG: SIF*, 501.

Vitousek, P. M. (1984). Litterfall, nutrient cycling, and nutrient limitation in tropical forests. *Ecology*, 65(1), 285-298.

Wagner, F., Rossi, V., Stahl, C., Bonal, D., & Herault, B. (2012). Water availability is the main climate driver of neotropical tree growth. *PLoS one*, 7(4), e34074.

Walker, T. W., & Syers, J. K. (1976). The fate of phosphorus during pedogenesis. *Geoderma*, 15(1), 1-19.

Wang, X., Comita, L. S., Hao, Z., Davies, S. J., Ye, J., Lin, F., & Yuan, Z. (2012). Local-scale drivers of tree survival in a temperate forest. *PLoS One*, 7(2), e29469.

Whitmore, T. C., & Burslem, D. F. R. P. (1998). Major disturbances in tropical rainforests. *Major disturbances in tropical rainforests.*, 549-565.

Wiemann, M. C., & Williamson, G. B. (2002). Geographic variation in wood specific gravity: effects of latitude, temperature, and precipitation. *Wood and fiber science*, 96-107.

Wittmann, F., Schöngart, J., & Junk, W. J. (2011). Phytogeography, species diversity, community structure and dynamics of central Amazonian floodplain forests. *Amazonian floodplain forests: ecophysiology, biodiversity and sustainable management*, 61-102.

Woodcock, D. W., & Shier, A. D. (2003). Does canopy position affect wood specific gravity in temperate forest trees?. *Annals of botany*, 91(5), 529-537.

Worbes, M. (1999). Annual growth rings, rainfall-dependent growth and long-term growth patterns of tropical trees from the Caparo Forest Reserve in Venezuela. *Journal of ecology*, 87(3), 391-403.

Worbes, M. (2002). One hundred years of tree-ring research in the tropics—a brief history and an outlook to future challenges. *Dendrochronologia*, 20(1-2), 217-231.

Wright, S. J., Kitajima, K., Kraft, N. J., Reich, P. B., Wright, I. J., Bunker, D. E., ... & Zanne, A. E. (2010). Functional traits and the growth–mortality trade-off in tropical trees. *Ecology*, 91(12), 3664-3674.

Zanne, A. E., Lopez-Gonzalez, G., Coomes, D. A., Ilic, J., Jansen, S., Lewis, S. L., ... & Chave, J. (2009). Global wood density database. Data from: Towards a worldwide wood economics spectrum. *Dryad Digital Repository*.

Zhao, M., & Running, S. W. (2010). Drought-induced reduction in global terrestrial net primary production from 2000 through 2009. *science*, 329(5994), 940-943.

Zhou, L., Wang, Y., Jia, Q., Li, R., Zhou, M., & Zhou, G. (2019). Evapotranspiration over a rainfed maize field in northeast China: How are relationships between the environment and terrestrial evapotranspiration mediated by leaf area?. *Agricultural Water Management*, 221, 538-546.

Zuidema, P. A., Brien, R. J., During, H. J., & Güneralp, B. (2009). Do persistently fast-growing juveniles contribute disproportionately to population growth? A new analysis tool for matrix models and its application to rainforest trees. *The American Naturalist*, 174(5), 709-719.

Zuidema, P. A., Brien, R. J., & Schöngart, J. (2012). Tropical forest warming: looking backwards for more insights. *Trends in ecology & evolution*, 27(4), 193-194.

Zuidema, P. A., Babst, F., Groenendijk, P., Trouet, V., Abiyu, A., Acuña-Soto, R., ... & Zhou, Z. K. (2022). Tropical tree growth driven by dry-season climate variability. *Nature Geoscience*, 15(4), 269-276.

TABELAS
E
FIGURAS

Table 4: Summary of dendrometric metrics in each investigated site along the Purus-Madeira interfluve, in central-south Amazonia. Plot identification (Plot Id.), mean aboveground biomass increments (MABI), mean diameter increments (MDI), and mean values of diameter at breast height (DBH), estimated height (m) and wood density (g/cm^3). Values calculated over 16 to 23 canopy trees sampled in each plot.

Site	Plot Id.	MABI (kg/year^{-1})	MDI (mm/year^{-1})	DBH (cm)	EH (m)	WD (g/cm^3)
M01	M01_TN_0500	23.08	2.96	40.37	22.89	0.68
M01	M01_TN_1500	39.28	6.86	42.79	24.65	0.7
M01	M01_TN_2500	29.46	5.16	42.58	24.1	0.65
M01	M01_TN_3500	17.28	2.44	42.38	23.44	0.66
M01	M01_TN_4500	23.6	3.60	41.95	23.57	0.62
M02	M02_TN_0500	25.86	4.45	43.64	24.33	0.71
M02	M02_TN_1500	20.19	2.42	43.11	24.08	0.75
M02	M02_TN_2500	23.05	2.35	41.96	23.96	0.78
M02	M02_TN_3500	24.93	3.16	41.61	23.99	0.79
M02	M02_TN_4500	21.39	3.08	38.7	23.26	0.77
M03	M03_TS_1500	20.07	1.52	36.44	23.52	0.92
M03	M03_TS_2500	19.95	2.27	49.3	20.93	0.76
M03	M03_TS_3500	18.13	3.46	36.82	21.4	0.9
M03	M03_TS_4500	22.73	2.90	38.05	21.1	0.76
M04	M04_TN_(-)0500	14.51	2.94	34.81	20.43	0.69
M04	M04_TN_0500	15.84	2.91	35.88	20.64	0.72
M04	M04_TN_1500	18.08	2.31	36.19	20.71	0.78
M04	M04_TN_2500	21.04	2.63	40.12	21.41	0.77
M04	M04_TN_3500	17.86	2.56	36.58	20.8	0.77
M05	M05_TN_(-)0500	19.38	3.32	34.32	21.62	0.69
M05	M05_TN_0500	17.12	2.90	36.11	21.93	0.66
M05	M05_TN_1500	19.34	2.22	42.26	23.14	0.69
M05	M05_TN_2500	15.43	2.41	32.77	20.98	0.79
M05	M05_TN_3500	22.37	2.21	39.41	22.56	0.79
M06	M06_TN_(-)0500	22.98	2.55	40.47	22.98	0.69

M06	M06_TN_0500	24.93	3.64	44.02	23.64	0.68
M06	M06_TN_1500	25.22	4.05	45.41	23.9	0.6
M06	M06_TN_2500	16.55	2.63	35.69	21.91	0.72
M06	M06_TN_3500	24.8	2.63	43.07	23.62	0.67
M07	M07_TS_0500	33.69	3.88	37.2	24.09	0.84
M07	M07_TS_1500	22.86	2.35	41.22	24.43	0.83
M07	M07_TS_2500	26.17	2.30	43.63	24.81	0.82
M07	M07_TS_3500	22.55	2.24	42.81	24.63	0.76
M07	M07_TS_4500	34.04	3.36	43.06	25.13	0.81
M08	M08_TS_0500	20.87	2.29	37.78	22.84	0.7
M08	M08_TS_1500	13.91	2.36	33.28	21.7	0.64
M08	M08_TS_2500	18.67	2.63	41.29	23.29	0.67
M08	M08_TS_3500	31.89	3.55	51.05	25.19	0.71
M08	M08_TS_4500	14.7	2.71	32.87	21.63	0.65
M09	M09_TS_0500	18.7	2.72	38.52	22.36	0.75
M09	M09_TS_1500	17.83	2.22	36.38	21.86	0.82
M09	M09_TS_2500	16.36	1.98	34.6	21.44	0.81
M09	M09_TS_3500	18.41	2.86	32.75	21.08	0.91
M09	M09_TS_4500	21.6	2.88	35.74	21.81	0.92
M10	M10_TS_0500	23.18	2.67	39.97	24.17	0.69
M10	M10_TS_1500	21.93	3.30	37.65	23.73	0.69
M10	M10_TS_2500	17.82	2.96	35.29	23.27	0.67
M10	M10_TS_3500	20.85	3.20	35.94	23.43	0.75
M10	M10_TS_4500	22.44	3.70	36.72	23.77	0.69
M11	M11_TN_0500	26.6	3.50	40.84	23.74	0.65
M11	M11_TN_1500	21.01	2.70	42.72	24.03	0.64
M11	M11_TN_2500	22.76	3.85	35.84	22.64	0.74
M11	M11_TN_3500	23.51	4.10	37.81	23.09	0.69
M11	M11_TN_4500	26.17	3.81	35.86	22.55	0.79

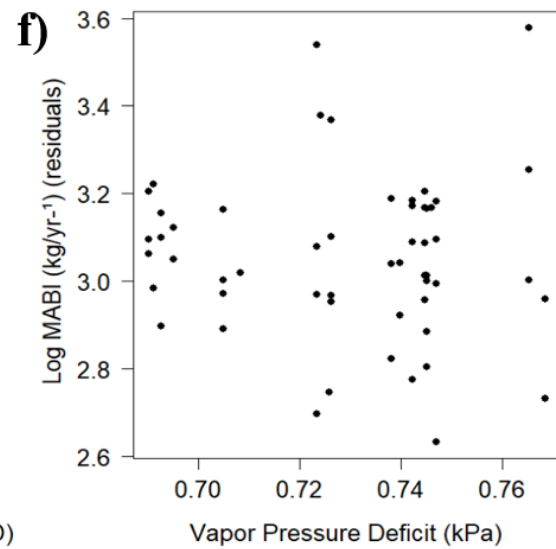
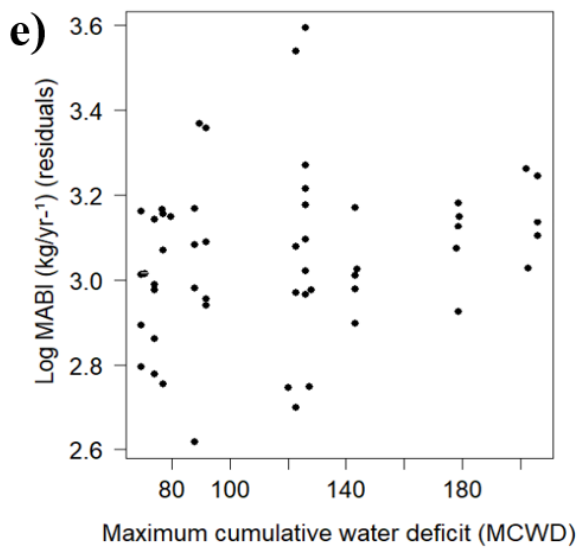
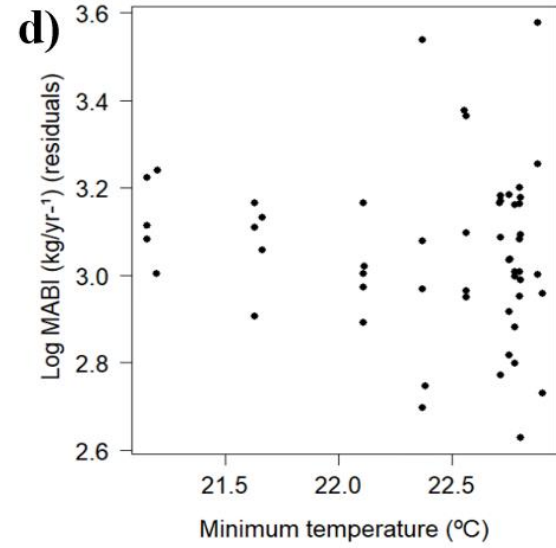
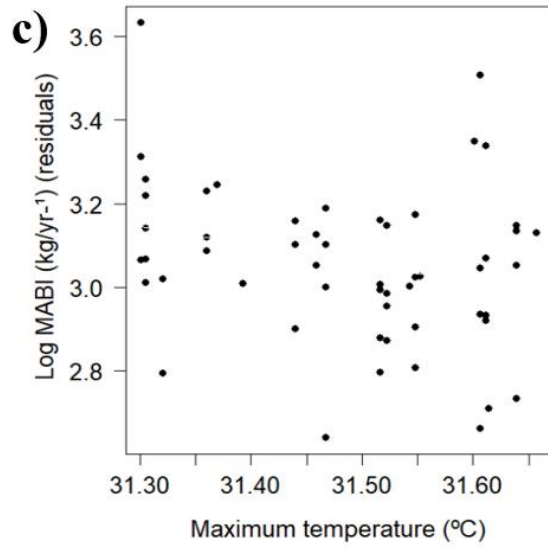
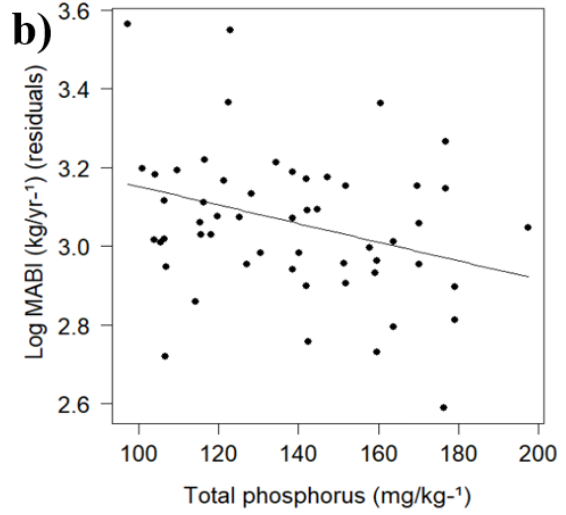
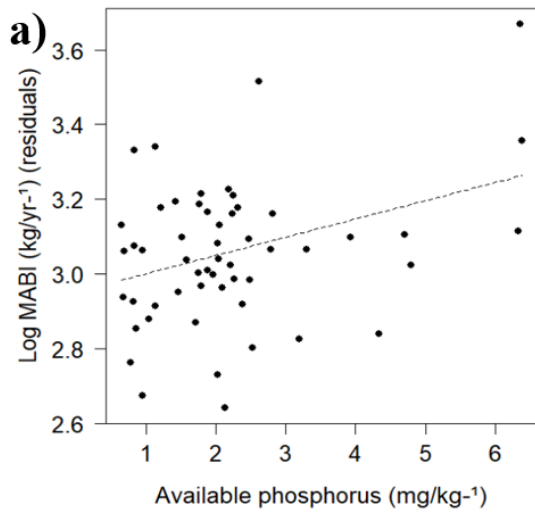


Figure 3: Partial regressions derived from the multiple regression models with higher support (see Table 2). Community-level mean increment of aboveground biomass based on individuals sampled in 54 plots along Purus-Madeira interfluvium. Partial regressions were derived from the mixed multiple regression model using the predictor variables considered in the selected models to explain the variation in above-ground biomass mean increment rates ($\text{kg}/\text{year}^{-1}$). Partial effect of: a) available phosphorus; b) total phosphorus; c) maximum temperature; d) minimum temperature; e) maximum cumulative water deficit (higher values indicate higher water deficit); and f) vapor pressure deficit (VPD). Black line represents the average trend line.

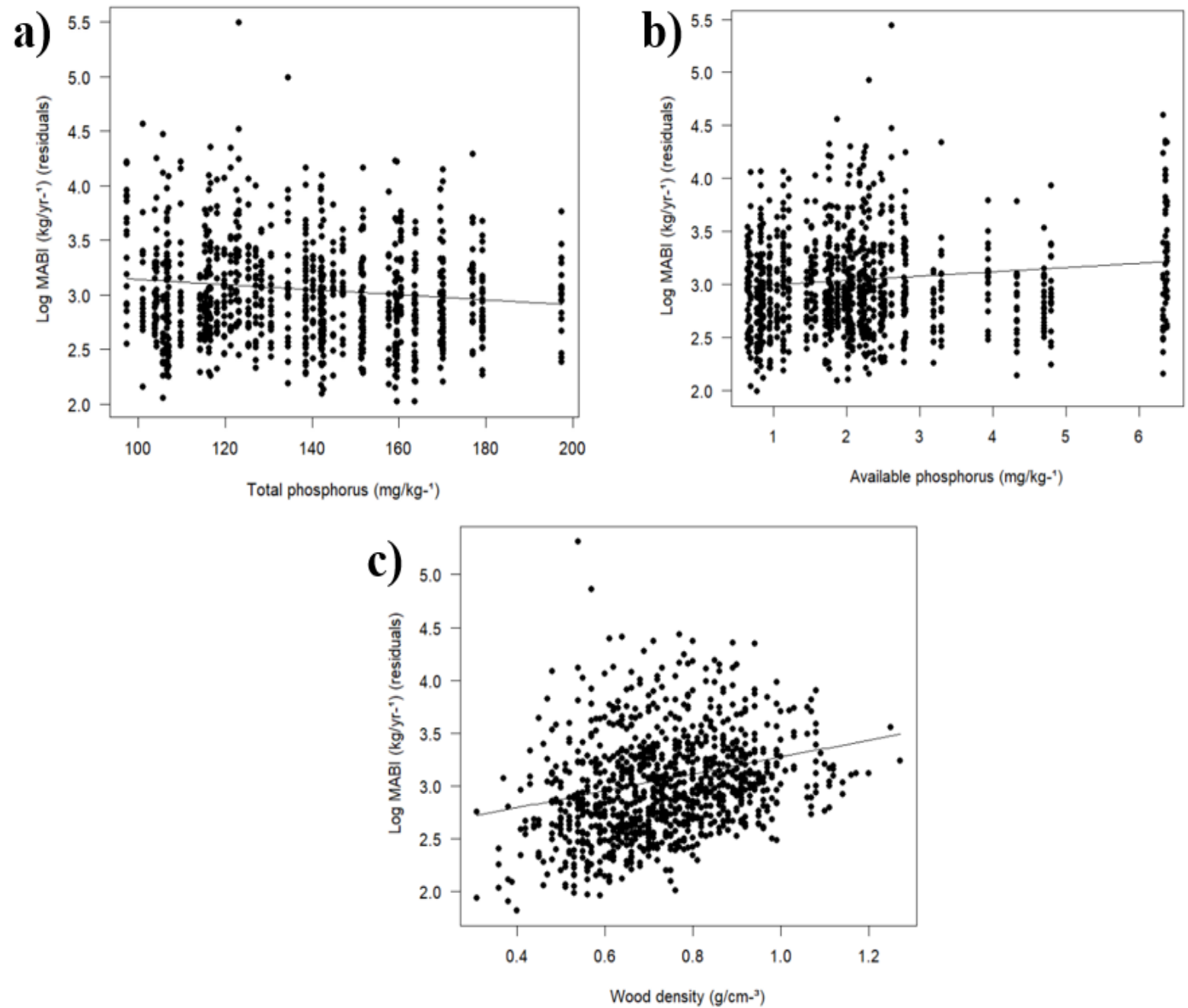


Figure 4: Partial regressions derived from the multiple regression models with higher support (see Table 3). Individual-level mean increment of aboveground biomass based on 1012 individuals along Purus-Madeira interfluvium. Partial regressions were derived from the multiple regression model using the predictor variables considered in the selected models to explain the variation in above-ground biomass mean increment rates (kg/year⁻¹). Partial effect of: a) total phosphorus; b) available phosphorus; and c) wood density. Black line represents the average trend line.

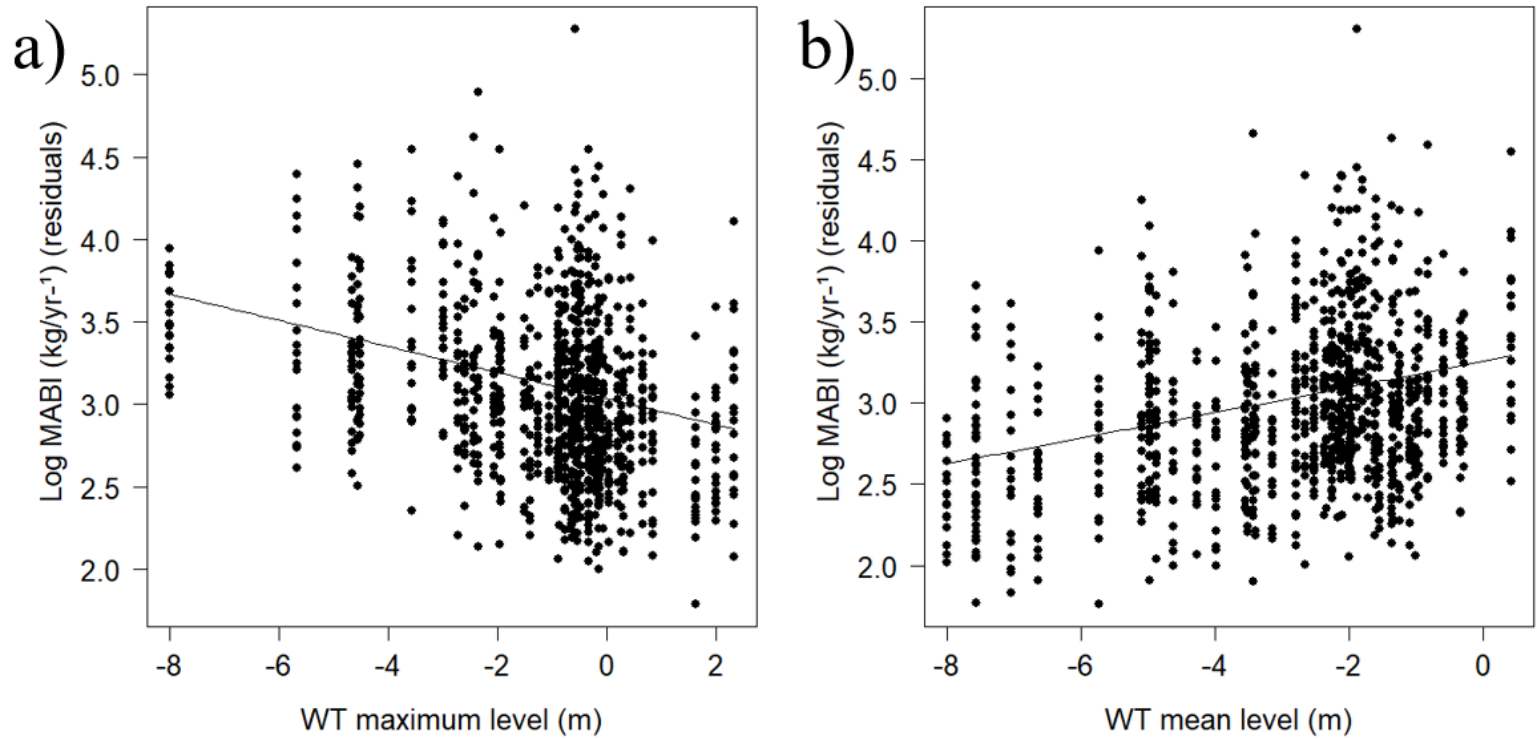


Figure 5: Partial regressions obtained from multiple regression model with Δ AIC = 2.15. Mean increment of above-ground biomass vs. water table measurements, considering 1012 individuals along the Purus-Madeira interfluve. Partial regressions were derived from the multiple regression model using predictor variables included in the selected model to elucidate the variation in mean above-ground biomass increment rates (kg/year⁻¹). Partial effects of: a) maximum water table level (m); and b) mean water table level. The black line depicts the average trend line. Negative values represent subsurface levels.

Supporting Information

Table S1: Summary of investigated variables in each site along the Purus-Madeira interfluve, in central-south Amazonia. Mean aboveground biomass increments (MABI); mean diameter increments (MDI); diameter at breast height (DBH); estimated height (m); wood density (g/cm³); vapor pressure deficit (VPD); maximum cumulative water deficit (MCWD); Maximum cumulative water excess (MCWE); water table depth (WTD) measurements (with negative values indicate subsurface depths) and soil characteristics. Bases, refers to the sum of the bases (calcium, magnesium and potassium) in exchangeable form expressed as milligram equivalents per 100 g of soil. Higher values of MCWD and MCWE indicate higher water deficit and excess, respectively.

SITE	MABI (kg/year ⁻¹)	MDI (mm/year ⁻¹)	DBH (cm)	EH (m)	WD (g/cm ³)	Age (years)	Annual precipitation (mm)	Maximum temperature (°C)	Minimum temperature (°C)	VPD (kPa)	MCWD (mm)	MCWE (mm)	WT minimum level (m)	WT maximum level (m)	WT mean level (m)	Range (m)	Standard Deviation	Available phosphorus (mg/kg ⁻¹)	Total phosphorus (mg/kg ⁻¹)	Bases (Ca ⁺⁺ , Mg ⁺⁺ , K ⁺)	Soil Index
M01	26.10	3.34	42.01	22.39	0.66	117	2226.19	31.31	22.89	0.767	126.8	910.36	-3.55	0.8	-0.99	4.35	1.44	5.34	139.82	0.31	10
M02	22.87	2.55	41.80	23.06	0.77	118	2207.34	31.31	22.8	0.745	126.2	878.89	-5.43	-0.57	-2.35	4.86	1.83	2.47	148.6	0.17	8
M03	20.36	2.84	40.15	20.90	0.81	106	2331.26	31.47	22.8	0.747	97.89	907.56	-4.91	1.25	-1.38	6.16	2.62	2.5	173.41	0.2	7
M04	17.52	2.56	36.72	19.96	0.74	114	2410.31	31.52	22.78	0.745	73.9	936.58	-2.52	-0.038	-1.07	2.14	0.75	2.04	236.99	0.17	7
M05	18.70	2.62	36.97	21.01	0.72	97	2456.6	31.55	22.75	0.739	69.8	949.2	-4.74	-1.89	-3.14	2.86	1.08	2.19	120.62	0.16	9
M06	22.79	2.88	41.73	22.25	0.67	117	2434.78	31.64	22.71	0.743	77.45	945.52	-6.18	-2.31	-3.84	3.87	1.38	1.84	123.09	0.15	6
M07	27.88	2.87	41.59	23.66	0.81	128	2535.38	31.61	22.56	0.726	91.29	869.75	-6.71	-2.27	-4.33	4.44	1.69	0.92	136.72	0.12	7
M08	20.00	2.70	39.25	21.98	0.67	113	2162.24	31.61	22.27	0.723	122.32	778.66	-4.81	-0.85	-2.33	3.96	1.47	1.59	129.54	0.13	5
M09	18.56	2.38	35.60	20.84	0.84	138	2116.37	31.53	22.11	0.706	143.35	751.11	-5.44	-0.45	-2.71	4.99	1.63	1.29	130.31	0.15	8
M10	21.29	2.88	37.11	22.73	0.7	103	2162.96	31.45	22.64	0.694	178.56	789.31	-7.39	-4.03	-6.57	3.36	1.18	1.66	126.63	0.12	3
M11	23.93	3.22	38.61	21.95	0.7	93	2202.73	31.37	21.17	0.691	204.48	816.99	-4.21	0.13	-1.9	4.35	1.71	2.68	162.83	0.13	9
MEAN	21.82	2.80	39.23	21.89	0.74	113.10	2295.11	31.49	22.50	0.73	119.28	866.72	-5.08	-0.93	-2.78	4.12	1.53	2.23	148.05	0.16	7.18

Table S2: Hydroclimatic selected variables for this study analyses and the mechanisms by which they can affect biomass increments and ultimately carbon sequestration.

Hydroclimate property	Variable selected for analysis	Mechanisms to affect biomass growth rates	References
Day-time temperature	Mean daily maximum temperature	Elevated daytime temperatures surpass the optimal conditions for photosynthesis, intensifying evaporative stress, increasing autotrophic respiration rates and evaporative demand. This, in turn, triggers stomatal closure, diminishing the time available for photosynthesis, and heightens the risk of mortality due to potential hydraulic failure and/or carbon starvation.	Clark et al., 2003, 2010; Fontes et al., 2018; Lloyd & Farquar, 2008; McDowell et al., 2018; Sullivan et al., 2020.
Night-time temperature	Mean daily minimum temperature	Higher temperatures accelerate respiration rates, possibly reducing carbon allocated to wood. Considering that respiration occurs continuously throughout day and night, while photosynthesis only happens during the day, night-time temperatures might offer a more accurate reflection of respiration effects, whereas day-time temperatures may better signify the impacts on photosynthesis.	Clark et al., 2003, 2010; Malhi, 2012; McDowell et al., 2018; Sullivan et al., 2020.
Atmosphere moisture availability	Vapor Pressure Deficit (VPD)	High VPD conditions reduce stomatal conductance and photosynthesis while simultaneously increasing plant water losses through transpiration. This defensive response results in a negative growth balance, depleting carbohydrate reserves and causing tissue-level carbohydrate starvation.	Oren et al., 1999; Fletcher et al., 2007; Barkhordarian et al., 2019; Grossiord et al., 2020; López et al., 2021.
Drought-related conditions	Maximum Cumulative Water Deficit (MCWD)	Prolonged water deficits lead to reduced photosynthesis, hindered growth, and an increased risk of mortality. Stomatal closure occurs to conserve water, limiting carbon assimilation, potentially causing hydraulic failure in xylem conduits (cavitation) and the rhizosphere, halting water flow and desiccating plant tissues.	Costa et al., 2022, 2023; Esteban et al., 2021; Esquivel-Muelbert et al., 2017, 2019; Restaino et al., 2016; Sousa et al., 2020, 2022.

Climatic water excess-related conditions	Maximum Cumulative Water Excess (MCWE)	An excess of rainfall can result in waterlogged soils, diminishing the availability of oxygen to roots and fostering anaerobic conditions. This can hinder nutrient uptake, disturb root function, and elevate the risk of diseases. While certain species adapted to flooding may thrive and continue to grow, others may cease or diminish in growth under flood conditions.	Costa et al., 2022; Esteban et al., 2021; Schöngart et al., 2002; 2004; 2011; Sousa et al., 2020, 2022.
Soil water condition	Water table depth (WTD)	Shallow water table (WT) can offer benefits by providing water to tree roots during moderate droughts; nevertheless, it also has the potential to induce anoxic conditions that hinder root respiration due to oxygen limitations resulting from increased rainfall. Conversely, deep WT do not directly influence soil water availability for trees, prompting tree roots to depend on rainfall for water supply. During drought-related conditions, deep WT are linked to diminished growth and an elevated risk of mortality, as there is a reduction in water availability for vital physiological processes.	Costa et al., 2022, 2023; Esteban et al., 2021; Sousa et al., 2020, 2022.

Table S3: Comparison between estimates of MABI (kg/year⁻¹), MDI (mm/year⁻¹) and WD (g/cm⁻³) of old-growth forests from this study, with estimates from non-flooded terra-firme, semi-evergreen forest, lowland tropical forests and whole Amazon from other studies.

	Area	MABI (kg/year⁻¹)	MDI (mm/year⁻¹)	WD (g/cm⁻³)
This Study	Purus-Madeira interfluvial region	21.87	3.02	0.73
Dias e Marengo (2016)	Central Amazonia terra-firme forest	-	2.04	0.75
van der Sande et al. (2015)	Semi-evergreen forest, Bolivia	105.4	-	-
Heráult et al. (2011)	Lowland tropical rainforest, French Guiana	-	3.31	-
Nogueira et al. (2007)	Whole Brazilian Amazonia	-	-	0.64
Vieira et al. (2004)	Central Amazonia terra-firme forest	-	1.70	-

Table S4: Partial effects of wood density (g/cm^{-3}) on elucidating the variability in the average aboveground biomass increment (gray) and mean diameter increments (white), incorporating coefficients for slope, intercept, coefficient of determination (R^2), and p-value stratified across three wood density classes.

Wood Density (g/cm^{-3})	Tree growth	Slope	Intercept	R^2	p-value
Soft (<0.50)	MABI	47.60	-3.90	0.05	0.006
	MDI	3.82	1.85	0.005	0.55
Medium (0.50-0.72)	MABI	24.80	4.86	0.01	0.01
	MDI	-0.001	3.04	0.001	0.99
Hard (>0.72)	MABI	3.99	20.32	0.001	0.43
	MDI	-0.51	3.39	0.001	0.51

Table S5: Species that were sampled in the study, specifically those with three or more individuals analyzed. It includes information on the mean diameter increments (MDI), mean biomass increments (MABI), wood density (g/cm^3), diameter at breast height (DBH) and estimated height (m).

<i>Species</i>	N° trees	MDI (mm/year⁻¹)	MABI (kg/year⁻¹)	WD (g/cm⁻³)	DBH (cm)	EH (m)
<i>Scleronema micranthum</i>	25	2.28	22.95	0.67	46.61	22.67
<i>Eperua purpurea</i>	24	2.75	29.17	0.68	54.30	24.55
<i>Brosimum utile</i>	21	2.47	21.55	0.62	47.71	22.89
<i>Chrysophyllum sanguinolentum</i>	20	3.00	18.37	0.74	39.73	21.19
<i>Licania oblongifolia</i>	16	3.05	24.00	0.96	43.17	21.18
<i>Brosimum parinarioides</i>	12	3.34	31.24	0.64	56.06	24.99
<i>Brosimum rubescens</i>	11	2.20	22.64	0.82	46.26	22.78
<i>Couma macrocarpa</i>	10	2.84	16.72	0.59	46.33	23.31
<i>Osteophloeum platyspermum</i>	10	3.11	22.22	0.57	51.99	24.05
<i>Caryocar glabrum</i>	9	2.46	20.46	0.80	41.73	21.52
<i>Carapa guianensis</i>	8	2.32	24.99	0.71	48.66	23.26

<i>Tachigali eriopetala</i>	8	2.49	15.00	0.56	40.15	20.79
<i>Goupia glabra</i>	8	4.24	30.87	0.83	45.41	22.41
<i>Micropholis guyanensis</i>	7	1.89	15.31	0.80	37.14	21.16
<i>Apeiba echinata</i>	6	3.28	22.06	0.55	47.08	22.71
<i>Erismia bicolor</i>	6	2.51	22.26	0.57	51.85	24.00
<i>Eschweilera coriacea</i>	6	3.30	22.98	0.89	45.45	23.19
<i>Licania micrantha</i>	6	3.11	16.75	0.90	33.88	19.52
<i>Simarouba amara</i>	6	6.55	24.79	0.49	42.05	20.57
<i>Hevea brasiliensis</i>	5	4.14	22.59	0.66	49.80	23.34
<i>Parkia nitida</i>	5	2.94	17.56	0.53	47.04	21.85
<i>Vochysia biloba</i>	5	3.65	10.62	0.50	36.96	19.64
<i>Anacardium parvifolium</i>	4	5.56	40.47	0.67	49.88	23.03
<i>Conceveiba guianensis</i>	4	3.09	14.65	0.66	38.63	22.10
<i>Ecclinusa guianensis</i>	4	2.90	16.96	0.76	36.53	20.55

<i>Licania discolor</i>	4	2.49	20.61	1.05	40.38	22.09
<i>Swartzia tomentifera</i>	4	2.87	17.16	0.89	35.80	20.65
<i>Abarema adenophora</i>	4	2.92	12.35	0.52	37.53	19.99
<i>Chrysophyllum ucuquirana-branca</i>	3	1.85	19.16	0.85	40.03	21.46
<i>Eschweilera tessmannii</i>	3	3.39	16.83	0.78	36.93	21.22
<i>Hevea guianensis</i>	3	3.02	16.05	0.67	40.87	21.44
<i>Hieronyma alchorneoides</i>	3	2.06	12.15	0.73	35.23	19.65
<i>Hymenaea parvifolia</i>	3	7.91	45.67	0.78	44.60	20.53
<i>Licania indet</i>	3	1.95	17.33	0.67	36.97	20.40
<i>Micrandra spruceana</i>	3	1.36	10.43	0.78	33.13	19.77
<i>Micropholis splendens</i>	3	2.85	20.71	0.80	40.03	20.77
<i>Micropholis venulosa</i>	3	4.23	26.45	0.70	46.63	23.35
<i>Moronobea coccinea</i>	3	2.51	16.78	0.79	34.63	18.84
<i>Ocotea indet</i>	3	2.36	17.77	0.64	47.23	23.96

<i>Pouteria laevigata</i>	3	4.46	21.32	0.62	44.37	22.61
<i>Tachigali amplifolia</i>	3	2.61	17.72	0.62	47.87	21.64
<i>Virola mollissima</i>	3	1.87	8.36	0.49	32.70	20.98
<i>Virola pavonis</i>	3	3.87	17.65	0.66	34.60	19.45
<i>Scleronema micranthum</i>	3	2.28	22.95	0.67	46.61	22.67

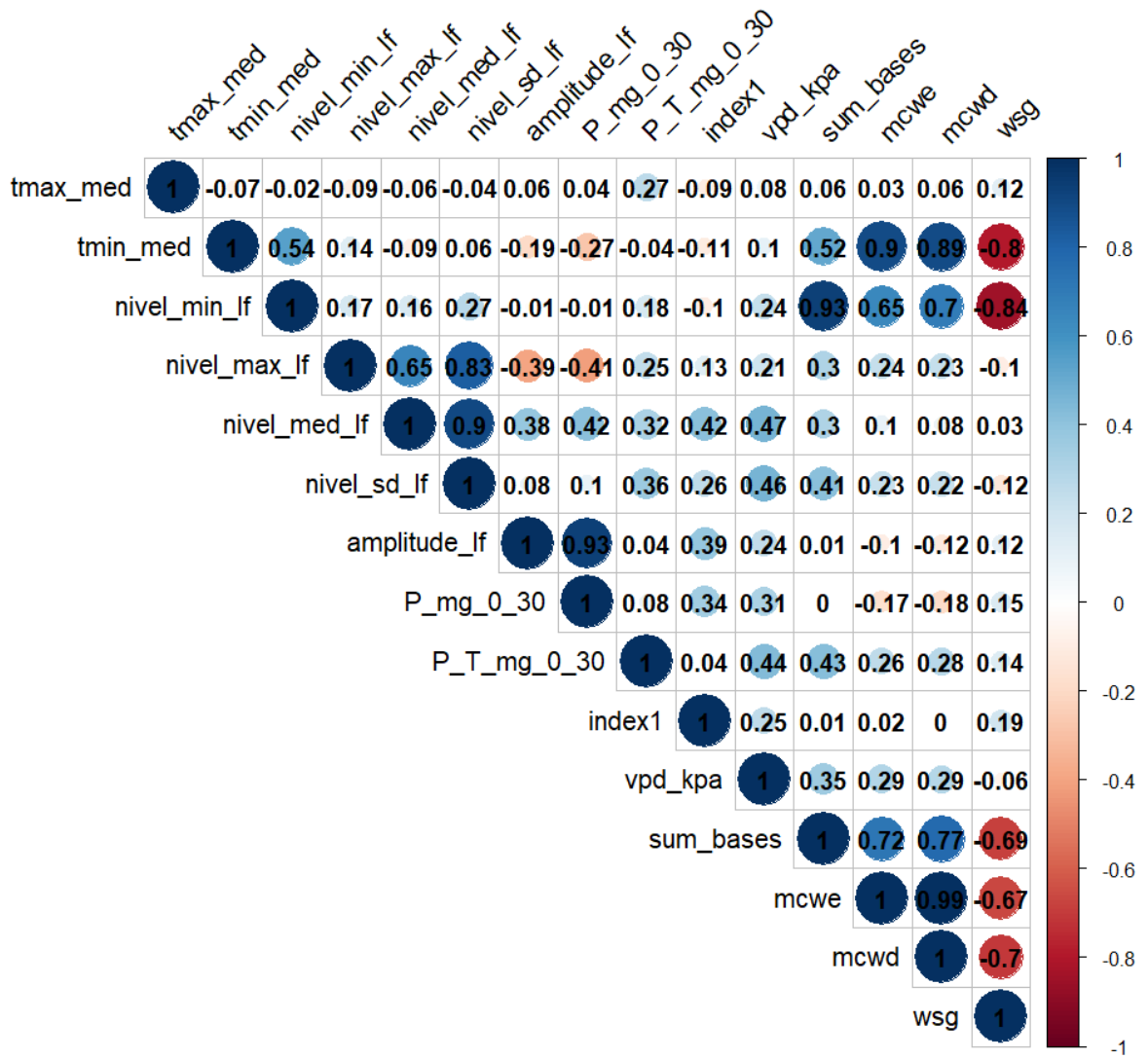


Figura S1: Pearson correlation matrix among the variables observed across the 54 studied plots.

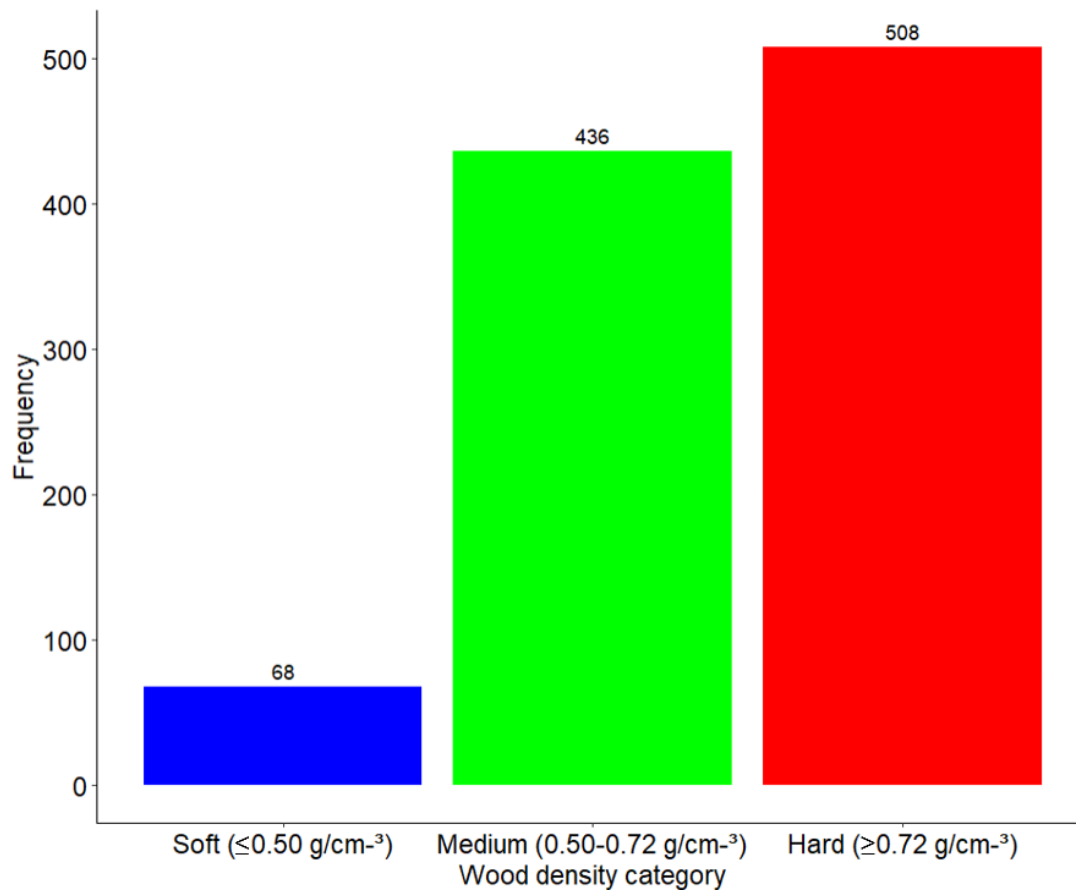


Figure S2: Boxplots illustrating the distribution of individual frequency across different wood density classes, categorized as "Soft ($\leq 0.50 \text{ g/cm}^3$)", "Medium ($0.50 - 0.72 \text{ g/cm}^3$)", and "Hard ($\geq 0.72 \text{ g/cm}^3$)", were defined based on specialized literature.

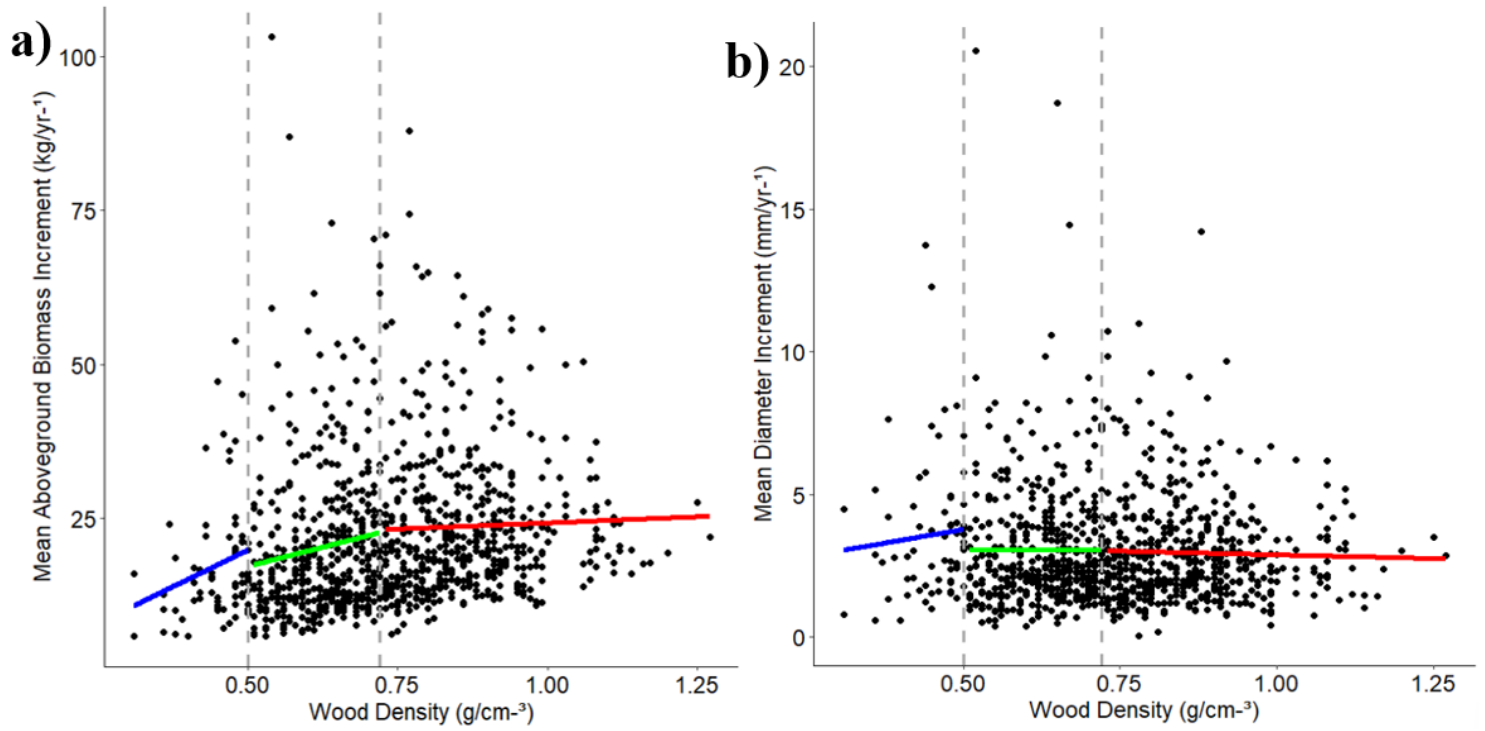
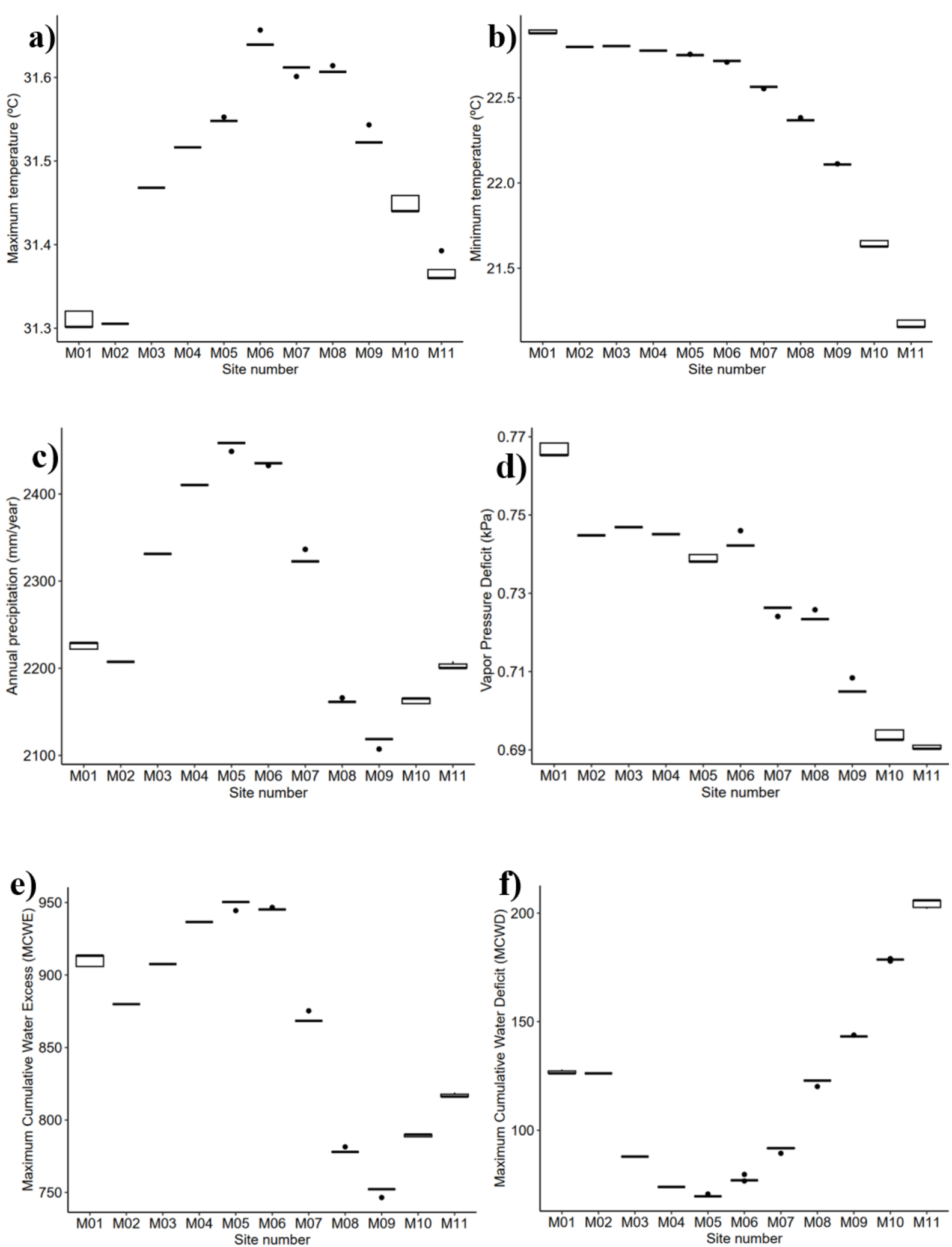


Figure S3: Simple correlation between: a) mean aboveground biomass increment and wood density; and b) mean diameter increment and wood density stratified across each density class (Soft < 0.50 g/cm⁻³ - blue line; Medium 0.50-0.72 g/cm⁻³ - green line; Hard > 0.72 g/cm⁻³ - red line). a) There is a significant positive overall trend ($\beta = 0.13$, $p = 0.001$). b) There is no significant overall trend ($p = 0.55$).



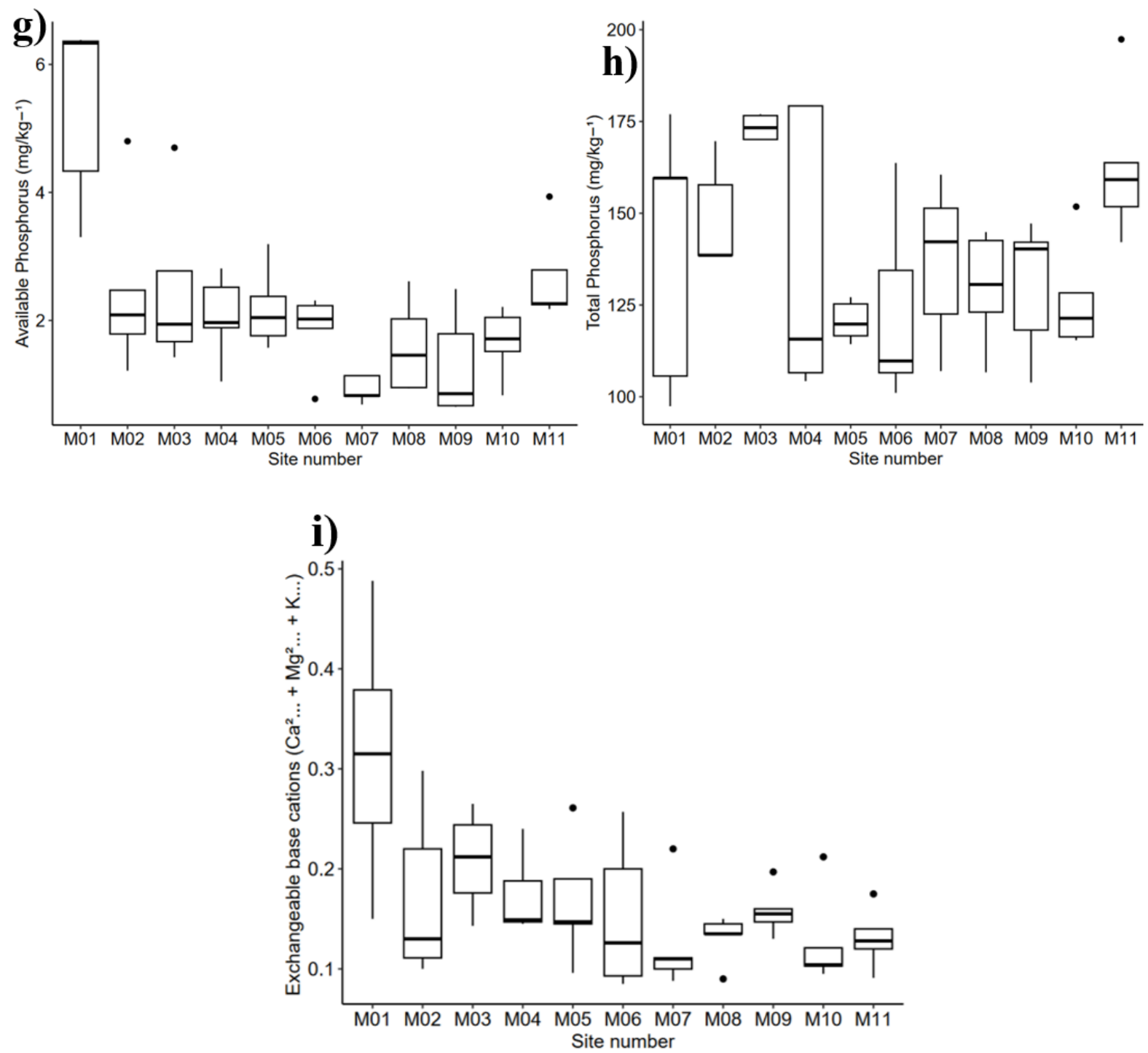


Figura S4: The eleven research sites (M01 - M11) located along the 600 km transect shown on the x-axis. Boxplots depict the variation of all climatic and edaphic variables analyzed.

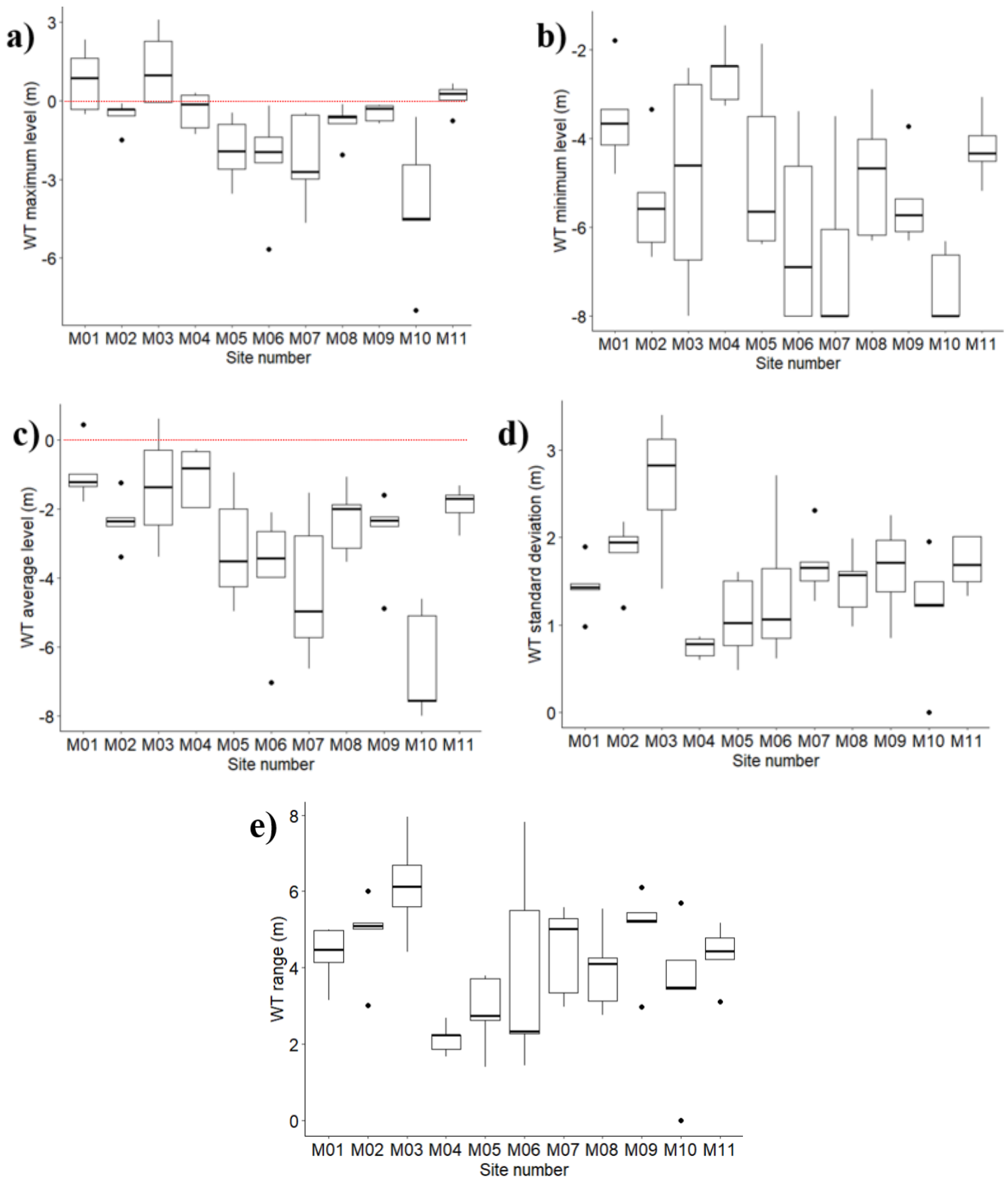


Figure S5: The eleven research sites (M01 - M11) located along the 600 km transect shown on the x-axis. Boxplots represent the variation of all the variables derived from the water table (WT) depth measurements analyzed. Negative values represent subsurface levels. Red dashed line indicates surface level.